2009-10-01

Thermal testing of innovative building insulations

Eoghan Frawley
Technological University Dublin

THERMAL TESTING OF INNOVATIVE BUILDING INSULATIONS

Eoghan Frawley B.E.

Masters of Philosophy

Dublin Institute of Technology

Supervisors: Dr. Anthony Reynolds & Dr. David Kennedy

School of Mechanical and Transport Engineering

October 2009

ABSTRACT

The main objective of this research was to design and develop a Hot Box to test the thermal properties of Eco-quilt multi-foil insulation. This work began by gaining an understanding into how multi-foil works, how it is installed and examining different variations of this insulation. It was clear at an early stage that there were two conflicting opinions on the thermal performance of multi-foils. One set of tests claimed that the insulation had a thermal resistance of approximately 5 $m^{2o}C/W$. These tests were carried out in real weather conditions, where temperatures were fluctuating, although one laboratory test achieved similar results. The second types of tests were based on standardised EN ISO test methods and the results were in general agreement that the thermal resistance of multi-foils was approximately 1.7 $m^{2o}C/W$.

The results of initial tests conducted on multi-foil with a basic testing facility were in general agreement with the results of the EN ISO test methods. It was noted that this initial testing facility had certain limitations and it was decided to build a more advanced test rig to conduct further tests on Eco-quilt. Research was conducted into three types of Hot Box testing apparatus and a new testing facility, based on a Guarded Hot Box, was designed and constructed.

A comparative test method was employed to evaluate Eco-quilt. This involved comparing insulation, with known thermal properties, directly with Eco-quilt while keeping the test conditions, for each test, as similar as possible. The results were in good agreement with the tests that found the thermal resistance equal to 1.7 $m^{2o}C/W$. Other tests conducted showed that the performance of multi-foil is reduced when manufacturers' installation procedures are not followed.

It was found that the testing facility produced repeatable and meaningful results and could be used in the future to offer a good indication of the thermal performance of new insulations being developed.

DECLARATION

I certify that this thesis which I now submit for examination for the award of Masters of Philosophy, is entirely my own work and has not been taken from the work of others save and to the extent that such work has been cited and acknowledged within the text of my work.

This thesis was prepared according to the regulations for postgraduate study by research of the Dublin Institute of Technology and has not been submitted in whole or in part for an award in any other Institute or University.

The work reported on this thesis conforms to the principles and requirements of the Institute's guidelines for ethics in research.

Signature_____ **Date:**_____

ACKNOWLEDGEMENTS

I would like to thank my tutors Dr. Anthony Reynolds and Dr. David Kennedy for their invaluable support and advice throughout the duration of this research. I would also like to express my gratitude to Brendan Dollard in Enterprise Ireland, for his time and input to the project, and to Dr. Fergal Boyle for reading this dissertation.

Many thanks also to Jim Mahon who gave me a helping hand with equipment during the testing phase of this study. I would like to thank my friends and family for their continued support during the past two years, and extend a special thanks to my girlfriend Louise for all her help and for feigning interest in heat transfer coefficients.

ABBREVIATIONS

PCM	= Phase Change Materials
CE	= Conformité Européenne
UKAS	= United Kingdom Accreditation Service
BRE	= British Research Establishment
CMM	= Confederation of Multi-foil Manufacturers
ETA	= European organisation for Technical Approval
BBA	= British Board of Approval
CEN	= Comite Europeen de Normalisation (European Committee for Standardisation)
GHB	= Guarded Hot Box
CHB	= Calibrated Hot Box
WGHB	= Wall and Edge Guarded Hot Box
BER	= Building Energy Rating

NOMENCLATURE

A_{ts} = Test specimen area (m^2)

A_{sp} = Surround panel area (m^2)

A_w =Metering box wall area (m^2)

A_n = Surface area normal to heat transfer (m^2)

C_p = Specific heat capacity of air @ 20°C (1.007 kJ/kg °C)

C_l = Combined loss heat transfer coefficient ($W/m^{2o}C$)

h_1 = Hot side test specimen surface coefficient ($W/m^{2o}C$)

h_2 = Cold side test specimen surface coefficient ($W/m^{2o}C$)

K_{ts} = Test specimen thermal conductivity (W/m^oC)

K_{sp} = Surround panel thermal conductivity (W/m °C)

$K_{polyiso}$ = Polyiso specimen thermal conductivity (W/m °C)

L_{ts} = Test specimen thickness (m)

L_{sp} = Surround panel thickness (m)

$L_{polyiso}$ = Polyiso specimen thickness (m)

$\dot{m}$ = mass flow rate (kg/s)

Q_{ts} = Heat transfer through test specimen (W)

Q_{in} = Heat input to metering box (W)

Q_w = Heat transfer through metering box walls (W)

Q_p = Heat transfer parallel to test specimen (W)

Q_e = Heat transfer through perimeter of test specimen/surround panel (W)

Q_{fl} = Flanking loss heat transfer (W)

Q_{sp} = Surround panel heat transfer (W)

Q_{heater} = Heater power (W)

Q_l = Combined loss heat transfer (W)

$R_{airgaps}$ = Air gap thermal resistance ($m^{2o}C/W$)

R_w = Wall thermal resistance ($m^{2o}C/W$)

R_{ts} = Test specimen thermal resistance ($m^{2o}C/W$)

$R_{Eco\text{-}quilt}$ = Eco-quilt thermal resistance ($m^{2o}C/W$)

$R_{multi\text{-}foil}$ = Multi-foil thermal resistance ($m^{2o}C/W$)

$R_{s\ 1}$ = Hot side surface resistance ($m^{2o}C/W$)

$R_{s\ 2}$ = Cold side surface resistance ($m^{2o}C/W$)

T1 = Average temperature in metering box (^oC)

T2 = Average temperature in Guard box (^oC)

T3 = Average temperature in Cold box (^oC)

T_{n1} = Metering box environmental temperature (^oC)

T_{n2} = Cold box environmental temperature (^oC)

$T_{hot\ ts}$ = Hot side test specimen surface temperature (^oC)

$T_{cold\ ts}$ = Cold side test specimen surface temperature (^oC)

$T_{hot\ sp}$ = Hot side test surround panel surface temperature (^oC)

$T_{cold\ sp}$ = Cold side test specimen surface temperature (^oC)

$T_{hot\ air}$ = Hot side air temperature (^oC)

$T_{cold\ air}$ = Cold side air temperature (^oC)

$T_{inside\ walls}$ = Inside metering box wall surface temperature (^oC)

$T_{outside\ walls}$ = Outside metering box wall surface temperature (^oC)

U_{sp} = Heat transfer coefficient of surround panel ($W/m^{2\ o}C$)

U_{ts} = Heat transfer coefficient of test specimen ($W/m^{2\ o}C$)

$(UA)_w$ = Heat transfer coefficient for metering box walls per unit area ($W/^oC$)

U_{TT} = Thermal transmittance ($W/m^{2\ o}C$)

ΔT_{ts} = Test specimen temperature difference (^{o}C)

ΔT_{sp} = Surround panel specimen temperature difference (^{o}C)

ΔT_{w} = Metering box wall temperature difference (^{o}C)

ΔT_{a} = Air temperature difference (^{o}C)

V = Volume flow rate (m^3/s)

$\dot{V}$ = Flow rate (l/s)

ρ_{air} = Air Density (1.18 kg/m^3)

ε = Emissivity

TABLE OF CONTENTS

TABLE OF FIGURES

LIST OF TABLES

CHAPTER 1 - INTRODUCTION

1.1 Background

In Ireland, energy demand is predicted to grow by 2-3 % annually until 2020 **[1].** With overall energy import dependency reaching 91 % in 2006 **[2]** and with increasing fossil fuel prices, it is essential that this energy is used efficiently**.** The Kyoto Protocol is a legally binding agreement by developed nations to reduce global green house emissions. The European Union (EU) has committed to reducing their green house gas emissions by 8 % below 1990 levels between the years 2008-2012. For Ireland, this means that we have to reduce emissions to 13 % above 1990 levels (which was breached in 1997). By investing in Ireland's renewable energy potential, reductions in CO_2 emissions and energy dependence can only benefit Ireland's economy in the future **[1]**. While reducing those parameters is important, making sure that this energy is used efficiently is vital.

Energy consumption can be divided into five groups; industry, transport, residential, commercial/public and agriculture. At 24.5 %, the residential sector is only second to transport in energy consumption **[2]**. Of that 24.5 %, space and water heating accounts for approximately 70 % of the energy costs in a typical dwelling, and without adequate insulation much of that energy is being wasted **[5]**. It is, therefore, easy to see why having an energy efficient building house is so important.

The Irish 1997 Building Regulations (Part L) sets minimum standards that buildings must meet to reduce energy consumption. These standards were further amended in 2002 **[3]**. Furthermore, an EU directive on the Energy Performance of Buildings (EPBD) **[4]**, which was brought into Irish law in 2006, contains provisions to improve

the energy performance of residential and non-residential buildings. As a result of this, new dwellings must have a Building Energy Rating (BER) certificate. Certificates range from an *A1* rating to a *G* rating, with *A1* the most energy efficient rating and *G* the most inefficient rating. This certificate clearly indicates the energy performance of a building to prospective buyers or tenants which in previous years would not have been available **[5].** As a result, manufacturers of building materials became increasingly aware that they would need some recognised and accurate way of testing their product to ensure that the product would be able to meet these requirements. This also makes the product more attractive to prospective buyers.

SmartRinsulations, an Irish company, manufacture a branded insulation called Eco-quilt. Eco-quilt is a multi-foil type insulation that is relatively new to the Irish market. Although multi-foils have been used in Europe since the 1980's, there has been considerable controversy to date over the thermal performance of the insulation. Conflicting test results show that when standardised test methods are employed [6], multi-foils perform poorly when compared to non-standardised tests. The standardised sets of tests were in general agreement that the thermal resistance of multi-foils was approximately 1.7 m2 oC/W, while test performed by multi-foil manufacturers showed that the insulation had a thermal resistance of approximately 5 $m^2\,^oC/W$.

SmartRinsulations and Enterprise Ireland commissioned this research to evaluate the thermal performance of Eco-quilt through agreed test methods. It was decided to base the tests in this research on the standardised Hot Box method as other test methods described in Section 2.4.1 – 2.4.4 were not recognised by the relevant authorities at the beginning of this project. Currently, there is no standardised Hot Box test facility in

Ireland and products must be sent to the UK where these test are carried out at great cost.

A method of testing insulation was developed at DIT previous to this research. Preliminary tests were conducted with a testing facility, as part of this research, before a new and more advanced test facility was designed. The purpose of these tests will be to give manufacturers an indication of how their particular product will perform before the specimen is sent to the UK for certification. This offers potential saving as the tests could give a strong indication of the eventual performance in the Standardised Tests.

1.2 Aims and Objectives

The main aims and objectives of this research were to:

1. Study multi-foil insulation and its thermal performance through defining multi-foil insulation, comparing it to other types of insulation and examining test reports and procedures.
2. Conduct preliminary thermal tests with the current testing facility at DIT, test Eco-quilt and gain a better understanding of how it performs.
3. Study Hot Box designs, types and testing through examining ISO standards, papers and case studies.
4. Design and manufacture a Hot Box for testing Eco-quilt insulation. This includes sizing and selection of equipment and agreement on a test procedure with project sponsors.
5. Calibrate the Hot Box and test multi-foil insulation with the use of calibration

panels.

6. Compare the test results with other test data for multi-foil insulation and to examine the suitability of Eco-quilt for meeting building regulations.
7. Provide a pre-test facility for industry.

1.3 Layout of Thesis

Chapter 1 is an introduction to the background of the research. The main goals of the project are also set out in this chapter.

Chapter 2 contains a literature survey on thermal insulation. It begins with a brief overview of different types of insulation, before focussing on multi-foil or reflective insulation. The thermal performance of multi-foil is discussed, and different test methods are detailed.

Chapter 3 contains a literature review of Hot Box testing apparatus and methodology. ISO Standards are also detailed in this chapter, along with relevant case studies on various Hot Box types.

Chapter 4 gives a detailed account of the design process involved in the test facility. It outlines the preliminary test rig and its limitations, along with design considerations for the eventual facility. The final design, construction, sizing and the equipment involved are described in this chapter.

Chapter 5 deals with the testing of the new test rig. Preliminary tests were conducted to ensure the equipment was working as intended, before calibration of the test facility took place. The remainder of the chapter describes tests performed on Eco-quilt, along

with an examination of the findings of the results of these tests.

Chapter 6 presents the conclusions and findings of this research, along with some recommendations for future work.

CHAPTER 2 – THERMAL INSULATION

2.1 Introduction

This chapter begins by describing common types of insulation that are commonly used in buildings today. Multi-foil insulation is then discussed in detail, with aspects such as what defines a multi-foil, how it works and how it is installed described. The thermal performance of multi-foils is examined by describing various thermal test reports that were conducted on multi-foil and their results. Hot Box thermal testing facilities are examined and three different types are described in detail. Hot Box testing theory is also described.

2.2 Thermal Insulation

Thermal insulation is one of the most effective energy conservation measures for cooling and heating in buildings **[7]**. The thermal conductivity (k) of an insulation is a measure of the effectiveness of the material in conducting heat **[13]**.

Two other properties related to the thermal performance of insulation are the thermal resistance (R) and the thermal transmittance (U). The thermal resistance of a material can be defined as the measure of the resistance to heat flow as a result of suppressing conduction, convection and radiation. It is a function of material thermal conductivity, density and thickness **[13].** The thermal transmittance is defined as the rate of heat flow through a unit area of a component with unit temperature difference between the surfaces of the two sides of the material. It is the reciprocal of the sum of the resistances of all layers composing that material plus the inside and outside air film resistances

[13].

Insulation types can be divided into four main groups **[8]**:

- Cellular insulation
- Fibrous insulation
- Flake/Granular insulation
- Reflective insulation **[8]**

Figures 2.1 a, b and 2.2 a, b show some of the most common types of insulations used in the the construction industry.

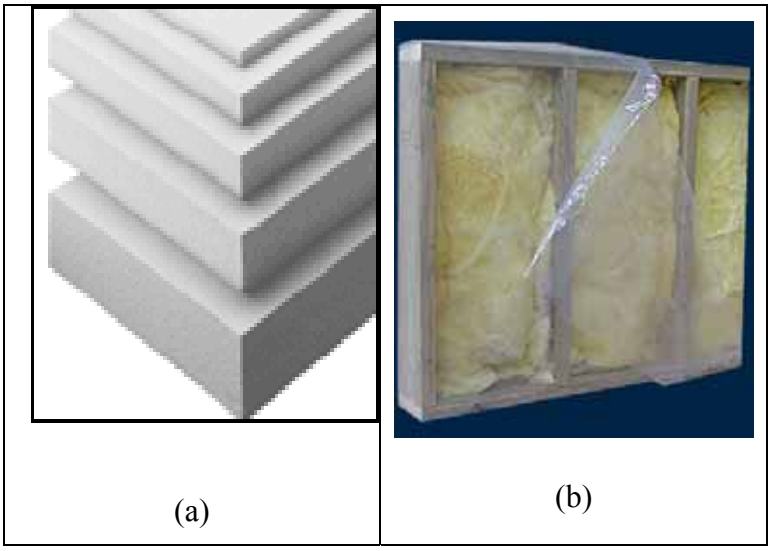

(a) (b)

Figure 2.1: a - Polystyrene (Cellular) Insulation; b - Fibreglass (Fibrous) Insulation **[9], [10]**

(a)

(b)

Figure 2.2: a - Flake/Granular Insulation; b - Reflective Insulation **[11], [12]**

Examples of cellular insulations are polystyrene, polyisocyanurate (Polyiso), foamed rubber and cork **[13].** Some of these insulations can be sprayed into the cavities of walls and all of them are produced in rigid sheet form (shown in Figures 2.1 a). This insulation is used in walls, roofs and under floors. Fibrous insulation such as rock wool, sheep's wool and fibreglass (shown in Figure 2.1 b) are commonly used for insulating attics and walls in buildings. They are generally manufactured in blanket rolls or rigid sheets **[14]**. Granular/Flake insulation consists of small nodules containing air pockets or small flakes that divide the air. They can be produced in the form of loose fill/pourable material or a mixing agent can be applied to achieve rigidity. An example of this is shown in Figure 2.2 a. This type of insulation is commonly used in attics. These types of thermal insulation are discussed in detail in the literature **[7], [8], [13], [14], [15].** Table 2.1 shows a list of common types of insulation and some of their associated properties. Reflective type insulation is discussed in detail in Section 2.3.

	Cellular Insulation		Fibrous Insulation		Granular/Flake Insulation	
Property	**Polystyrene**	**Polyiso**	**Fibreglass**	**Rockwool**	**Vermiculite**	**Perlite**
ρ (kg/m^3)	16-35	40-55	12-56	40-200	64-130	32-176
k (W/m^{0}C)	0.038-0.037	0.023	0.04-0.033	0.037	0.068-0.063	0.06-0.04
Fire Rating	Poor	Poor	Good	Excellent	Excellent	Excellent

Table 2.1: Characteristics of Some Insulations

Alternative types of insulation that exist are aerogels, vacuum insulated panels and Phase Change Materials (PCMs). Aerogel is a translucent silica based insulation that can have a thermal conductivity as low as 0.013 W/m^{o}C with a density of 120 kg/m^3 **[16]**. Due to its translucency, aerogel allows natural light to enter a building but does not allow heat leave it and this natural light has been proven to improve the performance of operators and workers in a building **[17]**. "Vacuum insulation panels (VIPs) are micro porous core materials that are sealed in a gas tight envelope at a very low pressure" **[18].** They can have a thermal conductivity as low as 0.005 W/m^{o}C, with a density from 80-140 kg/m^3. Originally used in refrigeration systems, VIPs have only been developed for use in building envelopes in recent years **[19].**

Research and investigation of PCMs suggests that they could be installed in the building envelopes to assist insulation and achieve higher energy efficiency for a building. PCMs store heat from the sunlight available in the day and release that energy when temperatures drop. This is achieved by its changing phase or state over a small

temperature range. Further information on the use of PCM along with conventional insulation can be found in the literature **[20 - 22].**

2.3 Reflective Insulation/Radiant Barriers

2.3.1 Introduction

Standard thermal insulation (e.g. fibreglass, foam etc.) are designed to lessen heat transfer by trapping air or a certain type of gas, thus reducing convection and conduction from one side of the insulation to the other. According to the Reflective Insulation Manufacturers Association (RIMA), radiation is often the major mode of heat transfer in a building envelope and some of the more conventional types of insulation are not well equipped to deal with this **[23]**. When discussing reflective insulation, it is important to distinguish between radiant barriers and reflective insulation (multi-foils).

Reflective insulation differs from conventional insulation for the following reasons:

1. Reflective insulation has very low emittance.
2. Reflective insulation traps air with layers of aluminium or some other highly reflective surface. Conventional insulations use fibres of glass, particles of foam or ground-up paper etc.
3. Reflective insulation does not have a large enough mass to absorb and retain heat **[23].**

2.3.2 Radiant Barriers

The generally accepted definition of a radiant barrier system is defined whereby one

reflective surface is facing an open air space **[23].** Radiant barriers do not have a thermal resistance themselves and must be installed beside an air gap. Radiant barriers are fixed on the surface of building components, such as foil backed plasterboard or foil backed sheets of insulation, or can be situated on their own near a building component. Their main function is not to radiate energy, but rather to reflect radiation that strikes the barrier. This is achieved by the radiant barrier having a very low surface emittance (usually $\varepsilon \leq 0.1$) **[24].** Figure 2.3 shows of a typical radiant barrier.

Figure 2.3: Radiant Barrier Insulation **[25]**

Studies carried out on radiant barriers show that heat loss in buildings can be reduced by using radiant barriers alone with no other insulation **[26 - 29]**. When radiant barriers were tested in conjunction with other insulation, heat loss through roof structures also fell. The effect of radiant barriers is reduced when the thermal resistance of insulation it is being used with increases. The performance of radiant barriers also varies in different climates **[30, 31].**

2.3.3 Reflective Multi-foil Insulation

Reflective insulations are defined as **"***Thermal Insulation consisting of one or more low*

emittance surfaces, binding one or more enclosed air spaces".

Reflective insulation generally comprises of layers of highly reflective aluminium, paper and/or plastic to trap air and thus reducing convection. As the layers of aluminium are highly reflective, radiation heat transfer through the multi-foil insulation is reduced. It is claimed in the literature that the foil material can reduce radiant heat transfer by as much as 97 % **[23].** The effectiveness of the insulation depends on the emittance of the materials, the size of the enclosed air space and the number of reflective layers. The smaller the air space, the less effect convection will have on the insulation. Therefore, the main function of multi-foil is to minimise radiation and convection heat transfer through the insulation by breaking an existing air space into several smaller cavities consisting of highly reflective layers. Figure 2.4 shows an example of multi-foil insulation.

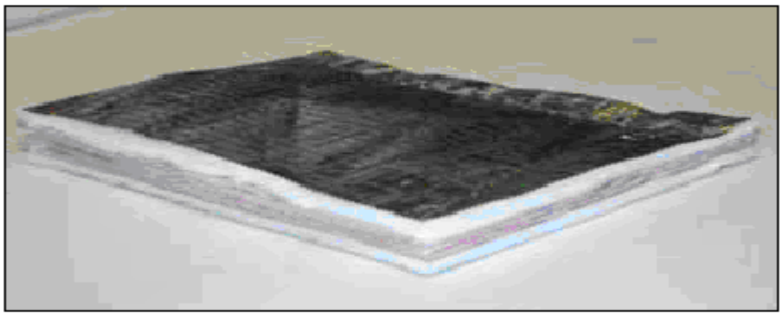

Figure 2.4: Example of Multi-foil Insulation **[12]**

One advantage of reflective insulation is its non-toxic nature, which therefore means it can be classed as an environmentally safe product. As reflective insulation is recyclable, it can be termed a Green Building Material. It can also serve as an effective vapour barrier **[23]**.

2.3.4 Examples of Reflective Insulations

There are many types of reflective insulations available in the marketplace today. As a generalisation, they can be separated into two groups. The first of these types are made of a number of layers of aluminium/plastic type reflective foil, separated by layers of plastic bubble wrap or some foam material. The second type also consists of multiple layers of aluminium, kraft paper and/or plastic with internal expanders **[23]**. Three multi-foils are described briefly.

2.3.4.1 ACTIS Multi-foil Insulation

ACTIS insulation, a French company, has manufactured multi-foil insulation for 25 years and holds a 65% share of the total European multi-foil market **[12].** They have two products; TRI-ISO Super 9 and TRI-ISO Super 10.

TRI-ISO Super 9 consists of 14 separate layers and is 25 mm thick when uncompressed. The layers comprise of the following **[32]**:

- 2 tear-resistant reinforced reflective films.
- 2 layers of soft, flexible wadding.
- 6 layers of closed cell foam.
- 4 internal reflective films.

TRI-ISO Super 10 is a newer product and consists of 19 separate layers and has an uncompressed thickness of 30 mm. The layers comprise of the following **[12]**:

- 2 external reflective films with reinforced reflective films.
- 3 wadding layers.

- 8 foam layers.
- 6 internal reflective films.

2.3.4.2 SmartRInsulations Multi-foil Insulation

Eco-quilt, the insulation tested for the purposes of this research, is manufactured by SmartRInsulations. This insulation is similar to TRI-ISO Super 9 as it consists of 14 separate layers and is 25 mm thick uncompressed. It consists of the following:

- 2 tear-resistant reinforced reflective films.
- 2 layers of soft, flexible wadding.
- 6 layers of closed cell foam.
- 4 internal reflective films.

2.3.5 Uses of Reflective Insulation

Multi-foil insulation is mainly installed in the roofs of dwellings. An air gap of at least 25 mm on either side of the multi-foil is always recommended by the manufacturer for best performance. Figures 2.5 and 2.6 show two methods of how multi-foil insulation can be installed in a roof structure. Figure 2.5 illustrates how the insulation is fitted between the breather membrane and the rafters. Battens are installed on top of the insulation to maintain the air gap between the multi-foil and the membrane. This is commonly referred to as over-rafter application. The installation procedure involves rolling out the insulation from the top of the roof and then stapling the rafters at approximately 500 mm intervals. The edges are overlapped and taped to ensure proper sealing.

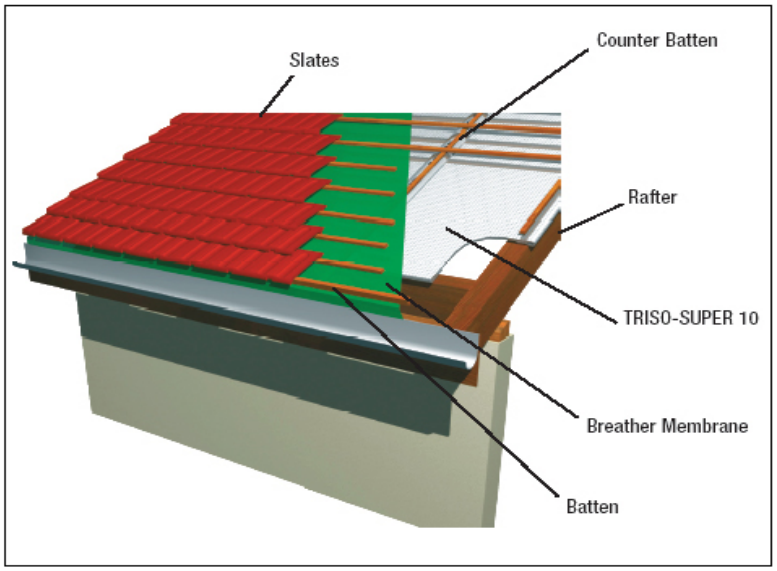

Figure 2.5: Over Rafter Application of Multi-foil Insulation **[12]**

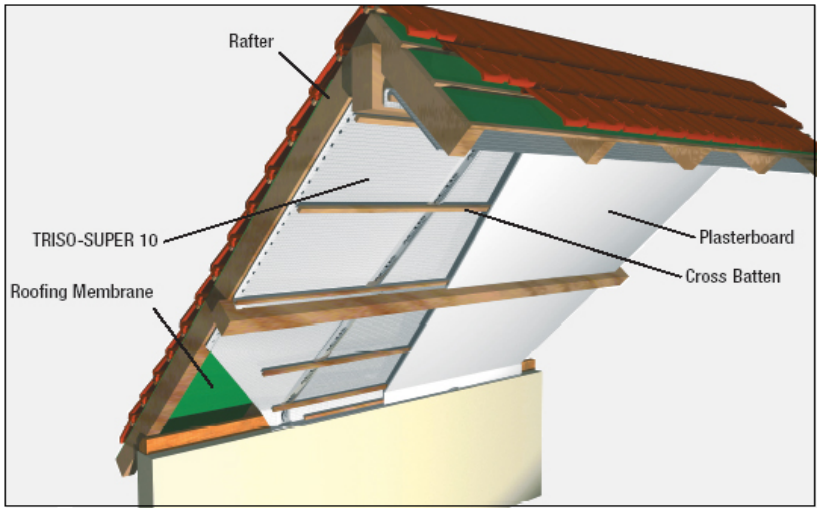

Figure 2.6: Under Rafter Application of Multi-foil Insulation **[12]**

If the tiles and the breather membrane are already present in a roof, the insulation can be stapled to the under-side of the rafters, a practice commonly referred to as under-rafter application. Figure 2.6 illustrates how the battens are fitted on the inside surface of the insulation (after the insulation has been stapled to the rafters) to maintain an air gap on either side of the insulation. Plasterboard would generally be screwed on to the battens to provide a finish for the inside attic space **[12], [33], [34]**.

Multi-foil insulation can also be used to insulate floors and walls. The method of installing this insulation is similar to that of the roof application. This method also recommends that an air gap of at least 20 mm between the wall battens and the plasterboard. The floor insulation also requires an air gap of at least 20 mm between the floor boards and the insulation, ensuring that the heat exchange occurs due to radiation and convection. This is shown in Figure 2.7 **[35]**.

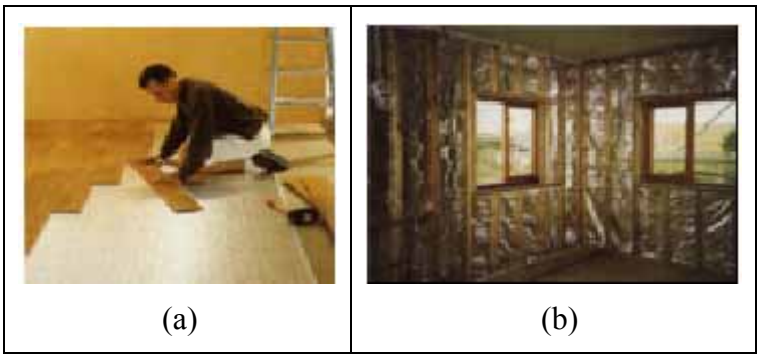

(a) (b)

Figure 2.7: a –Floor Installation; b - Wall Installation **[35]**

2.4 Thermal Performance of Multi-foil Insulation

There are two vastly different opinions on how multi-foil insulation performs. Some reports suggest that multi-foil insulation is equivalent to installing 200 mm wide of fibre glass which has an R-value of approximately 5 m^2 $^oC/W$ **[37, 38, 40, 42, 43]**. Other reports claim that the R-value of multi-foil is circa 1.7 m^2 $^oC/W$ **[45, 47, 54]**. This section describes the various different tests that have been performed on multi-foil and their conclusions.

2.4.1 Sheffield Hallam University Testing

The Centre for Infrastructure Management (CIM) is based in Sheffield Hallam University in the UK and offers advisory and independent testing services to the

construction and infrastructure industry. Two tests test were carried out by this organisation to evaluate the thermal properties of multi-foil insulation **[36]**.

2.4.1.1 Test 1: Evaluation of SuperQuilt Multi-layer Insulation Blanket in Roofs

This test was performed between December 2004 and January 2005 **[37]**. The aim of this test was to monitor the power consumption of two custom built enclosures replicating an enclosed roof space, while maintaining an inside temperature of 21 ^{o}C. Both roof models were exposed to outside winter conditions.

One of the enclosures was covered with 25 mm of SuperQuilt insulation (a multi-foil insulation). The other enclosure was covered with 200 mm of glass wool insulation.

The conclusions of this study found that the power consumption of the SuperQuilt was 26 % less than the power consumption of the glass wool enclosure while maintaining the required inside temperature.

As this was a comparative test, and the test report stated that 200 mm glass wool had a widely accepted R-value of 4.5 m^2 ^{o}C/W, it was calculated that the SuperQuilt had an effective thermal resistance of 6.1 m^2 ^{o}C /W and was equivalent to 270 mm of glass wool.

This report also stated that:

- "SuperQuilt insulation material was much easier to apply compared to standard glass wool" **[37]**
- "SuperQuilt provides a different insulating mechanism compared to standard glass wool. Heat was circulated more efficiently in the roof space insulated with SuperQuilt due to the highly reflective surface" **[37]**

2.4.1.2 Test 2: Assessment of Alumaflex Thermo-Reflective Insulation in Roofs

This comparative test was carried out at the CIM Sheffield Hallam University in August 2005. The aim of this test was to evaluate the thermal resistance of Alumaflex by comparing it to 200 mm of glass wool. Alumaflex consists of 14 separate layers and is 30 mm thick.

The main difference between this and the test outlined in 2.4.1.1 was that this experiment was carried out in a controlled environment. In the SuperQuilt test, the test rigs were exposed to outside weather conditions that were constantly changing. Accordingly, only one test enclosure was built, because the same conditions could be repeated for two different insulations on separate occasions.

A custom-built enclosure representing a roof space was built and the power consumption was measured to maintain an inside temperature of 21 ^{o}C. A hot spot ceramic heater was used to heat the enclosure. Thermocouples (type T) were placed inside and outside the enclosure to observe interior and exterior temperatures. A diagram of the enclosure is shown in Figure 2.8.

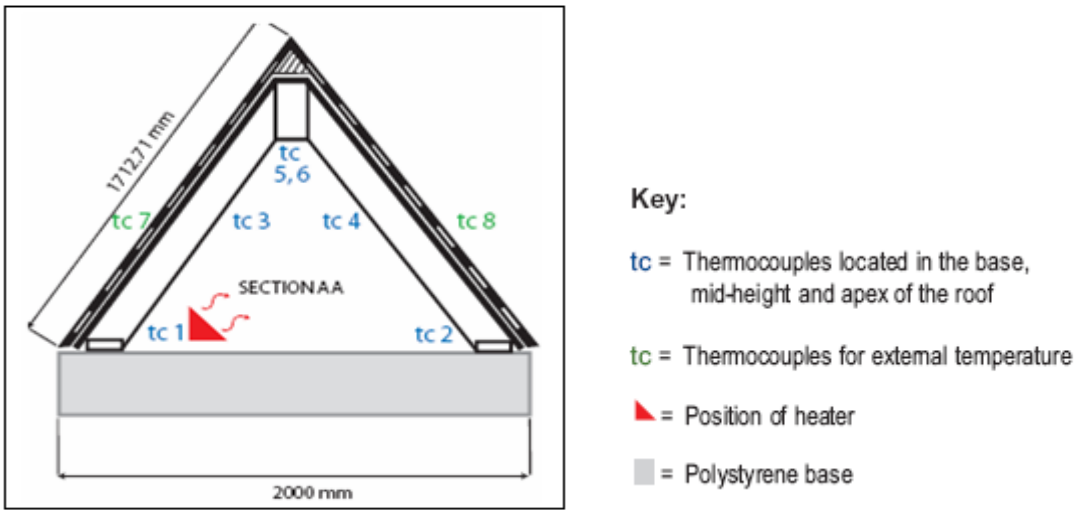

Figure 2.8: Diagram of Test Enclosure for Test 2.4.1.2 **[38]**

The enclosure consisted of a series of timber members. This timber frame was situated on a 100 mm polystyrene base. 100 mm of glass wool was fitted in between the rafters and an additional 100 mm was placed on top of the timber rafters. An air gap of 30 mm to 40 mm was maintained between the insulation and the external MDF boards. The same timber enclosure was used for Alumaflex. The reflective insulation was fitted over the outer surfaces of the rafters.

The enclosure was tested in a controlled room environment. Three tests were conducted, the first with the surrounding temperature steady at -5 ^{o}C, and the subsequent tests at 0 ^{o}C and +5 ^{o}C respectively. The duration of each test was 50 hours. Each test was given 6 hours for steady state conditions to exist and the remaining 44 hours were used for calculations.

Figure 2.9 illustrates the temperature profiles that occurred during the test. The temperature is on the Y-axis on the graph with the time on the X-axis. The time period for all tests was 50 hours. A measurement of the cumulative power consumption (quoted in KW in **[38]**) is also shown on the graphs. Figure 2.9 is the temperature profile for a controlled room temperature of 5 ^{o}C. The different temperatures measurements are colour coded and the key is shown.

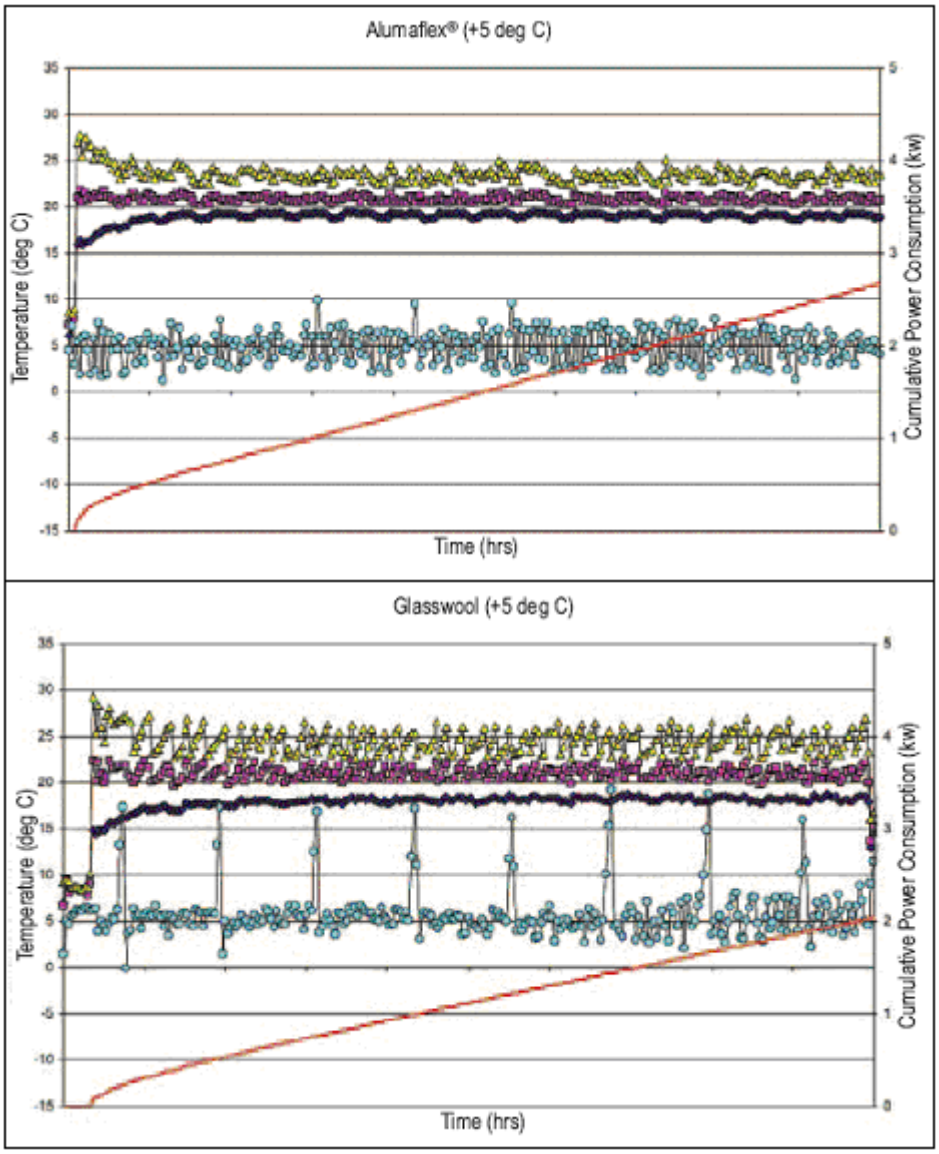

Figure 2.9: Temperature Profiles @ 5 ^{o}C (T0-T50 hrs)**[38]**

Key:

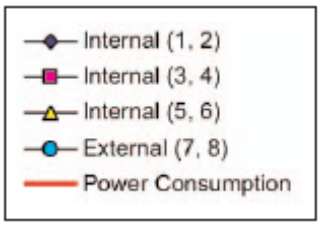

It was found that when the controlled room temperature was at -5 ^{o}C, Alumaflex was 39.8% more efficient than the glass wool over a 44 hour monitoring period. For

controlled room temperatures of 0 ^{o}C and + 5 ^{o}C, Alumaflex was 8.7 % and 2.8 % more efficient respectively.

As this was a comparative test, an effective thermal resistance was calculated by assuming that the glass wool had a thermal resistance of 5 m^2 ^{o}C/W. This report concluded that the thermal resistance of Alumaflex was at least the same as installing 200 mm of glass wool **[38]**.

2.4.2 TRADA Multi-foil Testing

TRADA technology is an independent consultant company based in the UK and offers commercial services to companies to certify products. A BM TRADA certificate offers assurance to contractors and purchasers that certified products will perform to a certain standard. TRADA also provides CE marking certification **[39]**.

The tests took place in 2006 in High-Wycombe in the UK. Three identical roof structures were built with one insulated with ACTIS TRI-ISO Super 10 multi-foil insulation, one insulated with 200 mm of glass wool and one with no insulation. The aim of this test was to compare the power consumption required to keep the inside temperature of these structures at 23 ^{o}C over several weeks. Figure 2.10 shows the roof structures constructed for these tests. Underneath the tiles was a layer of breather membrane and 150 mm deep rafters were used to support the roof **[40]**.

Figure 2.10: Outside View of Finished Test Structure, High-Wycombe **[40]**

Figures 2.11a and b shows the glass wool and TRI-ISO roof structures from the inside. It can be seen that the glass wool is installed between the rafters and is covered with a vapour barrier. The TRI-ISO was situated on top of the rafters. Figure 2.12 shows a how plasterboard was then fixed on the inside of the rafters to replicate how an actual roof would be finished. Both insulations were installed in accordance with the manufacturer's instructions.

(a)

(b)

Figure 2.11: a; b - Pictures of Installed Insulation **[40]**

Figure 2.12: Plasterboard Lining on inside of Test Structures **[40]**

The power consumption of each building was recorded over a 5 week period in 2006. TRI-ISO was found to perform better than the glass wool. These tests found that the TRI ISO was equivalent to 210 mm thick of glass wool **[40]**.

2.4.3 Fraunhofer Institute for Building Physics (IBP) Multi-foil Testing

Fraunhofer IBP carries out research, testing and consultant work in the field of building physics in Germany. They have several branches around Germany and the Holzkirchen branch, where the multi-foil tests were conducted, deals specifically with outdoor testing **[41].**

Two identical test houses were built with the roof of one house insulated with 200 mm of glass wool (with a thermal resistance of 5 $m^2\ ^oC/W$), and the roof of the other test house insulated with ACTIS prototype multi-foil insulation. The aim of this test was to compare the power consumption required to keep the inside temperature of these structures at 21 ^oC over several weeks. Figure 2.13 shows a picture of the two identical test houses.

Figures 2.14 and 2.15 are sections through each of the roofs. The reference roof (Figure 2.14) comprised of roof tiles sitting on battens, with under-tile lining beneath. The 200 mm of glass wool was then fitted into the roof and a vapour barrier covered the inside of the roof, before a layer of plasterboard finished the inside. The ACTIS roof (Figure 2.15) comprised of roof tiles sitting on battens, underneath which lay under-tile lining. An air gap existed between the lining and the ACTIS multi-foil; another air gap existed between the multi-foil and the plasterboard.

Figure 2.13: Holzkirchen Test House Image **[42]**

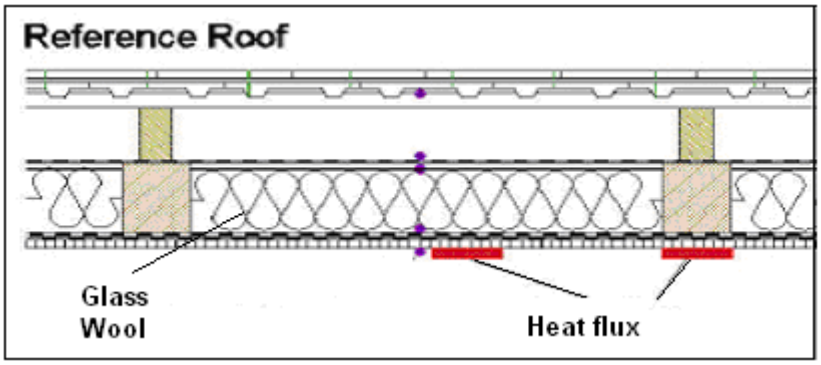

Figure 2.14: Glass Wool Roof **[42]** (Reference adapted)

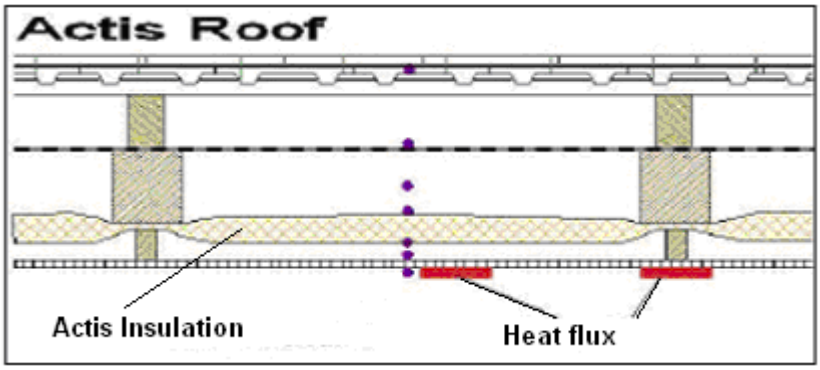

Figure 2.15: ACTIS Multi-foil Roof **[42]** (Reference adapted)

Measurements were taken over a period of time from the 26th of January to the 2nd March 2007. The power consumption of the house with 200 mm of glass wool was found to be 747.7 kWh. The power consumption of the house with multi-foil was found to be 749.5 kWh. These results showed that the multi-foil performed approximately the same as the 200 mm of glass wool **[42]**.

2.4.4 SFIRMM Testing of Multi-foil

SFIRMM are a French organisation that aims to promote the use of reflective multi-foil insulation products and also lobby for the creation of a European certification of these products. The aim of these tests was to monitor the power consumption of three test houses required to maintain a temperature of 23 ^{o}C over a period of 89 days. The test location was in Limoux in France and took place from December 16th 2006 to March 15th 2007.

Figure 2.16 shows one of the test houses. The roof of one of the test houses was insulated with an ACTIS multi-foil. The other (identical) test house was insulated with 200 mm of glass wool, with the last house having no insulation installed. The roof construction of the house with the glass wool and the multi-foil is shown in Figures 2.17

and 2.18 respectively. Although no specific details were given, Figure 2.17 show that the tiles were fixed on top of battens and that 200 mm of the glass wool was installed underneath the fixing battens. A layer of paper material was on the inside face of the glass wool, and the inside of the roof was finished with a layer of plasterboard. The configuration for the multi-foil roof was exactly the same as the glass wool roof except the layer of multi-foil (seen in blue in Figure 2.18) replaced the glass wool and paper combination.

Figure 2.16: Limoux Test House **[43]**

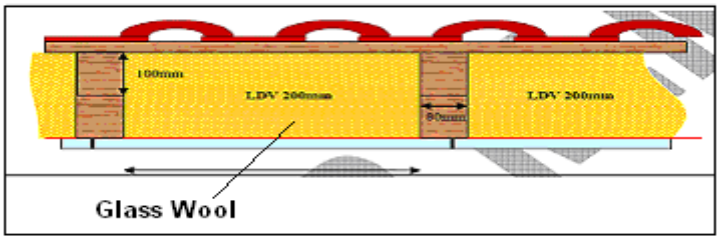

Figure 2.17: Glass Wool Roof Configuration **[43]**

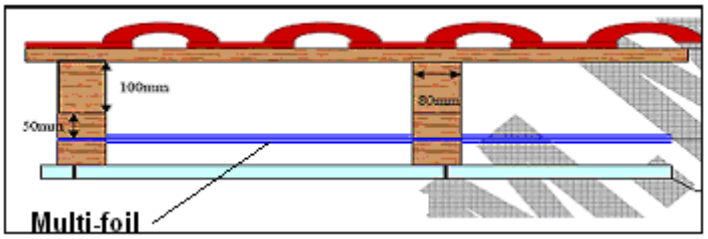

Figure 2.18: Multi-foil Roof Configuration **[43]**

Over the testing period, the multi-foil roof configuration was found to consume 28.4 % less power than 200 mm of glass wool **[43]**.

2.4.5 National Physics Laboratory (NPL) Test Report

The NPL is the national standards body of the United Kingdom and is known throughout the world to be a respected independent centre of research and development and knowledge transfer in measurement and material science **[44].**

This report was commissioned by Celotex Ltd. and issued on 13th August 2004. Celotex manufactures and sells polyiso insulation and is in direct competition with the multi-foil insulation industry.

This Wall and Edge Guarded Hot Box test conformed to EN ISO 8990 and is certified by UKAS (United Kingdom Accreditation Service). UKAS certification is recognised by the building regulations in the UK.

Hot Box testing is carried out under steady state conditions. The test rig has two chambers, one hot side and a cold side. The test specimen is placed in between the hot and the cold side and the heat flux (W/m^2) through the specimen is measured and the thermal resistance is extrapolated from that **[15].** This type of Hot Box is described in Section 2.5.4.1.

The multi-foil being tested was ACTIS TRI-ISO Super 9. As multi-foil is primarily a roof insulator, this insulation was tested at an inclination of 45 ^{o} (the Hot Box is fully rotatable) to represent a roof structure. The multi-foil was tested with an air gap on either side of the insulation. A diagram of how the test specimen was fitted, with the air

cavity on either side, into the surround panel of the Hot Box is shown in Figure 2.19.

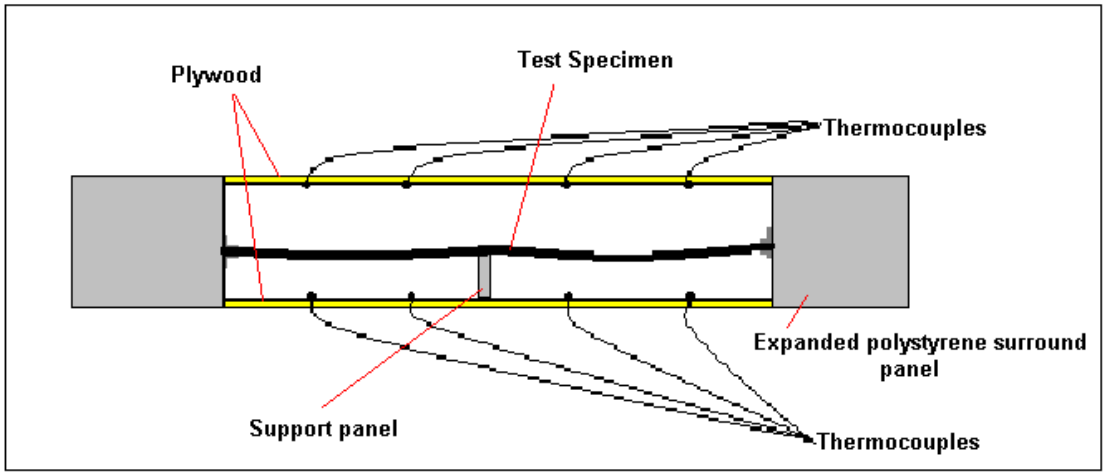

Figure 2.19: Test Specimen with Air Cavity **[45]** (Reference adapted)

It can be seen from Figure 2.19 that the thermocouples were placed on the inside surface of the sheet of plywood. The measurement procedure is described by the following points.

- The method of fixing the insulated quilt in the cavity and in the surround panel is shown in Figure 2.19.
- The test specimen was fixed 25 mm from the inside surface of the plywood sheet on the cold side.
- An expanded polystyrene support panel 10 mm thick x 85 mm high x 2000 mm long was fixed along the centre of the plywood sheet. This acted as a support to the quilted insulation during testing.
- The temperatures of the inside surfaces of both of the cavity walls were each measured using thermocouples.
- The thermal resistance of the cavity with the quilted insulation was then

calculated using the heat flow rate through the test specimen and the temperature difference across the cavity.

- The thermal resistance given for the insulated cavity was the mean value of four sets of readings taken at 2.5 hour intervals. The maximum variation between the four sets of readings was found to be less than 2 %.

The results from the test found that the thermal resistance for the insulated cavity was found to be 1.71 $m^2\,^oC/W$. This result differs greatly from the tests that were carried out by Sheffield Hallam University (a thermal resistance approximately three times greater than this test) **[45].**

The thermal performance of reflective insulation was discussed in a meeting held at the National Physics Laboratory (NPL) in February 2005. Two sample calculations were carried out to try and determine the best possible thermal resistance that reflective insulation could offer. There were two types of calculations involved **[46]**.

The boundary conditions for the first calculation are shown in Figure 2.20. It can be seen that the insulation is situated in the centre of an unventilated air cavity. The cold surface temperature is 10 ^oC and the hot surface temperature is 20 ^oC. The following points are a description of the steps and assumptions involved in the calculations **[46]**.

- The emissivity of surfaces 1 and surface 2 were assumed to be 0.05.
- No heat transfer due to radiation took place across the reflective insulation.
- The thermal conductivity of the insulation was assumed to be the same as still air at 0.025 W/m^oC. (i.e. no convection across the insulation.)

- The thickness of the insulation remained constant at 50 mm.
- Thermal resistance of each 25 mm air gap (using EN673 @ 45^0 with ε = 0.05) = 0.636 m^2 $^oC/W$.

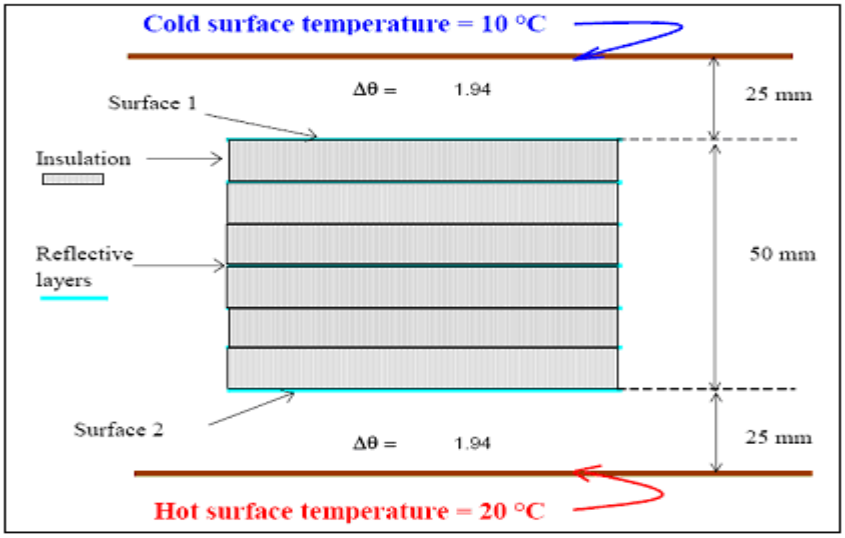

Figure 2.20: Unventilated Air Cavities either side of Reflective Insulation **[46]**

The thermal resistance of the insulation (with no convection and no radiation) plus the resistance of the air cavities on either side of the insulation was found to be 3.282 m^2 $^oC/$ W.

The boundary conditions for the second calculation are shown in Figure 2.21. It can be seen that the insulation is situated in large internal air spaces. The cold air temperature is 10 ^oC and the hot air temperature is at 20 ^oC. The following points are a description of the steps and assumptions involved in the calculations.

- The emissivity of surfaces 1 and surface 2 were assumed to be 0.05.
- No heat transfer due to radiation took place across the reflective insulation.
- The thermal conductivity of the insulation was assumed to be the same as still

air at 0.025 W/m^{o}C (i.e. no convection across insulation).

- The thickness of the insulation remained constant at 50 mm.
- The surface resistance of the cold side (using EN ISO 6946 ANNEX A –[heat flow upwards]) = 0.189 m^{2} ^{o}C/W.
- The surface resistance of the hot side (using EN ISO 6946 ANNEX A –[heat flow upwards]) = 0.190 m^{2} ^{o}C/W.

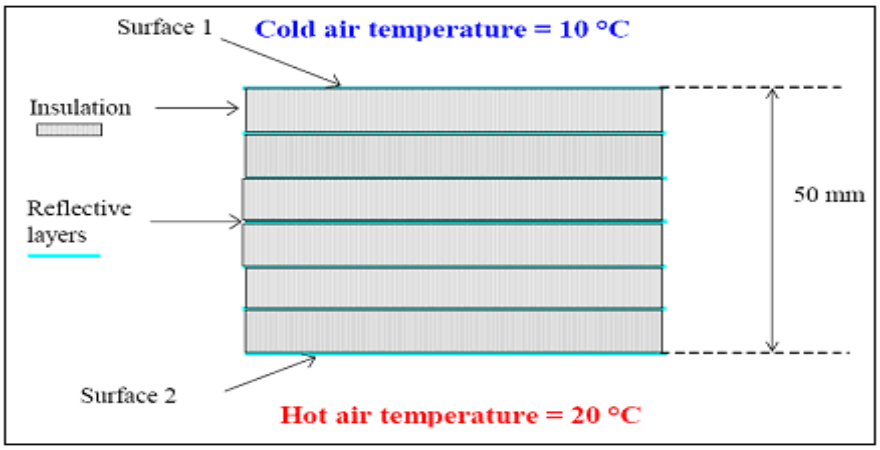

Figure 2.21: Reflective Insulation facing Large, Internal Air spaces **[46]**

Using those conditions and assumptions, the total thermal resistance of 50 mm thick reflective insulation with each reflective surface facing a large internal air space was calculated to be 2.379 m^{2} ^{o}C/W.

It was observed from the two calculations, even assuming that no heat transfer took place across the insulation due to radiation and convection, that the thermal resistance was lower than the tests described in Sections 2.4.1 – 2.4.4. The thickness of the insulation used for these calculations was 50 mm **[46]**.

2.4.6 The Thermal Performance of Multi-foil Insulation, BRE Scotland

This paper describes in-situ thermal tests on wall, floor and roof structures that contained multi-foil insulation. The results were then compared to existing values that are quoted for multi-foil insulation. These tests were done to clarify the conflicting opinions that exist in industry today. The insulation being tested was TRI-ISO Super 9.

The manufacturer of this insulation commissioned a report from a testing body known as TRADA Technology Ltd and it stated that "*TRI-ISO SUPER 9 had insulating properties equivalent to 200 mm of glass wool insulation. This provides thermal equivalent of an overall thermal resistance of 5* m^2 $^oC/W$".

The tests were carried out in accordance with ISO 9869 with the use of heat flow meters 100 mm in diameter. The tests took place in two separate locations. The first test took place on the walls of a Victorian flat that was dry lined with the insulation in Torry, Aberdeen. The second test took place on the roof and also on the floor of a temporary classroom in Alloa, Clackmannanshire. Starting from the inside and working out, each construction comprised of the following:

1. **External wall construction, Torry**

   12.5 mm plasterboard/25 mm unventilated cavity/ TRI-ISO/ 25 mm unventilated cavity/ Granite.

2. **Flat (low-pitch) Roof construction, Alloa**

   Plaster board/ 430 mm unventilated roof void/ TRI-ISO/ 15 mm slightly ventilated airspace/ Plywood/ Marleydek roof membrane.

3. **Floor construction, Alloa**

Chipboard/ 15 mm unventilated airspace/TRI-ISO/ ventilated under-floor.

The results for the tests are summarised in Table 2.2.

Location	Insulation	Measured U_m (W/m²K)	Estimated error in U_m (W/m²K)	Calculated U_c using R=5.0 m²K/W (W/m²K)	Ratio U_m/U_c
	Torry				
Wall 1	TRI-ISO SUPER 9® multi-foil insulation with adjacent airspace to each side	0.49	± 0.07	0.19	2.58
Wall 2		0.52	± 0.08	0.19	2.74
Wall 3		0.50	± 0.08	0.19	2.63
Wall 4		0.45	± 0.07	0.19	2.37
	Alloa				
Roof 1	TRI-ISO SUPER 9® multi-foil insulation with adjacent airspace to each side	0.85	± 0.13	0.19	4.47
Roof 2		0.76	± 0.11	0.19	4.00
Floor 1	TRI-ISO SUPER 9® multi-foil insulation with unventilated adjacent airspace to warm side and ventilated underfloor space to cold side	0.43	± 0.06	0.19	2.26
Floor 2		0.48	± 0.07	0.19	2.53

Table 2.2: Measured U-values and Calculated U-values - Summary of Results **[47]**

2.4.6.1 Test Results - Torry, Aberdeen

Table 2.2 shows the results for the four walls tested in Torry. The third column (Measured U_m) displays the results from the heat flow meter tests. These U-values ranged from 0.45 W/m^2 ^{o}C to 0.52 W/m^2 ^{o}C. The error estimation of each of the heat flow meter tests are shown in the fourth column. The fifth column (Calculated U_c), displays the results of a calculated U-value (U_c). The values used in the calculations were obtained in accordance with BS EN IS0 6946, but the R-value of the multi-foil insulation was assumed to be 5 m^2 ^{o}C /W. It was found that there were significant differences between the calculated U-values and the measured U-value as can be seen in the last column where the ratio of the measured U-value against the calculated value are shown.

At the time of the in-situ tests, inspection of the installation was not possible. It was

inspected some time later and the installation of the multi-foil was found to be fitted correctly. The conclusion for this test was that the thermal resistance for the in-situ tests were significantly less than the calculated results (assuming that multi-foil had a thermal resistance of be 5 m^2 $^oC/W$). An average U-value of 0.49 W/m^2 ^oC for the four tests was taken and the calculation procedure was worked back to find that the resistance of the multi-foil insulation was estimated at 1.72 $m^{2o}C$ /W. This value was in excellent agreement with the tests that were carried out by the NPL.

2.4.6.2 Test Results - Alloa, Clackmannanshire

The U-values for the flat roof and the floor were measured and are shown in Table 2.2. The floors had a ventilated under-floor space. The measured U-values of the floors were between 0.43 W/m^2 ^oC and 0.48 W/m^2 ^oC. The results of this test also found that the measured U-values were significantly less than the calculated values of 0.19 W/m^2 ^oC (assuming the insulation had an R-value of 5 m^2 $^oC/W$). Again, the measured results were in agreement with the NPL tests and not the calculated values.

In the roof construction, the insulation was laid on the outer surface of the rafters, before the roof deck was laid. This resulted in the air space between the roof deck and the outer surface of the insulation being smaller than the recommended gap. There was a 430 mm cavity adjacent to the inside surface of the insulation. The measured U-values were 0.85 W/m^2 ^oC and 0.76 W/m^2 ^oC. These values are not in agreement with the tests performed by the NPL. The authors of this paper reported that they were unable to inspect the installation of the insulation and suggested that the smaller air gap on the outer surface may have contributed towards the decrease in the thermal resistance for the roof in these tests.

2.4.6.3 Discussion of In-Situ Results

Table 2.3 shows the difference between the measured U-values (from the heat flow meter tests) and the calculated values when assuming the thermal resistance of the multi-foil insulation is 1.71 $m^2\,^oC/W$. It can be seen that these results are much closer to each other than the measured and calculated results in Table 2.2.

Location	Insulation	Um (W/m^2K)	Error (W/m^2K)	Uc (W/m^2K)	Um/Uc
	Torry				
Wall 1	TRI-ISO SUPER 9® multi-foil insulation with adjacent airspace to each side	0.49	± 0.07	0.49	1.00
Wall 2		0.52	± 0.08	0.49	1.06
Wall 3		0.50	± 0.08	0.49	1.02
Wall 4		0.45	± 0.07	0.49	0.92
	Alloa				
Roof 1	TRI-ISO SUPER 9® multi-foil insulation with adjacent airspace to each side	0.85	± 0.13	0.50	1.70
Roof 2		0.76	± 0.11	0.50	1.52
Floor 1	TRI-ISO SUPER 9® multi-foil insulation with unventilated adjacent airspace to warm side and ventilated underfloor space to cold side	0.43	± 0.06	0.49	0.88
Floor 2		0.48	± 0.07	0.49	0.98

Table 2.3: Measured U-values and Re-calculated U-values – Summary of Results **[47]**

This report found that the in-situ results were in good agreement with the tests that were carried out by the NPL on TRI-ISO insulation, and not in agreement with the tests on the same product that found the thermal resistance to be 5 $m^2\,^oC/W$. The work in this report was supported by the Office of the Deputy Prime Minister in the UK **[47]**.

2.4.7 ALBA Thermal Performance Appraisal of TRI-ISO Super 9

This study was conducted by Alba Building Sciences Ltd to assess the thermal performance of ACTIS TRI-ISO Super 9 in two separate apartments, in the same apartment block, in Torry, Aberdeen, Scotland. Alba Building Sciences are building

performance consultants and are members of the United Kingdom Thermography Association **[49]**. This report was done at the request of ACTIS Insulation UK and took place over a seven day period commencing on the 25th January 2006.

Two external walls were examined in two different apartments, 141b and 139a. Starting from the outside, the composition of both apartment walls were as follows:

1. **Torry Apartment – 141b**

   530 mm Granite External Wall/100 mm air gap/TRI-ISO Super 9/25 mm air gap/12.5 mm plasterboard

2. **Torry Apartment – 139a**

   300 mm Granite External Wall/100 mm air gap/ TRI-ISO Super 9/25 mm air gap/12.5 mm plasterboard

The air gaps were created by using timber battens as spacers. The heat flux through each wall was measured using an Alba Genius Device and temperature sensors monitored the inside and outside temperatures of the walls. No technical details were available for the device. Using data that was collected over a number of days, a heat transfer coefficient for each wall was calculated. Thermography was also used in the same part of the walls where the Alba Genius Device was used. Figure 2.22 shows this equipment in place on one of the walls. A picture of the external wall is also shown.

Figure 2.22: Alba Genius Device used to measure U-value of a Wall **[48]**

2.4.7.1 Test Results

The U-value for the apartment walls was found to be 0.446 W/m^2 ^{o}C for apartment 139a and 0.259 W/m^2 ^{o}C for apartment 141b. The report accounted for the difference between the two values in the thermography results. These results showed some cold spots in both walls, but found more for the wall in apartment 139a. A thermal image for both test areas is shown in Figures 2.23a and 2.23b, illustrating the cold air leakage was greater in apartment 139a. The report concluded that possible cold air infiltration occurred through both the multi-foil insulation test walls due to poor installation procedures and warned that incorrect installation would hamper the performance **[48]**.

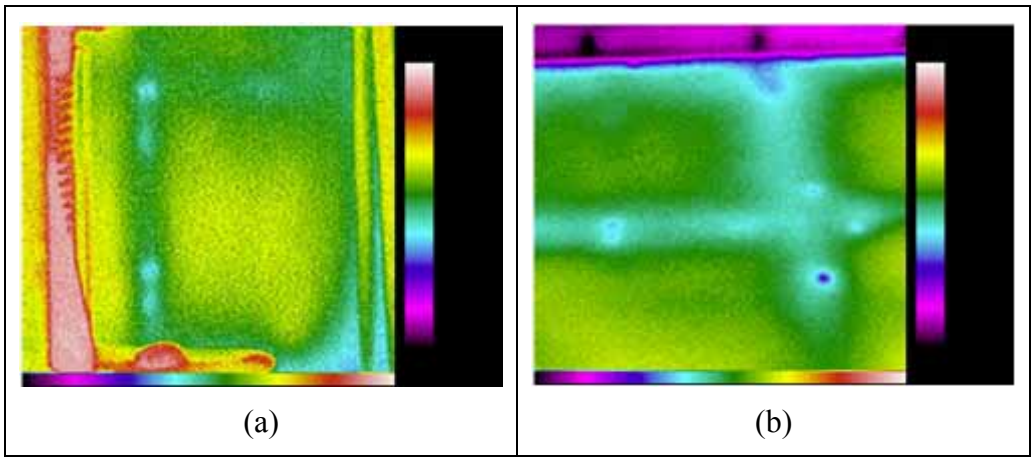

(a) (b)

Figure 2.23: a, b - Thermal Image of Apartments 141b and 139a **[48]**

2.4.8 ASA (Advertising Standards Authority) Adjudication

The Advertising Standards Authority (ASA) in the UK recently made adjudication on the thermal performance of ACTIS TRI-ISO Super 9 Multi-foil insulation. A complaint was made concerning a brochure that was released by ACTIS in 2005. The complaint challenged the claim that the insulation was "Thermally equivalent to 200 mm of mineral wool" and quoted thermal resistance of "RT = 5". The claim was based on tests that were conducted and certified by BM TRADA in Limoux in France in early 1997.

The adjudication found that the building was not representative of a real building and found evidence that the mineral wool was not installed properly which would lead to poor performance. ACTIS maintained that TRADA were aware of the issues and that the problems had been rectified. The adjudication, however, did not find sufficient evidence in the test report to show that the problems had been addressed.

The adjudication also understood that the claim "RT = 5" was a symbol of thermal resistance and had the units of $m^2\ ^oC/W$. ACTIS agreed to include the units in future publications. The ASA used a field expert to examine the test report and from the recorded test data, the expert found that the thermal resistance of the multi-foil could be estimated between 1.6 $m^2\ ^oC/W$ to 1.8 $m^2\ ^oC/W$ and not 5 $m^2\ ^oC/W$. ACTIS did not agree with these findings. The report also noted that ACTIS have stopped advertising TRI-ISO Super 9. ACTIS maintain this was because "it has been replaced by their new product TRI-ISO Super 10" **[50]**.

2.4.9 Multi-foil Research Conclusions

Two types of tests for multi-foil insulation were described in the previous sections. One

type of test was to compare the performance of multi-foil with 200 mm of glass wool by recording the power usage to maintain a pre-determined temperature inside a structure. Table 2.4 shows a summary of the first type of tests.

Location	**Power Usage for Multi-foil kWh**	**Power Usage for 200 mm Glass Wool kWh**	**Average Result**
TRADA UK **[40]**	-	-	Multi-foil equivalent to 210 mm of glass wool
IBP Germany [**42]**	747	749.5	Multi-foil used 0.2% more power than 200 mm glass wool
SFIRMM France [**43]**	666	930	Multi-foil Used 28.4 % less power than 200 mm glass wool
Sheffield UK 1 **[37]**	-	-	Multi-foil Used 26% less power than 200 mm glass wool
Sheffield UK 2 (Three tests @ Different temperatures) [**38]**	152.5 120.8 92.3	198.0 116.0 74.0	**Best result**: Multi-foil used 39.8 % less power than 200 mm of glass wool. **Worst Result**: Multi-foil Used 2.8 % less power than 200 mm of glass wool

Table 2.4: Summary of Comparative Tests Reviewed

In the second type of tests, the thermal characteristics of the test elements were directly measured and a thermal resistance was calculated from those tests. Table 2.5 shows a summary of those test results.

Location	**Test Specimen**	**Average Thermal Resistance ($m2^o$ C/W)**
BRE Tests UK (in-situ) **[47]**	Walls With Multi-foil Roofs With Multi-foil Floors with Multi-foil	2.04 1.24 2.2
Alba Tests, UK (in-situ) **[48]**	Wall with Multi-foil Wall with Multi-foil	2.24 3.86
NPL Tests UK (Laboratory) **[45]**	Unventilated Multi-foil with air cavity	1.71

Table 2.5: Summary of Calculated Tests Reviewed

The test results fell into two categories. All the comparative tests suggested that multi-foils with an air cavity on either side had a thermal resistance of at least 5 m^2 $^oC/W$. These values were based upon the fact that glass wool has a widely accepted thermal conductivity of 0.04 W/ m^oC. and that a 200 mm thick sheet of glass wool would have a thermal resistance of 5 m^2 $^oC/W$. Where the multi-foils performed better than the glass wool, it was suggested that the thermal resistance was even greater. The tests conducted by ALBA building consultants aimed to show that the thermal performance of multi-foils is highly dependent on the installation of the insulation. The test methods used for all these tests are not standardized or recognized by the EN ISO standards. The tests conducted by the NPL and BRE were in good agreement that the thermal resistance of multi-foil (with an air gap either side) was approximately 1.71 m^2 $^oC/W$. They both used

recognised and standardised testing apparatus and procedures for these tests.

The manufacturers of multi-foil accept the results of the standardised tests but maintain that the testing methods are not suited to multi-foil as they "do not take into account temperature variation, changes in humidity and the impact of real life conditions such as wind, sun and rain have on the thermal performance of the material". The test described in Section 2.4.1.2 detailed a steady state test performed in a laboratory where all conditions were kept constant; this test found that multi-foil performed better that 200 mm of glass wool which had a thermal resistance of 5 $m^2\,^oC/W$. This result was in good agreement with the other field tests conducted where the multi-foil was tested in real weather conditions.

2.4.9.1 Multi-foil Certification

At present, the prescribed way to certify multi-foil insulation with an EU national accreditation service certificate, is to test the material in accordance with BS EN 8990 (Hot Box testing), BS EN 12664 or BS EN 12667 (Hot-plate testing) **[3], [51].** Multi-foil is better suited to Hot Box testing as it can be tested with an air gap either side of it. In 2006, the UK Building Regulations were updated and made particular reference to multi-foil insulations. Paragraph 11 of AD L1b of these regulations stated that "U-values must be calculated using the methods and conventions set out in the 2006 version of BR 443" **[80]**. BR 443 stated that multi-foil must be tested by a "Notified body accredited for thermal testing by an EU national accreditation service" **[51].** This meant that multi-foil insulations would not be accepted as having a thermal resistance of around 5 $m^2\,^oC/W$, and that the field tests and certifications such as the BM TRADA certificate would not be recognised by the UK Building Regulations.

As a result of this change in the regulations, ACTIS Insulation were successful in bringing a case against the DCLG (Department for Communities and Local Government) in the UK for the publication of the BR443 document. In November 2007, a judgment found it unfair that the DCLG did not consult with multi-foil manufacturers when adapting the building regulations and found that it would damage the multi-foil industry. As a result of this judgment, Local Building Authorities in the UK can now use their discretion in allowing other test methods to be accepted under the building regulations while the regulations are being re-assessed **[52]**.

It is not clear what the outcome of this amendment to the building regulations will be. It does offer a reprieve for the multi-foil industry but does not offer any guarantee that their method of testing will be accepted. The members of the Confederation of Multi-foil Manufacturers (CMM) are currently working with the European organisation for Technical Approval (ETA) to establish a specific test method for multi-foil insulation **[53].**

Thinsulex insulation is the only multi-foil insulation that has BBA certification (British Board of Approval.) This insulation was tested using the Hot Box method, a procedure that is recognised by EU National Accreditation Service. The tests showed that Thinsulex had a thermal resistance of 1.69 $m^2\ ^oC/W$ when installed with an air gap on either side. Thinsulex can meet the Building Regulations if it is used in conjunction with other insulations. This certificate ensures that all local building authorities can use this insulation **[54].**

After studying the thermal performance of multi-foil insulation, it was noted that in all the tests that claimed a thermal resistance of approximately 5 $m^2\ ^oC/W$, the multi-foil

had been compared with glass wool insulation. It is difficult to achieve a consistent thickness when using glass wool as it is a loose-knitted material which is easily compressed and stretched. This would imply that the thermal resistance of glass wool would not be uniform. As fibre glass works by trapping air within the fibres, it is important that a layer of plastic is used to stop mass air transfer from one side of the insulation to the other. Any perforations or punctures in the plastic sheeting would also lead to reduced thermal performance. Comparing multi-foil with a rigid insulation would alleviate the possible problems with glass wool as it has a constant thickness, a stable thermal conductivity and is not porous. For these reasons, it was decided to avoid using a fibrous form of insulation for the purposes of testing in this research.

CHAPTER 3 HOT BOXES

3.1 Introduction

Through consultation with the sponsors of this project, it was decided to design a test facility, based on the Hot Box method and to test the Eco-quilt multi-foil insulation. This section details the design of various types of Hot Box.

3.2 General Information on Hot Boxes

The primary purpose of a Hot Box is to test the thermal properties of a particular material or a composition of materials. This is achieved by trying to quantify the total heat flow through the material. After obtaining this information, it can be converted into a heat transfer coefficient or a U-value for that material **[55]**.

There are many different designs of Hot Boxes used around the world. These different designs can generally be split into two groups; Guarded Hot Box (GHB), and a Calibrated Hot Box (CHB). There are other types of methods being used in the Baltics, but they are not widely used and are changing their approach to suit the CEN standards **[55]**.

Hot Boxes are commonly used to measure building envelopes with a composition of different materials such as cavity walls **[56 - 60].** Even though the individual thermal properties of a composition might be known, aspects such as thermal bridging **[61 - 63],** heat transfer by convection and radiation inside the composition need to be physically tested to obtain a thermal resistance for the whole test specimen. Hot Boxes are also frequently used to test window structures **[64 - 66]**. By controlling the relative humidity

and the temperature on either side of the test specimen, moisture transfer within building envelopes can also be tested **[67]**. With the use of computer modelling, Hot Boxes are often used to validate the thermal properties of building components that have been calculated **[68]**.

3.3 Calibrated Hot Box (CHB)

One of the earliest CHB to be built was in the 1970's **[69].** CHBs can vary in their design from the more conventional CHB **[70]** (similar to Figure 3.1) to the Hot Box built by Mamow **[71]**. Figure 3.1 shows a cross section of a simple CHB. The CHB consists of two chambers, the metering box (also referred to as the indoor chamber or hot side) and the cold side (can be referred to as the outdoor or environmental chamber) **[72]**. Both chamber walls are made from a material with a very high thermal resistance. The walls are made very thick to try and keep the heat loss to the surroundings at a minimum. This has to be the case as the energy flow, through the test specimen, from hot to cold is being measured; therefore, major losses would lead to inaccuracies.

The test specimen is fixed into the surround panel that is located between the two chambers. This is also made from a highly resistive material. The thickness of the surround panel varies according to the standard the Hot Box adheres to.

As suggested in the name, the Hot Box has to be calibrated with a test specimen of known U-value in order to calculate all the losses to the surrounding environment **[55]**.

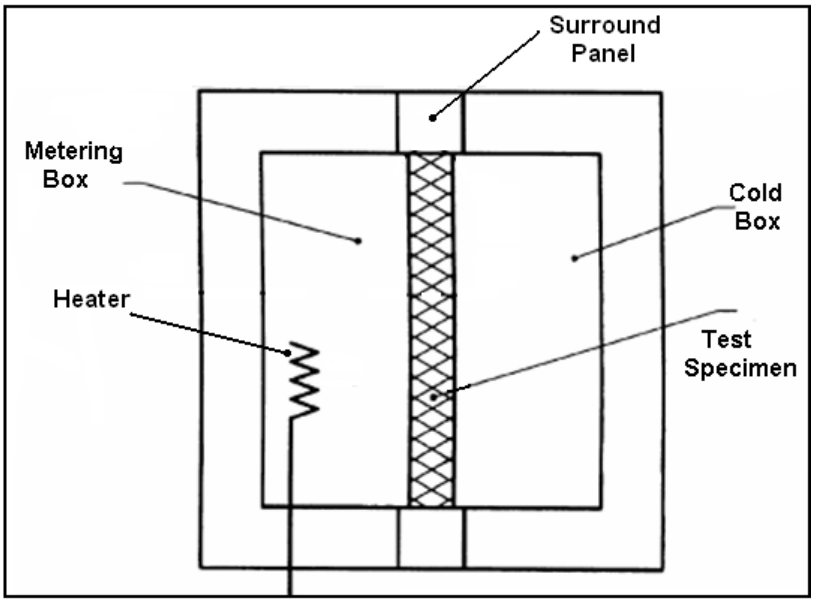

Figure 3.1: Calibrated Hot Box **[6]**

3.3.1 Case Study: Design and Calibration of a Rotatable Thermal Test Facility

This paper describes the design, building, instrumentation and preliminary calibration of the testing facility. One unique aspect to this paper is that it describes a rotatable facility and it gives a detailed description of how a frame was constructed in order to make the Hot Box rotate. This rotatable CHB was built from early 1979 to late 1981 at the University of Massachusetts at Amherst. The total cost of the testing facility amounted to approximately $100,000 **[73]**.

The CHB was designed to measure the heat transfer through various specimens. The heat transfer was found by measuring the input power of the metering chamber. The heat transfer through the metering chamber walls and the flanking losses around the perimeter of the specimen were taken into account. Calibration runs on different calibration panels produce these values. The losses through the metering walls were minimised by using polyiso foam insulation.

The rotatable CHB was designed to provide horizontal through vertical testing. In each hot and cold chamber, a small fan in a sheet metal duct drives the air. This in turn is connected to a linear air diffuser that distributes the air evenly between the baffles and the test specimen. The baffles are painted matt black so that the test specimen sees a high emittance low reflectivity surface. An open wire electric coil in the metal duct heats the warm air. The cold air circulates in the opposite direction as the warm air is cooled by an evaporator freezing coil.

The walls of each chamber are covered with eleven layers of one inch thick foam. These were glued together using construction adhesive and subjected to heavy weights to improve the contact. The walls were then attached to an internal wooden frame, constructed of lengths of 50 mm x 4 mm wooden batons. A diagram of the CHB is shown in Figure 3.2.

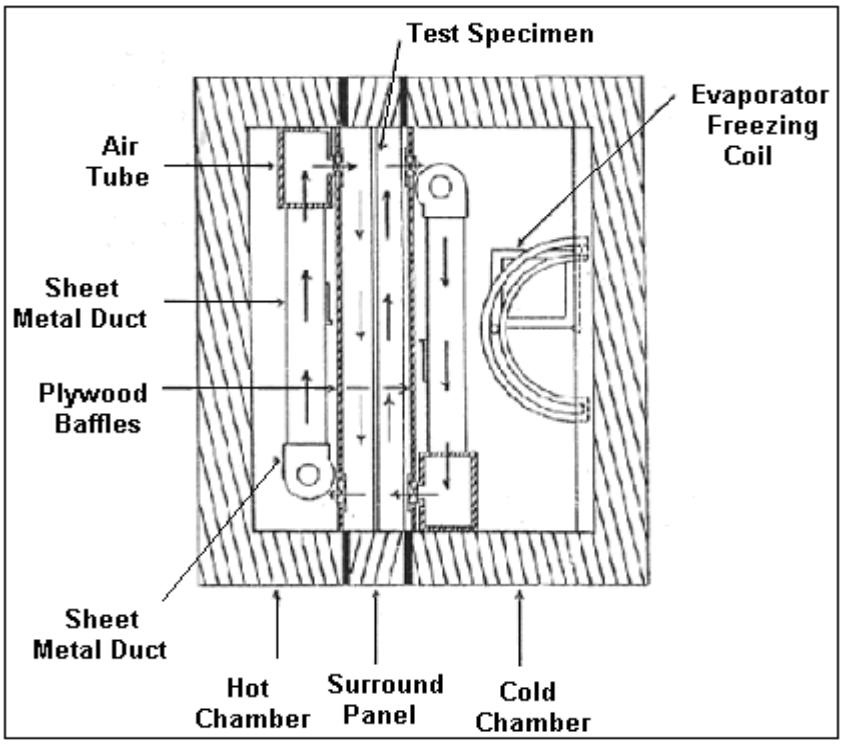

Figure 3.2: Schematic of CHB Test Facility **[73]** (Reference adapted)

The primary objective of the metering chamber is to provide a controlled temperature and to enable parameters such as wind velocity and heat transfer through the specimen to be measured. When steady state is reached the input power to the metering chamber is equal to the heat transfer through the test specimen minus the losses. These losses are found through calibration tests, and, as this is a CHB, there is no guard area and the heat loss through the walls of the apparatus must be accounted for.

The outer dimensions of the hot side are 3.04 m x 3.04 m x 0.76 m deep externally and 2.43 m x 2.43 m x 0.45 m deep internally. The external surface of the box was covered with 12 mm plywood to add rigidity to the box. All the joints were caulked to seal the metering chamber. A diagram of the metering chamber is shown in Figure 3.3.

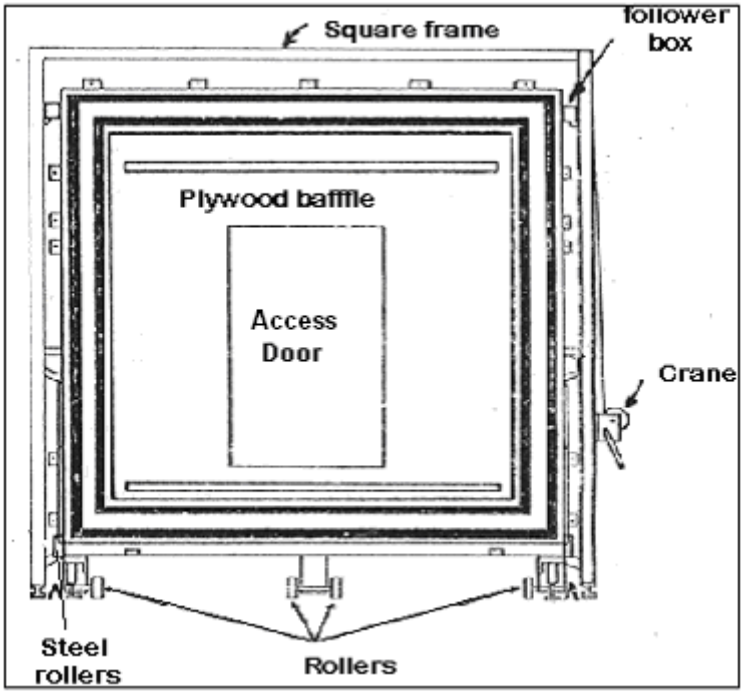

Figure 3.3: Hot Chamber **[73]** (Reference Adapted)

As the weight of the metering chamber was considerable, a rocker frame was built to hold the metering chamber in place when in the vertical position and when rotation was

taking place. The rocker frame was supported by two adjustable steel stands. These were only used when the apparatus was in the vertical position. There were also four steel rollers that acted as a guide and a support when the hot side was rotated. These rollers travelled along v-shaped tracks at the back of the hot side.

The crane mechanism provided the force to rotate the hot side. The square frame was constructed with an aluminium I-beam and was permanently bolted to the floor. Two pulleys were used to rotate the hot side and were located at the top of the frame. A steel chord fixed to one side of the frame passes through these pulleys and two follower boxes that are connected to the hot side. The follower boxes were constructed with two steel plates with plastic rollers and provided easy sliding into the slots in the aluminium frame. These slots, in the aluminium frame, are used to halt the rotation of the box at a given angle. Schematics of the crane mechanism are shown in Figures 3.4 and 3.5.

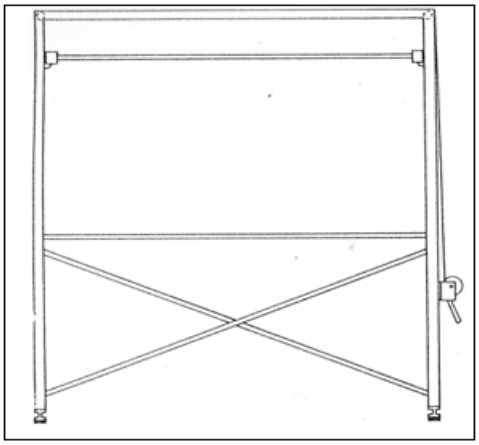

Figure 3.4: Crane Mechanism Square Frame **[73]**

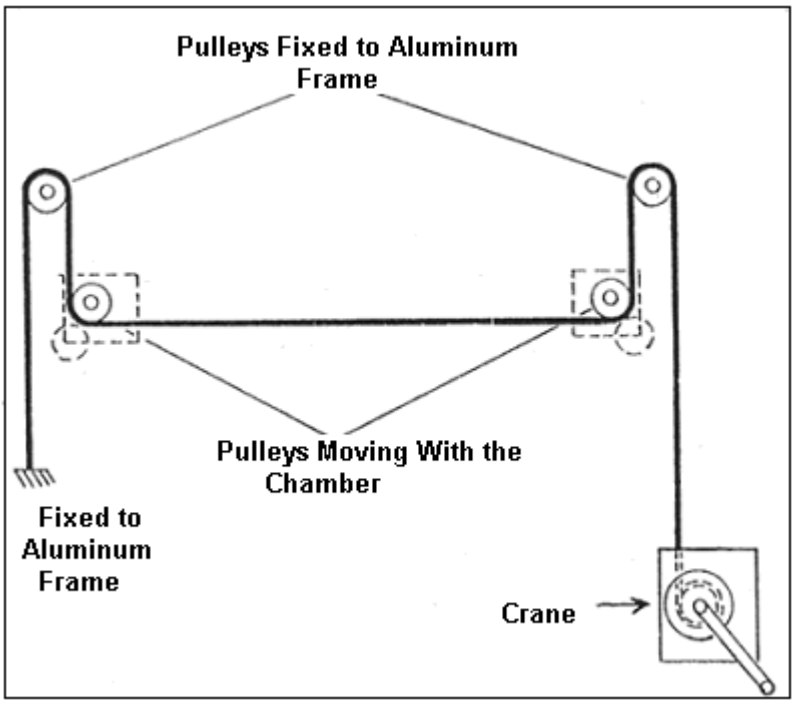

Figure 3.5: Operation of the Crane Mechanism **[73]** (Reference Adapted)

The climatic chamber is where the rotatable part of the CHB lies and was constructed similarly to the hot chamber. The power input to the refrigeration system did not have to be measured as the temperatures were held to a constant value.

The external dimensions of the cold chamber were 3.1 m x 3.1 m x 1.2 m and the internal dimensions were 2.4 m x 2.4 m x 0.9 m. The cold side of the chamber was deeper than the hot side because the refrigeration system had to be placed in the cold side. A steel frame around the perimeter supported the chamber. This frame was bolted to the rotating hubs that are on either side of the chamber. These hubs allowed the chamber to be rotated 360^{o} about its axis. The hubs were welded to follower boxes that slid up or down the uprights on either side. Schematics of the cold chamber are shown in Figure 3.6.

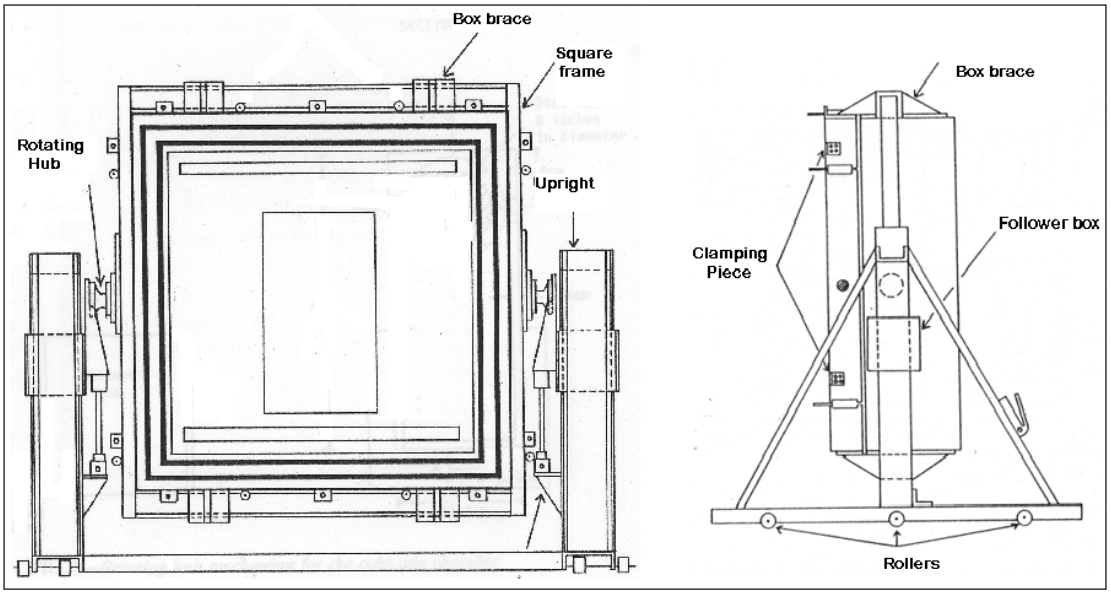

Figure 3.6: Cold Side **[73]** (Reference adapted)

The function of the surround panel is to hold the test specimen in place and also to provide high resistance perimeter insulation. The surround panel walls were constructed with the same material (poyiso) that was used to insulate both chamber walls. The surface that the specimen fits into is in contact with reinforced fibre glass plastic. This has a higher thermal conductivity than the polyiso, but the reinforced fibre glass plastic is more durable. The CHB must be calibrated each time the orientation of the Hot Box changes as the losses may not be the same as before **[73]**. The location of the surround panel is illustrated in Figure 3.2.

3.4 Guarded Hot Boxes (GHB)

The first GHB was built in the late 1930's to test over 120 different wall configurations **[69]**. The main difference between this and the CHB is that the GHB has a metering box inside a guard box. This reduces the heat loss through the metering box to a minimum as the metering box and the guard box temperatures are kept the same **[55]**. This is

shown in Figure 3.7.

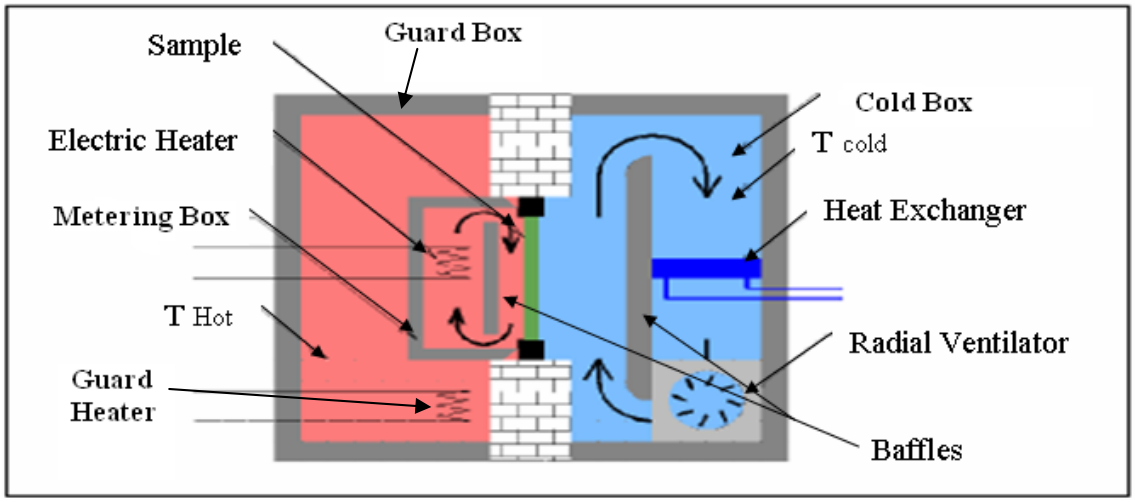

Figure 3.7: Guarded Hot Box **[74]** (Reference adapted)

The CHB is, in the main, better suited to testing full-scale systems since they measure total heat transfer through a complete test specimen. GHBs can test the centre portion of larger assemblies **[75],** and it is more accurate as it has fewer losses to the environment. One problem with the GHB is that it takes smaller test specimens than the CHB, (for the same exterior size) because of the extra enclosure on the hot side of the box. The costs to build these would generally be the same, as the cost of having very thick walls for the CHB would approximately be equal to the cost of constructing an extra wall in the GHB. Figure 3.7 is a conventional GHB design and is similar to the Hot Boxes described by Versluis **[76]**, Kosney **[77]** and Nussebaumer **[78]**. A GHB built by the National Research Council Canada **[79]**, to test skylight windows, shows that alternative designs can be used when building GHBs.

3.4.1 Case Study: University of Ulster Guarded Hot Box

The author visited this testing facility in November 2006. As part of this research, a

Guarded Hot Box was built to test the insulating properties of evacuated glazing, and the research was completed in 2002. This GHB was built in accordance with BS EN ISO 8990. Figure 3.8 shows a cross-section of the GHB **[80].**

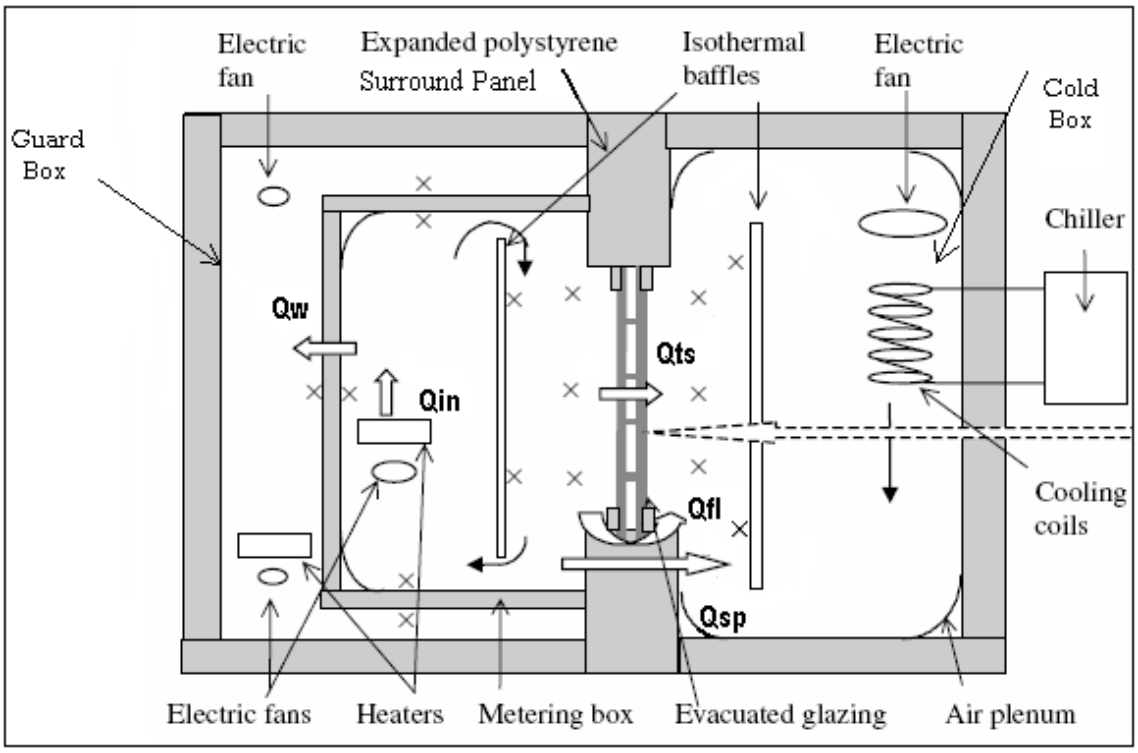

Figure 3.8: Cross-section of GHB **[81]** (Reference adapted)

The metering box was constructed from plywood and its inner dimensions were 1600 mm high x 1600 mm wide x 550 mm deep. A 20 W DC heater and electric fan was used to heat the metering box. These two components can affect the uniformity of the temperature inside the metering box because of their radiative exchange with the box walls. To eliminate this risk, a 1100 mm x 1100 mm x 2 mm thick baffle was installed parallel to the test specimen as shown in Figure 3.8. A smaller baffle was installed behind the DC heater. The thermocouples (marked with an x in Figure 3.8) were all connected to a 64-channel Data Logger that recorded all the temperatures in the Metering Box. A rubber sealant was fixed around the perimeter of the metering box to

achieve air tightness.

The guard box was built to reduce the heat flow through the metering box walls to a negligible level. Inside the guard box, four electric fans were installed to eliminate stagnant air pockets, along with a 60 W AC electric heater to heat the guard box. The guard box heater was controlled with a custom-built PID (Proportional Integral and Derivative) controller that kept the air temperature difference between the metering box and the guard box to less than 0.1 ^{o}C. This resulted in heat transfer through the metering box walls close to 0 W. The guard box was constructed with sheets of 150 mm Styrofoam insulation.

The cold box provided controlled low temperature conditions between 0 ^{o}C and 5 ^{o}C. To achieve this, a 6 m long cooling coil was installed in the cold box and was connected to a chiller. Another 1100 mm x 1100 mm copper baffle was fixed parallel to the test specimen to avoid radiative exchanges between the specimen and the cooling pipes. A 40/60 mix with antifreeze and water was used in the reservoir of the chiller. A 20 W electric fan was mounted above the cooling coil to provide the air circulation. The air velocity over the specimen was measured to be 2 m/sec. All the thermocouples were connected to the 64 channel Data Logger.

The dimensions of the surround panel were 2400 mm x 2400 mm x 300 mm thick with a 500 mm x 500 mm aperture cut out for the test specimen to be inserted. The surround panel was constructed from Styrofoam IB insulation, a mass type insulation with a thermal conductivity of 0.033 W/m^{o}C and a density of 28 kg/m^{3}. Two moveable platforms were designed to support the GHB and to separate the cold side from the hot side when different specimens had to be placed onto the surround panel. All the

different enclosures were clamped together with ratchets and straps when thermal tests were being performed. The thermal testing facility is shown in Figure 3.9 **[80]**.

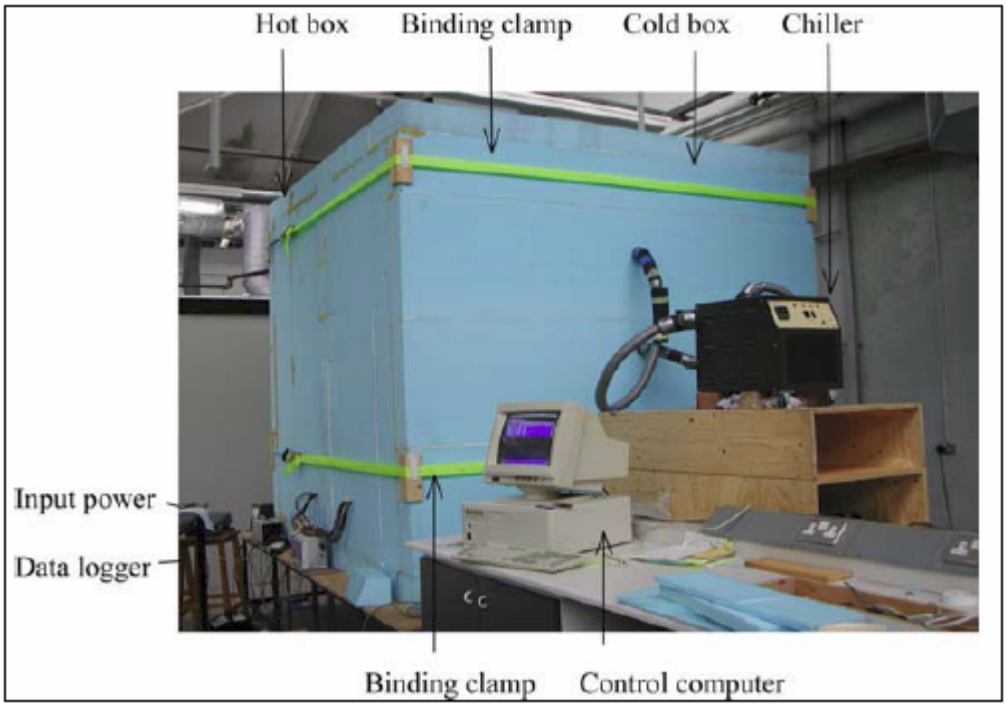

Figure 3.9: GHB at University of Ulster **[82]**

3.5 Wall and Edge Guarded Hot Box (WGHB)

This is a third type of Hot Box and is described as a combination of the GHB and the CHB. With this type of Hot Box, the metering walls are guarded with plate metal heaters in the wall of the hot side. This ensures that there is no temperature difference therefore, no heat transfer can take place between the inside surface and the outside surface of the metering box **[83].** This design can be the most accurate of all, but the control system is quite complex. It also requires highly skilled operators to perform the tests. This type of Hot Box was originally developed in the UK **[83]**.

3.5.1 Case Study: The National Physics Laboratory (NPL), Rotatable Wall and Edge Guarded Hot Box

A Rotatable WGHB was designed and built by the NPL to perform thermal tests on insulating panels, windows and door configurations as well as wall and roof structures. This Hot Box is an improved version of the original Wall Guarded Hot Box and retains all of its advantages. This WGHB was developed because it offered better control over the operating environment and is more compact than the traditional calibrated Hot Box.

The maximum size of the test specimen that the WGHB can accommodate is 2.4 m x 2.4 m x 0.15 m. The cold side temperature ranges from -20 ^{o}C to + 20 ^{o}C. The hot chamber has a maximum temperature of 35 ^{o}C. The minimum temperature of the hot chamber is limited to 3 ^{o}C above the surrounding room temperature.

In the original GHB, the primary function of the guard box is to reduce the heat flow through the metering box walls to a minimum. Although this system works, it reduces the size of the metering box, thus reducing the size of the test specimen. In the RWGHB, the two-box system is eliminated by controlling the temperature of the outside surface of the metering box to the same temperature inside the metering box. This means that there is now no guard area in the apparatus and that a larger test specimen can be used **[84]**.

This type of Hot Box was designed to be fully rotatable. This permits the RWGHB to be arranged at any orientation from the cold side horizontally positioned above the Hot Box, through the vertical position, to the hot side being located above the cold side. A photograph and a schematic of the apparatus is shown in Figures 3.10 and 3.11.

Figure 3.10: Photograph of NPL WGHB **[84]**

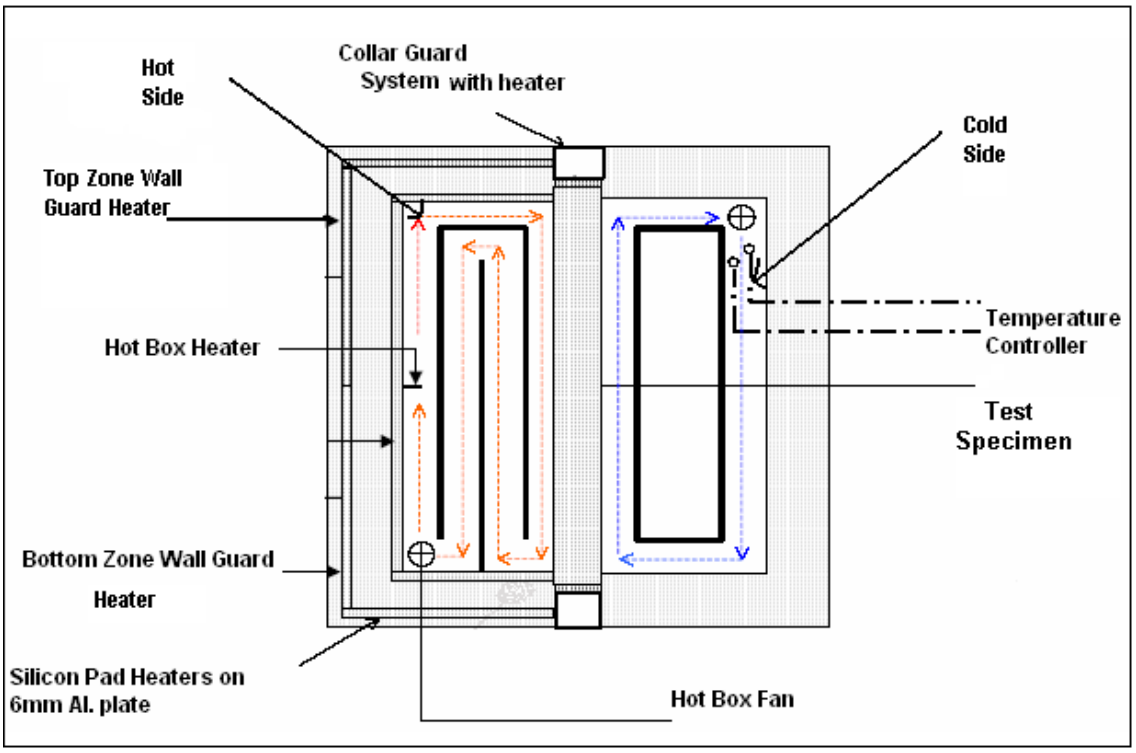

Figure 3.11: Cross-section of NPL WGHB **[84]** (Reference adapted)

The heaters on the wall guard are self-adhesive silicon heater pads. These are attached consistently around the edges that are made from 6 mm plate of aluminium. The temperature in the plates is controlled using a thermistor inserted into the one of the plates. The heater system is separated into different areas. The bottom area is controlled comparatively to the top area. Each area is independently heated and the temperatures are then matched. Heat flow meters are fitted into the Hot Box walls to measure the amount of heat flow through them with great accuracy.

The collar guard heater system is shown in the Figure 3.11. These are located all around the test specimen perimeter and are attached to the support panel. They comprise of heater strips that are connected to a 0.5 mm thick stainless steel plate and are attached close to the edge of the hot chamber. The opposite side of the stainless steel plate is gripped by a copper cooling fin that extends 75 mm into the cold box. This creates a temperature gradient for the edge guarding. Thermocouples are attached to the centre of the stainless points to establish the mean temperature. This system minimises losses from the edge of the test specimen to the surrounding room. The heaters are controlled to match closely the temperature gradient across the test specimen. This facility has a repeatability of 1.1 % and an uncertainty of +/- 3.6 % when measuring the thermal resistance of a homogeneous specimen **[84]**.

3.6 ISO Standards on Hot Box Testing

EN ISO 8990 *"Thermal insulation – Determination of steady state thermal transmission properties – Calibrated and Guarded Hot Box"* refers to the minimum requirements that are in place for the design and construction of a CHB or GHB. It also gives information on how the Hot Boxes should be calibrated and how to deal with losses

that lead to inaccuracies in the tests. It gives a description on how the test procedure should be carried out and a description of the apparatus needed to comply fully with the standard.

3.6.1 Hot Box Losses

As described earlier, there are two main types of Hot Box, the calibrated Hot Box and the Guarded Hot Box. Although they are quite similar, the losses that occur in each are different.

Figure 3.12 is a schematic of a GHB illustrating the losses that it can incur. Losses through the metering box are kept to a minimum by maintaining similar conditions in the guard box and the metering box. These conditions also minimise lateral heat flow parallel to the test specimen. In an ideal situation, when a homogenous test piece is in the test apparatus, the guard box and metering box temperatures are equal, and the cold side temperatures and the surface coefficients are uniform, a temperature balance for the air on both sides implies a state of equilibrium on the surface. This suggests that the imbalance heat flow rate parallel to the specimen and the heat flow rate through the metering walls are equal to zero. This means that the input power will equal the energy transfer through the test specimen. In reality, this is never likely to happen. This is referred to as an imbalance. A basic heat balance is shown in Equation 3.1 for the GHB that shows all the losses that can occur in this type of Hot Box.

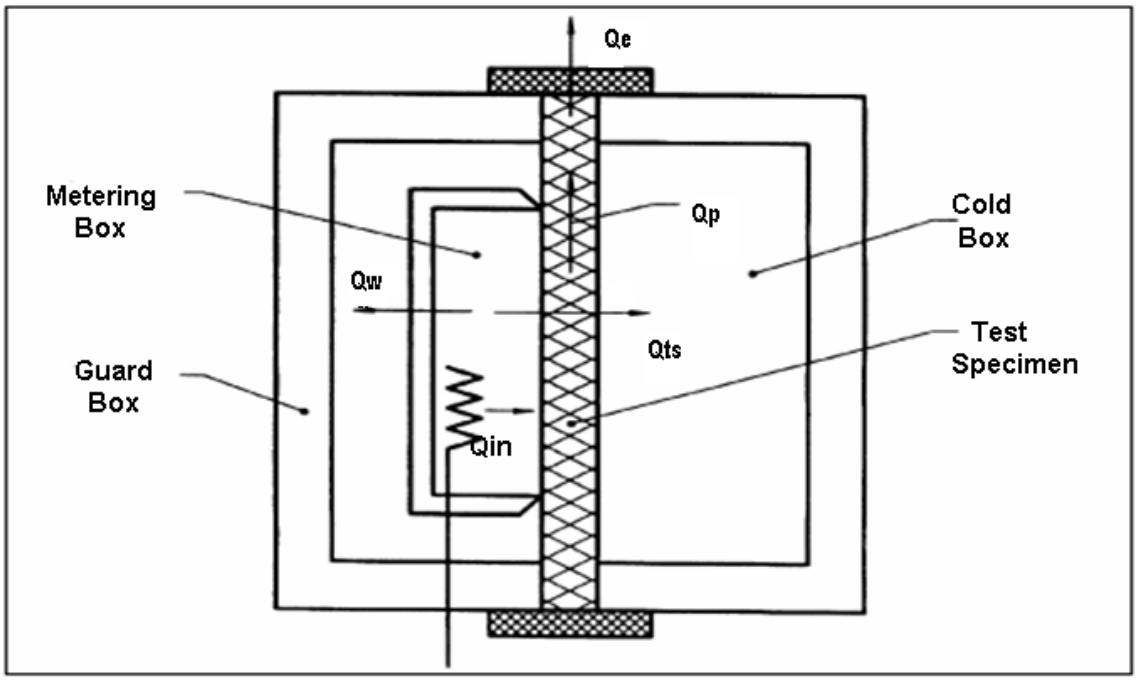

Figure 3.12: Guarded Hot Box Losses **[6]** (Reference Adapted)

$$Q_{ts} = Q_{in} - Q_p - Q_w \qquad \textbf{3.1}$$

Where;

Q_{in} = Total power input (W)

Q_{ts} = Heat transfer through test specimen (W)

Q_p = Heat transfer parallel to test specimen (W)

Q_w = Heat transfer through metering box walls (W)

As described earlier, the CHB is surrounded, on both sides, by a thick highly thermal resistive wall. This is to keep the losses through the metering box at a minimum. The total power input has to be corrected to accommodate for this loss. Another loss that occurs is the Flanking Loss, Q_{fl}. This is heat loss around the edges of the test specimen. A correction for this loss is found by calibrations on specimens with known thermal properties. When accounting for this loss, the known specimen should cover the same thickness and the same thermal resistance range of the unknown specimen. It should

also be tested over the same temperature range. The CHB losses are illustrated in Figure 3.13. Equation 3.2 shows a heat balance for CHB.

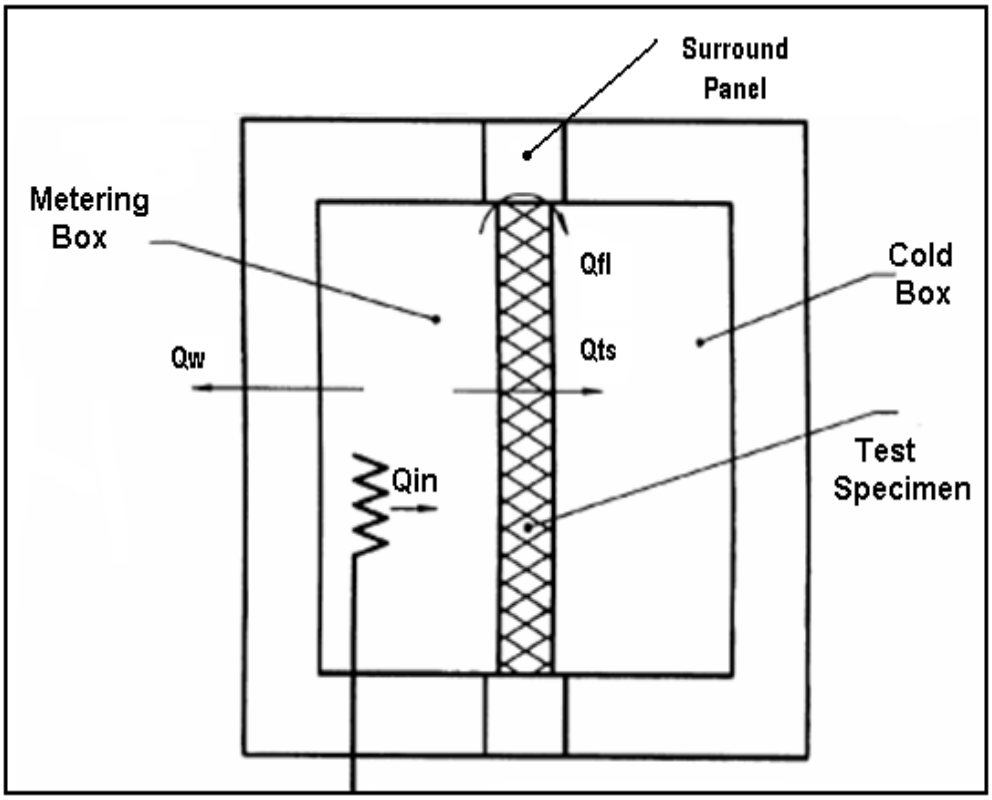

Figure 3.13: Calibrated Hot Box Losses **[6]** (Reference Adapted)

$$Q_{ts} = Q_{in} - Q_w - Q_{fl} \qquad \textbf{3.2}$$

Where;

Q_{fl} = Flanking loss heat transfer (W)

3.6.2 Calibration of Hot Box

By using calibration panels with known thermal properties, the losses in both Hot Boxes can be calculated or minimised to an acceptable level. In the GHB, the imbalance heat flow parallel to the test specimen can be made very small by keeping the temperature uniformity between the metering box and the guard box as close as possible, so that the

imbalance heat flow is negligible compared to the heat flow through the test specimen. Applying sufficient insulation to the outside of the test specimen can reduce the peripheral loss, Q_e in the GHB to a negligible level. By recording the temperature difference across the calibration panel (with known thermal properties) and the total power input, the losses for the metering box walls can be calculated using Equation 3.1. This principle can also be applied to the CHB where the metering box wall losses (Q_w) and flanking losses can be found using Equation 3.2. Surface temperatures are measured in such a way as not to affect the temperature of the surface at that point. This can be achieved by using thermocouples with a diameter less than 0.25mm, with at least 100mm of adjoining wire that is in thermal contact with the surface. Cement or tape with similar emissivity to the test specimen can be used to fix the thermocouple to the test specimen.

Once the losses have been accounted for, a specimen with unknown thermal properties can be tested. The thermal resistance of the specimen can be calculated using Equation 3.3.

$$R_{ts} = \frac{A_{ts}(\mathrm{T_{hot\ ts}} - \mathrm{T_{cold\ ts}})}{Q_{ts}} \qquad \textbf{3.3}$$

Where;

R_{ts} = Test specimen thermal resistance ($m^2\ ^oC/W$)

A_{ts} = Test specimen area (m^2)

$T_{hot\ ts}$ = Hot side test specimen surface temperature (^oC)

$T_{cold\ ts}$ = Cold side test specimen surface temperature (^oC)

For the thermal transmittance calculations, heat transfer into and out of the specimen through radiation and convection are taken into account. The radiation heat transfer is

dependent on the radiation exchange between the specimen and the surfaces seen by the specimen. Heat transfer by convection is dependent on the air temperature and the air velocity over the specimen. The thermal transmittance for a test specimen can be written as Equation 3.4.

$$U_{TT} = \frac{Q_{ts}}{A_{ts}(T_{n1} - T_{n2})} \quad \textbf{3.4}$$

The surface coefficients are expressed in Equations 3.5 and 3.6.

$$h_1 = \frac{Q_{ts}}{A_{ts}(T_{n1} - \mathrm{T}_{\text{hot ts}})} \quad \textbf{3.5}$$

$$h_2 = \frac{Q_{ts}}{A_{ts}(T_{\text{cold ts}} - T_{n2})} \quad \textbf{3.6}$$

Where;

T_{n1} = Metering box environmental temperature (^{o}C)

T_{n2} = Cold box environmental temperature (^{o}C)

U_{TT} = Specimen thermal transmittance (W/m^2 ^{o}C)

h_1 = Hot side test specimen surface coefficient (W/m^2 ^{o}C)

h_2 = Cold side test specimen surface coefficient (W/m^2 ^{o}C)

The concept of the environmental temperature, $T_{n,}$ combines the air and radiant temperatures used to calculate the thermal transmission. It is a calculated value and is a function of air temperatures, mean radiant temperatures, mean surface temperatures and the heat flux per unit area. Further reading on the environmental temperature can be found in this standard **[6]**. Hot Boxes built to this standard can achieve accuracies of +/- 5 % **[84]**. For more detailed requirements for standardised Hot Boxes, further reading is also found in References **[85]**, **[86]**.

3.7 Flanking Losses in Hot Boxes

To evaluate the specimen heat flow in a Hot Box, the heat input must be known and the losses accounted for. Originally, it was thought that all the losses occurred through the metering walls and the specimen heat flow was calculated after that. Further developments showed that there was an additional loss between the metering chamber and the cold chamber that was occurring through the specimen frame (surround panel). This heat flow is called flanking loss and it is found during the calibration procedures. Flanking losses are mainly a function of air to air temperature difference between the hot and cold side and also the specimen thickness. Varying test specimen conductivity does not strongly affect the flanking loss **[87]**. Flanking losses always occur in the CHB because the test specimen comes into contact with the surround panel in the metering box. It only occurs in the GHB when the test specimen is smaller than the metering box area. This can be seen in Figure 3.8 (Ulster University), where the test specimen sits in the aperture of the surround panel in the metering chamber. Figure 3.12 shows a GHB where flanking losses (Q_{fl}) do not occur as the test specimen area is greater than the metering area.

Yuan **[64]** used test specimens (with known thermal properties) of different thicknesses, while maintaining the same air-to-air temperature difference, to calibrate a CHB for flanking losses. This CHB was used for testing window structures. Figure 2.38 shows a schematic of the CHB used. It can be seen that the test specimen is smaller than the metering area and a 102 mm thick surround panel holds the test specimen in place. A heat balance for the CHB is shown in Equation 3.7.

$$Q_{ts} = Q_{in} - Q_w - Q_{sp} - Q_{fl} \qquad \textbf{3.7}$$

Where;

Q_{sp} = Surround panel heat transfer (W)

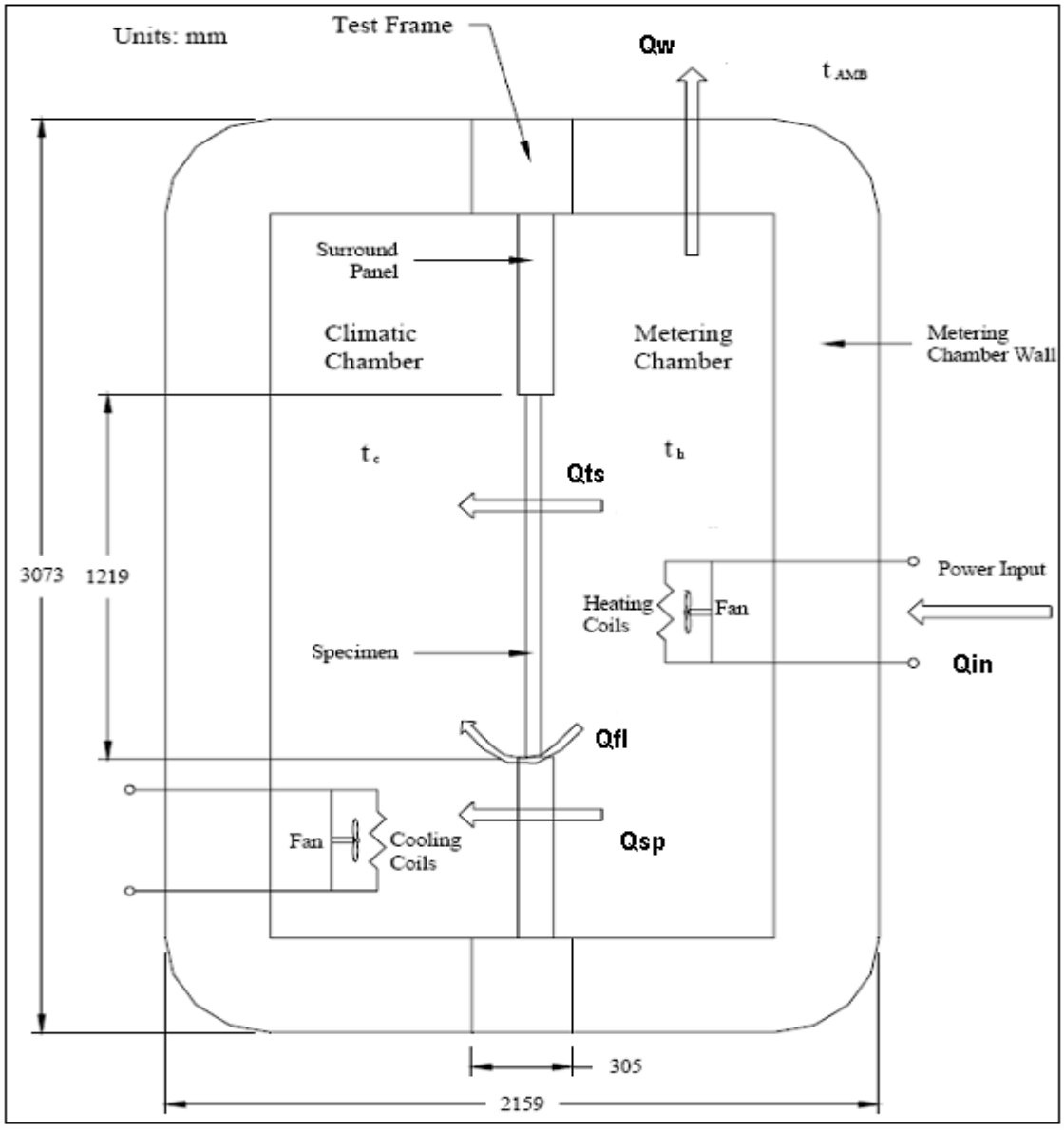

Figure 3.14: CHB Flanking Loss **[64]** (Reference adapted)

The wall losses and heat flow through the surround panel and test specimen were

known from previous calibration testing. The results for the flanking loss calibration tests are shown in Figure 3.15.

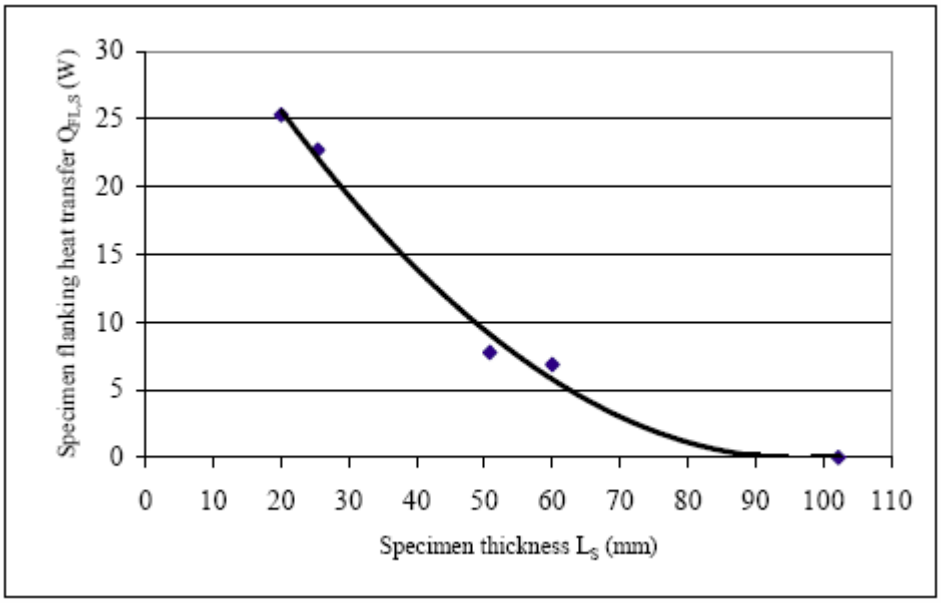

Figure 3.15: Flanking Losses v. Specimen Thickness **[64]**

It can be seen from Figure 3.15 that the flanking losses decrease with increasing specimen thickness. When the test specimen thickness is equal to the surround panel thickness, the flanking losses do not exist. A relationship between the flanking loss and specimen thickness was found through regression analysis and is described by Equation 2.8 **[64]**.

$$Q_{fl} = 40.798 - 08475(L_{ts}) + 0.0044(L_{ts})^2 \qquad (0 < L_{ts} < 102\ mm) \qquad \textbf{3.8}$$

Where;

L_{ts} = Test specimen thickness (m)

Tests were then conducted on a double glazed window, with a frame thickness of 68 mm. This thickness was used to calculate the flanking losses for the window (L_{ts}) in Equation 2.8. The thermal transmittance of the window was found to be 1.95 W/m^2 ^{o}C.

The heat transfer coefficient for the 60 mm calibration panel was approximately 0.45 $W/m^2\ ^oC$. Although there was a big difference between the thermal properties, this method showed that thermal conductivity does not have a big effect on the flanking losses and that when the air to air temperatures are held constant, the only other major factor influencing the flanking losses is the specimen thickness. This research was part of an inter laboratory project and this result was compared with other tests on the same type of window from different laboratories around Europe. All these tests achieved very similar results **[64]**.

3.8 Hot Box Research Conclusions

Three types of Hot Box were analysed before the design of the new testing facility took place. Standards on Hot Box design helped gain an understanding on the losses that occur in each type of Hot Box as well as the standardised calibration procedures for those losses. By reading case studies, knowledge on the different materials and equipment used to build Hot Boxes was gained. This information was used to help with the design of the new test facility.

CHAPTER 4 -TESTING FACILITY DEVELOPMENT

4.1 Introduction

There were two separate testing facilities used in this project. The design of the first test rig was based on the Calibrated Hot Box (CHB) and was developed prior to the current research. A series of tests were conducted with this test rig and the results can be found in Appendix A. On completion of these tests, the facility was evaluated, and based on this assessment, a new and more advanced test rig was designed and produced. This chapter describes the preliminary test rig and the design and construction of the new facility.

4.2 Preliminary Hot Box

Tests were carried out with this apparatus to gain an indication of the thermal properties of the multi-foil insulation. These tests took place between late January and early March 2007.

4.2.1 Description

Figure 4.1 shows the initial Hot Box prototype. The inside of the box acted as the hot side with the surrounding room acting as the cold side. The walls of the hot chamber were constructed with 80 mm polyiso insulation, with an inner and outer shell of 12 mm plywood to add stability to the box. The surround panel (that holds the specimen in place) was originally constructed with 80 mm polyiso insulation and supported with plywood on both sides.

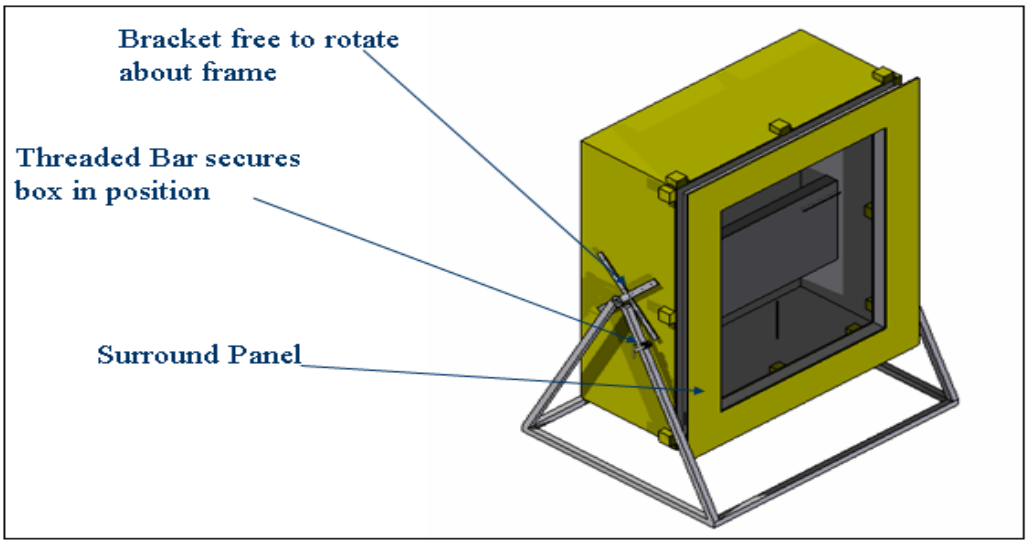

Figure 4.1: Preliminary Hot Box

A new surround panel was constructed to accommodate a thicker test specimen for the preliminary tests. The test specimen was fixed into the surround panel and sealed around its perimeter to ensure that no mass transfer occurred. A frame was constructed to keep the hot chamber off the ground and also to enable it to rotate through 360°.

Seven Type T thermocouples were used for temperature measurement. Six thermocouples were positioned inside the hot chamber, and one thermocouple was outside the hot chamber. These were used to monitor the air temperatures on both sides of the specimen during testing. A simple On-Off controller was used to regulate the temperature inside the box and was wired to a 100 W AC enclosure heater. A 12 W AC fan circulated the air inside the box to create a uniform temperature. A baffle was placed in front of the heater and the inside surfaces of the hot chamber were painted matt black to reduce radiative effects (from the heater) to the test specimen.

The temperature readings were captured by the data logger which recorded readings of

the thermocouples every minute. This was then outputted to an Excel spreadsheet. Kilowatt-hour meters recorded the power input to the Hot Box throughout the duration of the tests.

4.2.2 Testing Procedure

The calibration test determined the heat losses through the metering box walls and the surround panel. This was done by testing specimens with known thermal properties. If the thermal resistance of the specimen was known, the losses could be found by using the temperature differences across the specimen and the average power used during the test. These losses were then represented by a heat transfer coefficient for the box walls and surround panel.

4.2.2.1 Calibration Panel Tests

The inside of the hot chamber was heated to a set temperature and left for approximately 12 hours for steady state conditions to exist. Figure 4.2 illustrates a test specimen in the test rig. T1 represents the hot air temperature and T2 represents the cold air temperature. This results in a temperature gradient existing across the test specimen.

The hot temperature and cold temperatures were recorded during this period to ensure that they remained relatively constant. At the start of the testing the kilowatt-hour meters were switched on to record the power consumption (Q_{in}) into the hot side. Newton's Law of Cooling **[88]** was applied to the heat transfer across the test specimen in Equation 4.1 and also applied to a heat balance for the test rig as shown in Equation 4.3.

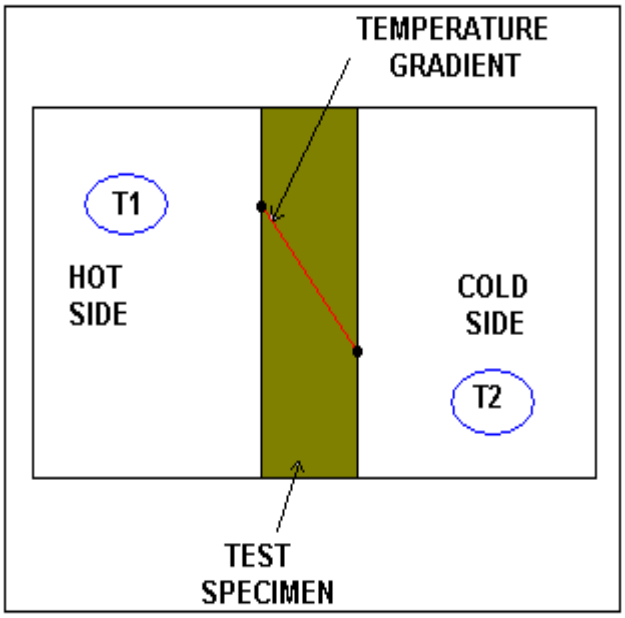

Figure 4.2: Temperature Gradient across Test Specimen

$$Q_{ts} = U_{TT} A_{ts} \Delta T_a \qquad \textbf{4.1}$$

Where;

ΔT_a = Air temperature difference (^{o}C)

As the temperatures being measured across the test specimen were air temperatures, a surface resistance at either side of the test specimen existed. These surface resistances were approximated using EN ISO 6946 **[93].** U_{TT} in Equation 4.1 is calculated as in Equation 4.2.

$$U_{TT} = \frac{1}{R_{s1} + R_{ts} + R_{s2}} \qquad \textbf{4.2}$$

Where;

$R_{s\,1}$ = Hot side surface resistance (m^2 ^{o}C/W)

$R_{s\,2}$ = Cold side surface resistance (m^2 ^{o}C/W)

A heat balance for the test rig is shown in Equation 4.3

$$Q_{in} = Q_w + Q_{ts} \qquad \textbf{4.3}$$

Re-arranging Equation 4.3 with the heat flow through the walls and surround panel as the subject of the heat balance gives

$$Q_w = Q_{in} - Q_{ts}$$

Substituting Equation 4.1 into 4.2 and applying Newton's law of cooling to Q_w gives

$$(UA)_w \Delta T_a = Q_{in} - (U_{TT} A_{ts} \Delta T_a)$$

Where;

$(UA)_w$ = Heat transfer coefficient for metering box walls per unit area (W/^{o}C)

All values were known except U_w. The heat transfer coefficient for the box walls was calculated using Equation 4.4.

$$(UA)_w = \frac{(Q_{in} - (U_{TT} A_{ts} \Delta T_a))}{\Delta T_a} \qquad \textbf{4.4}$$

4.2.2.2 Unknown Test Specimen

Once a heat transfer coefficient for the box walls and surround panel was found, a specimen with unknown thermal properties could be tested and a heat transfer coefficient for the unknown specimen could be computed. The heat balance for the test rig is shown in Equation 4.5, with the heat flow through the test specimen as the subject.

$$Q_{ts} = Q_{in} - Q_w \qquad \textbf{4.5}$$

Since the losses through the walls and surround panel were found from calibration procedure, Equation 4.4 could be used to solve for the test specimen thermal transmittance. This is shown in Equation 4.6. Possible errors associated with the specimen thermal transmittance are discussed in section 4.2.3.

$$U_{TT} = \frac{(Q_{in} - (UA)_w \Delta T_a))}{\Delta T_a A_{ts}} \qquad \textbf{4.6}$$

4.2.3 Limitations of Testing Facility

It was apparent from some of the preliminary tests conducted, and from observations made, that the test rig had some limitations. This was an important part of the research as it resulted in determining many of the design requirements that had to be employed in order for a new and better test facility to be built. The following is a list of possible errors that could be associated with the estimation of U_{TT}.

- Absence of a cold side
- Metering box wall errors
- Lack of equipment

It became apparent from an early stage of testing that a cold side to the Hot Box would be required. Successful testing would depend on the room temperature remaining relatively constant throughout the test. This proved to be problematic because of significant temperature differences between night and day. Many tests had to be delayed or cancelled due to this problem. Another problem that occurred was that the air velocity across the surface of the cold side of the test specimen could not be kept constant for the duration of the test. The absence of a cold side also allowed radiation from hot surfaces (such as roofs heated by the sun or through windows) in the surrounding room to interact with the surface of the test specimens. This led to inaccuracies as the environmental conditions could vary during and between tests.

Another possible source of error was that the metering box walls may have been

subjected to a change in room temperature during testing. This affected the temperature difference between the inside and outside of the walls which resulted in the box losses varying between the tests.

There were only seven thermocouples used to gather data from the test rig. More thermocouples would give better information and improved temperature profile inside and outside the test rig. Placing thermocouples on the surfaces of the test specimens and walls could give more accurate and accountable thermal resistances for them. Other factors also had to be taken into account and are discussed in Section 4.2.4.

4.2.4 Other Design Considerations

The following design considerations are discussed:

- Hot box size
- Health and safety
- Installation of measurement components
- Sealing of the Hot Box

This first step in the design process was to size the Hot Box. As the Hot Box was to be constructed in a different location to where the tests would be conducted, the apparatus had to be small enough to enable movement between locations. This was a constraint that affected the exterior dimensions and in turn affected the size of the test specimen.

The Hot Box was also designed so that it could be operated by one person. The surround panel, for example, would have to be manageable in terms of handling and ease of movement. In addition, the test specimens would have to be fixed into the surround panel with the minimum of effort.

The heating and measuring equipment, including the heater, fan and thermocouples, would need to be accommodated inside the Hot Box. Specified holes would have to be drilled through the walls to feed electrical connections to these components.

One major factor that would affect the success of the tests was sealing of the Hot Box. All the joints, inside and out, would require careful sealing so that no air would leak through the walls. Joints between the surround panel and the metering box, and between the guard box and the surround panel, would also have to be airtight. Another concern was the joint between the perimeter of the surround panel and the test specimen. All of these parameters were considered during the design process.

4.3 Design of Testing Facility

After studying the different methods and test rigs used in industry, the relevant ISO standards **[6] [85] [86]**, and the preliminary test rig, a testing facility was designed that was suitable for the type of tests conducted in this project. From the outset of this project, it was clear that not all of the conditions of the ISO standards could be met due to practical and budgetary constraints. The key to the design was to balance those constraints with the information received in the relevant standards and case studies and arrive with the best possible solution.

The Hot Box was designed with the aid of Solid Works. Solid Works is a drawing computer package which aids in the design of products and structures. Once a series of parts were drawn up they could be assembled together in a drawing. If certain parts did not fit into the assembly as intended, that part could be altered without making changes to the overall drawing. This was helpful in the design of the Hot Box as dimensions for

different parts were refined and finalised before construction took place. Possible difficulties in construction could also be seen before they took place.

4.3.1 Choice of Hot Box Type

The first step of the design process was to make a decision on which type of Hot Box to build. As discussed in detail in the literature survey, there are generally three types of Hot Boxes used for testing materials: Calibrated Hot Box (CHB), Guarded Hot Box (GHB) and Wall and Edge Guarded Hot Box (WGHB). The first stage of the design process was to decide which of the three Hot Box types the design would be based upon.

The WGHB is a design that is based on the CHB. This was the first design to be discarded because of the following points.

- Expensive to build.
- Silicon pad heaters are required on the outside perimeter of the metering chamber and heaters were required around the edges of the specimen. This was deemed overly complex to implement for the time frame allowed.
- A complex control system would have to be designed to cater for all the heaters.

After considering the benefits and disadvantages of both the GHB and the CHB, a decision was made to design the test rig based on the GHB. The deciding factor was based on analysis of the surrounding room in which the testing facility would be located. From performing tests with the preliminary test rig, it was noted that there was significant temperature variations in the room throughout the day. This temperature had an undesirable affect on the temperature inside the metering box that caused it to

fluctuate. Through building a GHB, this error was significantly reduced as the guard box temperature was controlled to keep the temperature variation as small as possible even when the room temperature was varying a considerable amount. Air velocities in the metering chamber, cold chamber and guard areas would also be constant due to fans moving the air around the guard box to maintain a uniform temperature. This was also beneficial as the air velocity in the test room would be affected by doors or windows being left open.

The ISO Standards outlined in Section 3.6 recommend a negligible heat transfer through the metering box walls into the guard box area. This would require the design of a custom PID controller along with the acquisition of the relevant equipment. Minor fluctuations in the conditions either side of the metering box walls would cause heat transfer in or out of the metering box and would have to be accounted for. However, it was decided to employ a comparative method of testing as outlined in Section 5.5 for practical reasons, as the limits outlined in the ISO Standards could not be attained with the available equipment and in the specified time.

The comparative testing method is based on maintaining a higher temperature in the metering box than in the guard box. Maintaining an average temperature difference would mean that the losses through the metering box walls would be constant and therefore produce repeatable results. An arbitrary average temperature difference of 2 ^{o}C was chosen.

4.3.2 Guarded Hot Box Dimensions

The first course of action was to determine the overall dimensions of the Hot Box. This

process started by trying to keep the test specimen size as large as possible while keeping in mind the maximum dimensions possible in order for the test facility to be moved into any test location. The maximum allowable height that the Hot Box could reach was found to be 1.96 m with a maximum possible width of 1.4 m.

As described in Section 3.6, one of the losses associated with the GHB is the peripheral loss. This is a heat flow parallel to the specimen at the edge of the specimen. To minimise this loss, the surround panel would have to be made with a material of high thermal resistance and also have a significant distance between the perimeter of the test element and the inner surface of the metering box. As a balance between protecting the test specimen from these losses while maintaining a meaningful test specimen size, a distance of 200 mm was chosen. As a result of this, different test specimens could be inserted into the surround panel, but the peripheral loss through the surround panel would remain constant.

The distance between the perimeter of the metering box and the inside of the guard box walls was chosen to be 150 mm. This was done to achieve a uniform temperature in the guard box and reduce the risk of stagnant air pockets forming, while remaining within the maximum height allowed.

4.3.3 Material Selection

The material chosen to manufacture the shell of the Hot Box was plywood sheeting. Plywood is strong, relatively cheap and can be cut easily. It was also used in the Hot Boxes described in Sections 4.3.1 and 4.4.1.

Polyiso was chosen to insulate the walls of the metering box and guard box. Polyiso

foam is a rigid foam that has the highest insulating values of any conventional foam insulation available in industry today. It can be seen in Table 2.1 that 50 mm thick polyiso offers approximately 40 % better thermal performance than polystyrene of the same thickness. Along with the very low conductivity of the foam, there are also gases trapped in the foam that add to its thermal resistance. Polyiso is moisture resistant, dimensionally stable and air tight.

4.3.4 Hot Side Overview

Figure 4.3 shows the hot side of the GHB with the key to the diagram. It can be seen that the metering box sits inside the guard box. A gap of 150 mm between the outside perimeter of the metering box and inside perimeter of the guard box was chosen to avoid any stagnant air pockets in the guard area.

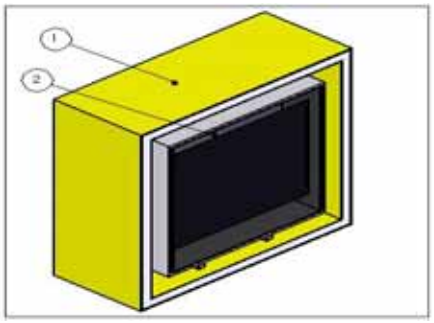

Key:
1: Guard box
2: Metering box

Figure 4.3: Hot Side Drawing

4.3.4.1Guard Box Design

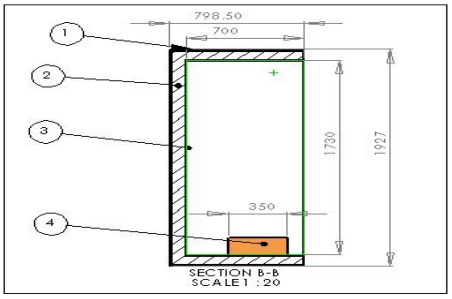

Key:
1: Outside plywood shell
2: Guard box insulated wall
3: Inner plywood shell
4: Metering box holders

Figure 4.4: Section View – Guard Box (Dimensions: mm)

The inner dimensions of the guard box were designed to be 1730 mm high x 1730 mm wide and 700 mm deep. This provided enough space above and between the perimeter of the metering box and guard box for air to circulate. This also allowed for an air gap behind the metering box for a fan and heater to be fitted to the inside of the guard box. This resulted in the outer dimensions of the guard box to be 1927 mm high x 1927 mm wide and 798.5 mm deep. The outer dimensions of the guard box were below the maximum allowable dimensions set out in Section 4.2.2.

4.3.4.2 Metering Box Design

The metering box sits inside the guard box on the hot side of the test specimen. It was designed by taking into account some of the dimension requirements addressed in Section 4.2.2. A sectional view of the metering box is shown in Figure 4.5.

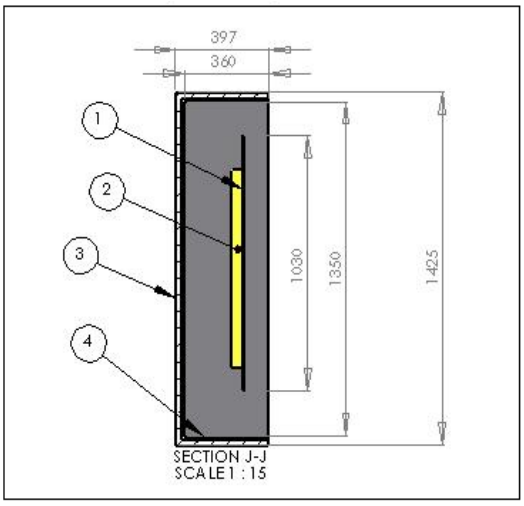

Key:
1: Baffle
2: Timber Battens
3: Insulation
4: Plywood Shell

Figure 4.5: Section View through Metering Box (Dimensions: mm)

The metering box had to be wide enough to be able to facilitate the heaters and fans to fit behind the baffle. The width of the metering box was designed to be 360 mm. The dimensions that were chosen for the test specimen were 950 mm x 950 mm and

that resulted in the inner dimensions being 1350 mm high x 1350 mm wide.

The composition of the metering box was the next stage in this part of the design. There were two main choices. The first was to put the wooden sheet on the outside of the metering box with the insulation on the inside. The second was to put the wood sheeting on the inside with the insulation on the outside. The latter was chosen because it offered a strong fixing surface for the heaters, fans and baffle to be attached to the inside of the metering box walls.

The inside surface of the wooden sheeting would be painted a matt black colour so that the radiation from the hot surface of the heaters would not be reflected from the box walls to the specimen surface. Surfaces seen by the test specimen should achieve a desired emissivity of at least 0.8 because of this **[6]**. A 1030 mm high x 1350 mm wide x 2 mm thick matt black aluminium baffle was installed in the metering box to shield the specimen surface from direct radiative heat transfer from the heaters and fans.

4.3.5 Cold Box Design

The cold box was designed to provide a cold and stable environment for the test specimen and surround panel. An isometric view of the cold side is shown in Figure 4.6. The structure was strong enough to be clamped to the surround panel and hot side. From a practical point of view, the cold box was designed to be easily manoeuvrable. This was because the guard box combined with the metering box was a heavy structure and could not be moved easily. Having a light and moveable cold side would make it easier for the for test specimens to be fitted into and removed from the surround panel by one person. This was achieved by having a single shell of plywood sheeting, and covering

the outside of the structure with a light reflective multi-foil insulation.

Figure 4.7 shows a section view of the cold box. The inside dimensions were designed to be 1902 mm high x 1902 mm wide x 348 mm deep. The height and width of the cold box had to be at least the same size as the guard chamber. A 1200 mm high x 1902 mm wide x 1.5 mm thick matt black aluminium baffle was installed in the cold box to shield the specimen surface from direct radiative heat transfer from the cold air ducts and cold box walls. The cold box had to be deep enough to facilitate the refrigeration ducts and the baffle. The battens that are labelled 4 in Figure 4.7 were designed to hold the baffle in place. The baffle was designed to be installed into the cold box to shield the test specimen from radiative transfer with the cold box walls.

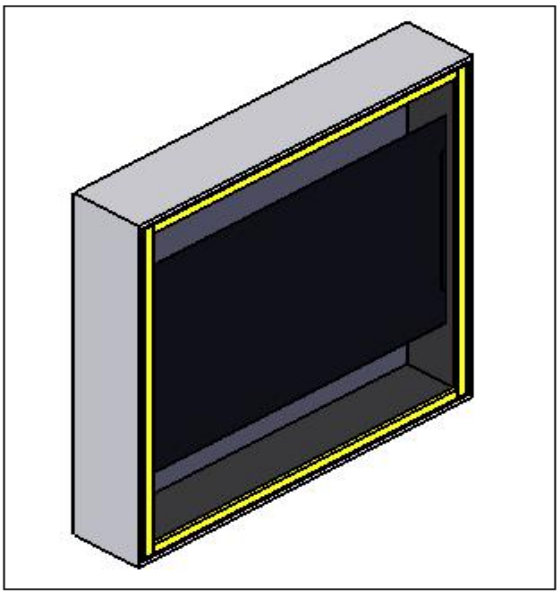

Figure 4.6: Cold Box Isometric View

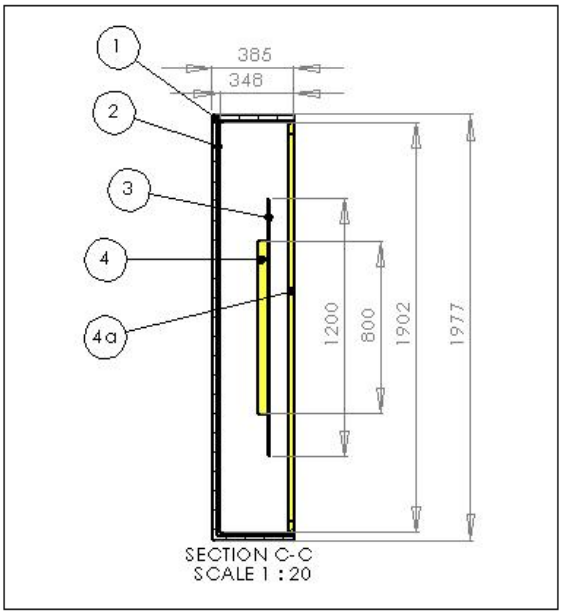

Key:

1:Reflective quilted insulation

2: Plywood shell

3: Baffle

4, 4a: Timber Battens

Figure 4.7: Section View through Cold Box (Dimensions: mm)

During a test, the cold box was to be clamped up against the surround panel. As the surround panel was constructed from polyiso insulation, too small a contact area (12.5 mm wood sheeting) would create indentations into the surround panel. 50 mm x 25 mm battens (labelled 4a in Figure 4.7) were fixed to the perimeter of the cold side to increase the area of contact between the cold side and the surround panel thus protecting the surround panel from damage.

4.3.6 Surround Panel Design

Figures 4.8 a and b show drawings of the surround panel. The outer dimensions of the surround panel were designed to be 1902 mm high x 1902 mm wide. These dimensions were the same as the exterior dimensions of the insulation in the guard box. The test specimen sits into the surround panel and the dimensions of the test specimen were designed to be 950 mm high x 950 mm wide. The surround panel was designed to be 160 mm wide. This was the maximum intended width of the test specimens.

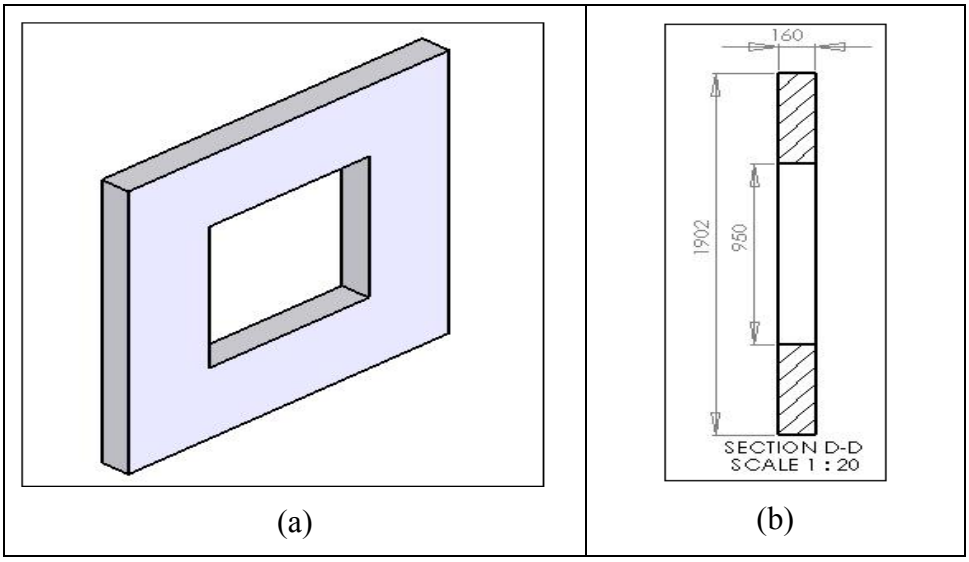

Figure 4.8 a) Isometric View Surround Panel b) Section View

4.3.7 Finished Design

Figure 4.9 shows a section view of the complete design of the GHB. All the separate designed parts were assembled together to make up the final design of the GHB. This is the intended assembly of the GHB during a test. The metering box is designed to sit into the guard box and is fixed to the metering box holders. The surround panel is located between the hot side and cold side.

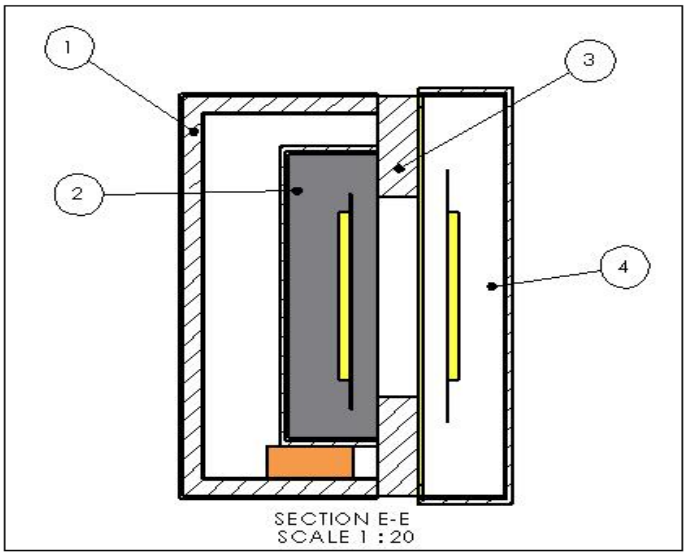

Key:

1: Guard Box

2: Metering Box

3: Surround Panel

4: Cold Box

Figure 4.9: Section View of GHB

4.4 Associated Guarded Hot Box Equipment

4.4.1 Introduction

All the control and monitoring equipment associated with the GHB is summarised below:

To control and maintain a uniform temperature inside the guard box, the following were used:

- A 100 W AC enclosure resistance heater.
- 12 W AC fan.
- PID temperature controller with a solid state relay.

To control and maintain a uniform temperature inside the metering box, the following were used:

- 4 PTC element enclosure heater 15W (12 V-24 V DC).
- 2 VAPO bearing axial fan each with a with a volumetric flow rate of 32.8 m^3/hr (12 V DC).
- DC power supply. Two channels. Max voltage 30 V, max current 3 A.

To control and maintain a uniform temperature inside the cold box, the following was used:

- Refrigeration unit from laboratory.

4.4.2 Guard Box Heater Selection

The guard box heater was chosen after some preliminary calculations were carried out to size it. The heat created by the fan was ignored for calculation purposes and it was

assumed that the total power input to the guard box was from the heater alone.

A maximum temperature difference between the inside and outside of the guard box was chosen to be 35 ^{o}C. This was an over-estimated figure to ensure that the heater would not be undersized. The thermal resistance of the guard box walls and surround panel were approximately 3.5 m^2 ^{o}C/W and 7 m^2 ^{o}C/W respectively. Equation 4.7 was used to estimate the heater size **[94].**

$$Q_{heater} = \frac{A_n x \Delta T_n}{R_w} \qquad \textbf{4.7}$$

Where;

Q_{heater} = Heater power (W)

R_w = Wall thermal resistance (m^2 ^{o}C/W)

Area of guard box walls $= (1.73 \times 1.73) + 4(1.73 \times .70) = 7.84\ m^2$

Area of surround panel in guard box $= 4(1.52 \times 1.73) = 1.05\ m^2$

$$Q_{heater} = \left(\frac{7.84x35}{3.5} \right) + \left(\frac{1.05x35}{7} \right)$$

$$Q_{heater} = 83.64\,\text{W}$$

As a result of this a 100 W AC enclosure resistance heater was chosen. The type of heater used is shown in Figure 4.10.

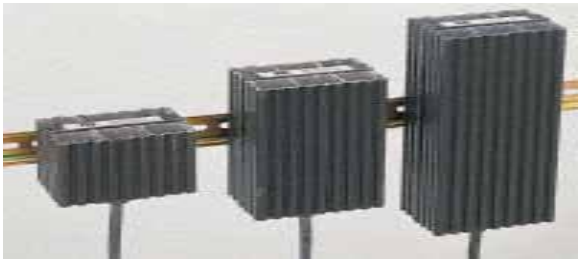

Figure 4.10: Enclosure Heaters **[93]**

4.4.3 Metering Box Heater Selection

The same procedure as described in Section 4.3.1 was used to size the heaters. A DC heater was used because it was important to be able to accurately know the heat input to the metering box. DC power can be more accurately recorded than AC power **[85]**.

A temperature difference between the inside and outside surfaces of the metering box was chosen to be 2 ^{o}C. The resistance of the metering box walls and surround panel was conservatively estimated to be 0.7 m^2 ^{o}C/W and 7 m^2 ^{o}C/W respectively. The lowest thermal resistance envisaged for the test specimen was 2 m^2 ^{o}C/W. Equation 4.7 was used to estimate the heater size.

Area of metering box walls = 3.82 m^2

Area of surround panel in metering box = 1.08 m^2

Area of test specimen in metering box = 0.90 m^2

$$Q_{heater} = \left(\frac{3.82x2}{0.7} \right) + \left(\frac{1.08x35}{7} \right) + \left(\frac{0.90x35}{2} \right)$$

$$Q_{heater} = 32.16 \text{ W}$$

Four PTC 12V-24V DC element enclosure heaters, each with an output of 15 W, were chosen for the metering box. **[89]**. Even though three of these heaters would have delivered enough power into the metering box, four were chosen to speed up the heating time for the metering box to arrive at the desired temperature.

4.4.4 Guard Box Fan Selection

The function of the fan was to circulate the air and to achieve a uniform air temperature

throughout the guard box. The major factor in determining the uniformity of the air temperature in an enclosure is the fan's air flow. The fans were sized on this basis. A desired air temperature difference of 1 ^{o}C was chosen. This would ensure that the surface temperature of the outside of the metering box walls would remain uniform.

A 12 W, 230 V AC fan was chosen. It was used in the preliminary test rig and no technical data was available. It was noted that the air temperature difference in the preliminary test facility was less than 1 ^{o}C and therefore would perform the same task in the guard box.

4.4.5 Metering box fan selection

The same method used by Ye **[94]** was employed to size the metering box fan. Equation 4.8 was used to calculate the required mass flow rate.

$$Q_{heater} = \dot{m} C_{p\,air} \Delta T_a \qquad \textbf{4.8}$$

Where;

$\dot{m}$ = mass flow rate (kg/s)

$C_{p\,air}$ = Specific heat capacity of air @ 20^{o}C (1.007 kJ/kg ^{o}C)

$$\dot{m} = \frac{0.032}{1.007} \text{ kg/sec}$$

$$\dot{m} = 0.032 \text{ kg/sec}$$

From there, the mass flow rate was converted to air velocity in litres per second by using Equation 4.9.

$$\dot{m} = \rho_{air} \text{ V} \qquad \textbf{4.9}$$

Where;

ρ_{air} = Air Density (1.18 kg/m^3)

V = Volume flow rate (m^3/s)

$\dot{V}$ = Flow rate (l/s)

$$V = \frac{0.032}{1.18}$$

$$V = 0.0271 \text{ m}^3/\text{ sec}$$

$$\dot{V} = 27.1 \text{ l/sec}$$

Two 12V DC VAPO bearing axial fans were chosen. Each fan has an airflow rate of 15.55 l/sec **[93]**. A picture of the fans is shown in Figure 4.11.

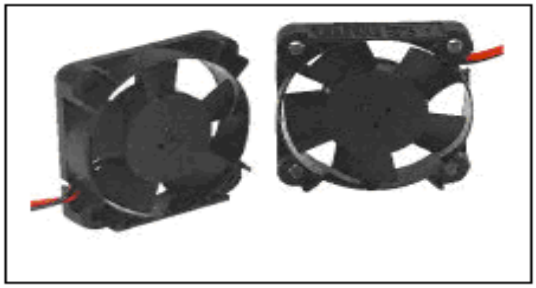

Figure 4.11: Metering Box Fans **[89]**

4.4.6 Guard Box Temperature Control

The temperature in the guard box had to be controlled in order to keep the outside temperature of the metering box walls constant. A (PID) temperature controller was chosen to carry out that task. This would have to be connected to a certain type of relay that could switch the heater on and off to maintain the temperature in the guard box.

A DATALOGIC QS/QD PID controller was chosen for this. This controller could be powered by mains voltage. The controller then sent a 12 V DC signal to a relay to turn the heater on and off. The controller had to be programmed before use. When using a PT 100 platinum resistance thermometer as the sensor input a temperature uniformity of

+/- 0.2 ^{o}C could be achieved **[90]**. A solid state relay was chosen as a method of switching the heater on and off.

4.4.7 Metering Box Temperature Control

As well as controlling the temperature in the metering box, the power consumption also had to be measured. A two-channel IPS2303 DC power supply was used to provide power to the fans and the heaters in the metering box. A digital readout on the power supply displayed the current and voltage on each channel. The accuracy of the voltage and current readings were not clear from the specifications. For this reason, two multimeters with known accuracy were used during testing to record these parameters.

The fan and heater voltages were measured using a Fluke 70 III multimeter with an accuracy of 0.3 % **[91]**. The voltage display from the power supply read to the nearest 0.1 V while the multimeter read to the nearest 0.01 V. Although the multimeters were always used for recording test data, the power supply readout always agreed with the multimeter to the nearest 0.1 V.

A Fluke 189 True RMS multimeter was used to measure the heater current in the metering box with an accuracy of +/- 0.5 % **[89]**. The current display on the power supply read to the nearest 0.01 A. The difference between the two readings never deviated by more than 0.01 A. As the Fluke 189 True RMS multimeter was used to measure the heater current, it could not be used to measure the fan current. As the voltage and current fan settings were intended to stay constant for all tests, and the power supply readings were in excellent agreement with the multimeter readings, the current drawn by the fans was recorded from the power supply.

4.4.8 Temperature Measurement and Recording

Type T thermocouples were chosen to measure the temperatures of the test specimens, walls and air temperatures. These thermocouples give a large signal output per ^{o}C and offer high stability **[94].** They were also used by Ye **[94]**, Fang **[81]**, and Yuan **[64]**. To record and save the temperatures, a PICO TC08 data logger was used. When used in conjunction with the PICO data logger, a temperature resolution of at least 0.1 ^{o}C could be achieved **[92]**. The data logger had eight channels available at any time to read the temperatures and had in-built cold junction compensation. A sample number of thermocouples were connected to the data logger and the temperature readings were compared with an ISOTECH Venus Calibrator thermometer calibration device. The liquid bath in the calibration device was set to three different temperatures covering the intended range of temperature measurements. The readings from the Venus calibrator agreed with the data logger readings to the nearest 0.1 ^{o}C (See Appendix C).

4.4.9 Cold Box Temperature Control

A refrigeration unit was needed to keep the temperature stable in the cold box. A refrigeration unit that was available from the thermodynamics laboratory was used. It had a controller installed in it to set the temperature. The refrigeration unit was designed to be situated outside the cold box with flexible plastic ducting used to deliver and remove the air in and out of the cold box. A fan in the refrigeration unit was constantly blowing air into the cold box with the refrigerator switching on and off each time the air temperature rose above or below the set point. This resulted in a constant airflow in the cold box that maintained a uniform temperature. There was no technical data available

on the refrigeration unit but it was found to be suitable through tests that were carried out when the GHB was built and are shown in Section 5.2.1.

4.5 Construction of Guarded Hot Box

The construction of the GHB took place from late June 2007 to early September 2007. This process included not only the construction of the main elements of the GHB but also the installation of all the associated equipment.

4.5.1 Hot Side Construction

The hot side of the GHB comprised of the guard box and the metering box.

4.5.1.1 Guard Box Construction

The outer shell of the guard box was constructed from sheets of 12 mm plywood cut to the size required and then screwed together. Sheets of polyiso, 80 mm thick, were then glued to the inside of the outer shell to act as the insulation in the guard box wall. The guard box was then finished by gluing sheets of 6 mm plywood to the inside of the insulation. To ensure a proper contact between the insulation and the plywood each side was glued separately with weights placed on the surface. Each side took approximately 24 hours for the glue to set. All the joints were sealed with silicon to ensure an airtight guard box during testing. The sheets of plywood added the required strength and stability to the structure to accommodate the metering box and to provide a solid fixing surface for the heaters and fans. Figure 4.12 shows the constructed hot side.

4.5.1.2 Metering Box Construction

The metering box was built from 12 mm of plywood and 25 mm of polyiso insulation.

The plywood was used as the inner shell, with the polyiso glued to its outside surface. A 1.5 mm thick aluminium baffle was situated in the metering box to encourage uniform airflow over the specimen and to shield the specimen surface from direct radiative heat transfer from the heater and the fans. A rubber draught excluder was installed around the perimeter where the metering box meets the surround panel to stop air transfer between the metering box and the guard box during testing. The inside surfaces and the baffle of the metering box were painted matt black. The constructed metering box, along with the guard box, is shown in Figure 4.12.

Figure 4.12: Hot Side Image

4.5.2 Surround Panel Construction

The surround panel separates the metering and guard box from the cold side. The surround panel also accommodates the test specimen. Polyiso insulation was chosen to

fabricate the surround panel. Two sheets of 80 mm polyiso were glued together and then the aperture for the test specimen to sit into was cut out of the centre of the surround panel. The glue took approximately 24 hours to set. A thin green strip of polyester was then glued to the aperture of the surround panel. This was done to protect the polyiso from wear as different test specimens would be inserted and removed from test to test, possibly resulting in damage to the aperture. The surround panel is shown in Figure 4.13.

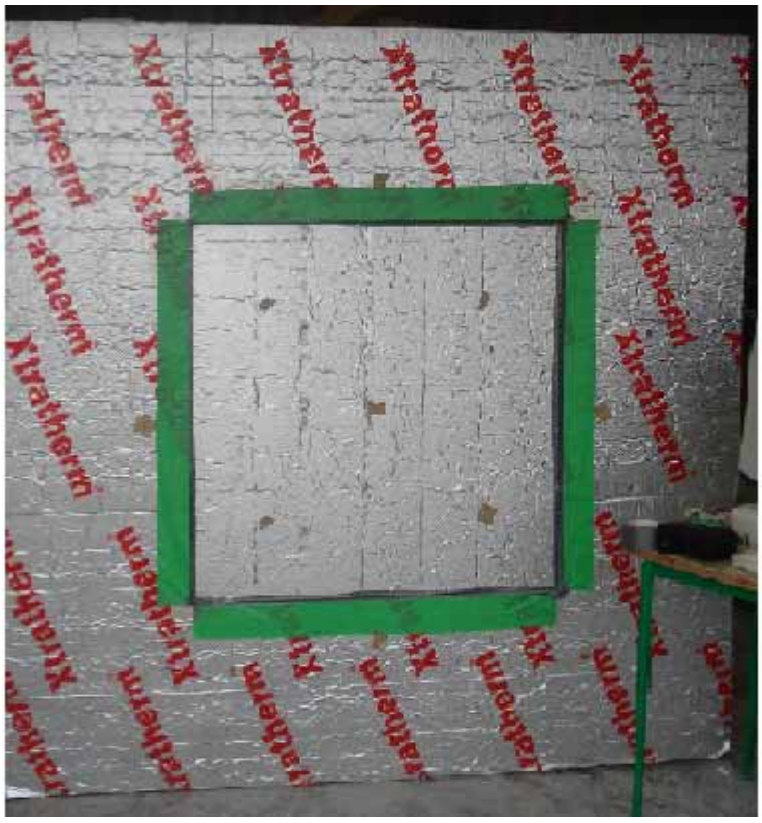

Figure 4.13: Surround Panel with Test Specimen

4.5.3 Cold Box Construction

The cold box was constructed with 12 mm plywood and reflective insulation. A 2 mm aluminium shield was fixed into the cold side to shield the specimen from radiative affects from the cold box walls. Battens were then screwed on to the inside walls on the

open face of the cold box (facing the surround panel). This was done to keep the dimensions of the cold box square and to increase the contact area between the cold box and the surround panel when the whole test facility was clamped together. A picture of the cold box and the hot side is shown in Figure 4.14, the cold box being on the left side of Figure 4.14.

Figure 4.14: Cold Box and Hot Side

4.5.4 Refrigeration Unit

Figure 4.15 shows the refrigeration unit with the adaptations that were made. The three plastic ducts coming out of the top of the unit all carry the cold air into the cold box. These were fixed in three separate positions behind the baffle, the left side, the right and the middle of the cold box. The flexible ducting at the bottom of the unit carries air out of the cold box. This air was fed back into the air intake fan of the refrigeration unit to reduce the energy consumption of the unit.

Figure 4.15: Refrigeration Unit

4.6 Testing facility Development Conclusions

A Hot Box based on the GHB was designed and manufactured. The design began by evaluating the preliminary test rig and trying to improve the testing procedure and conditions. The exterior dimensions of the GHB were curtailed by the requirement to move it into different locations and the rest of the dimensions were based around that factor. Heaters and fans were sized and appropriate equipment was chosen to control the temperature in all enclosures.

CHAPTER 5 - TESTING OF THE GUARDED HOT BOX

5.1 Introduction

Once the GHB was designed and built, the testing stage of this research could begin. The first set of tests were conducted to ensure the equipment was performing as it was intended to. This chapter describes the preliminary tests that took place and the testing procedure employed to calibrate the GHB and test the multi-foil insulation. The results of these tests are then discussed.

5.2 Preliminary Testing of the Guarded Hot Box

The preliminary tests began in early October to November 07.

5.2.1 Air Temperature Distribution Testing of Guarded Hot Box

Before calibration took place, a series of tests were carried out to ensure the equipment was performing as intended. These tests examined the temperature distribution in the different enclosures associated with this GHB. Three tests were carried out.

- Cold side air temperature distribution.
- Metering box air temperature distribution.
- Guard box air temperature distribution.

Figures 5.1, 5.2 and 5.3 show the locations of the thermocouples in the different enclosures for the three tests that were completed. The red circles represent the thermocouple positions in the relevant enclosures. Six thermocouples were used for the cold side test and eight thermocouples were used for both the metering box test and the

guard box test. All thermocouples for all tests were fixed to the surfaces with small strips of masking tape.

Figures 5.4, 5.5 and 5.6 are graphs of the maximum and minimum temperatures in each enclosure, at the given location, over a period of time. All the other temperatures that are not shown lie in between the maximum and minimum and are not included in the graphs for clarity.

The results of these tests showed that the temperature distribution in each enclosure was small, and therefore proved the air flow in each enclosure was sufficient to achieve temperature uniformity throughout the GHB. The maximum air temperature differences for the cold box, the metering box and the guard box air temperatures were found to be 0.47 ^{o}C, 0.56 ^{o}C and 0.77 ^{o}C respectively.

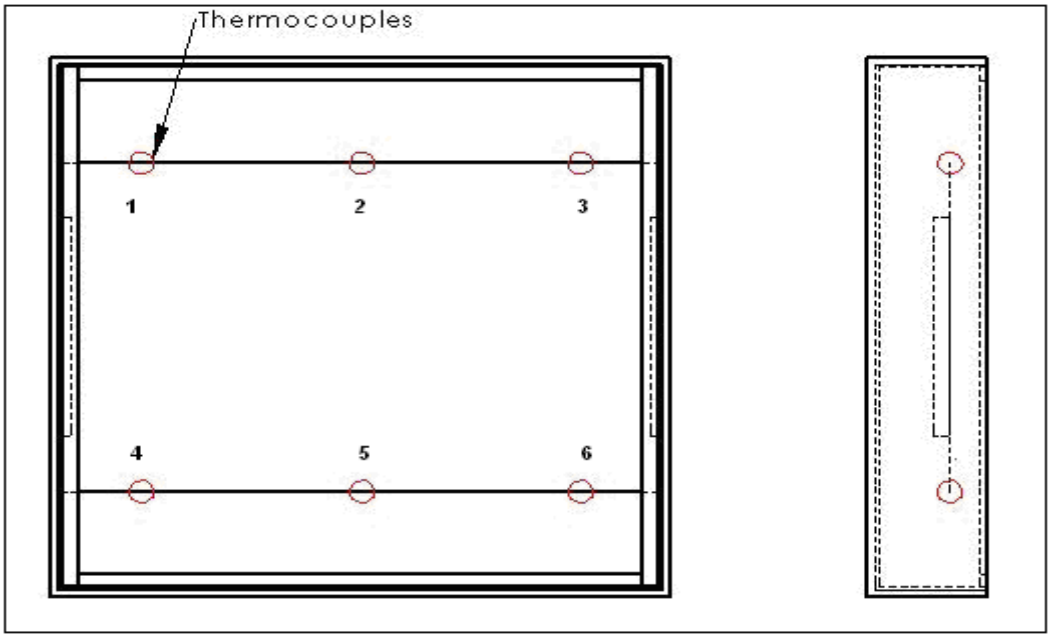

Figure 5.1: Thermocouple Placement for Cold Box

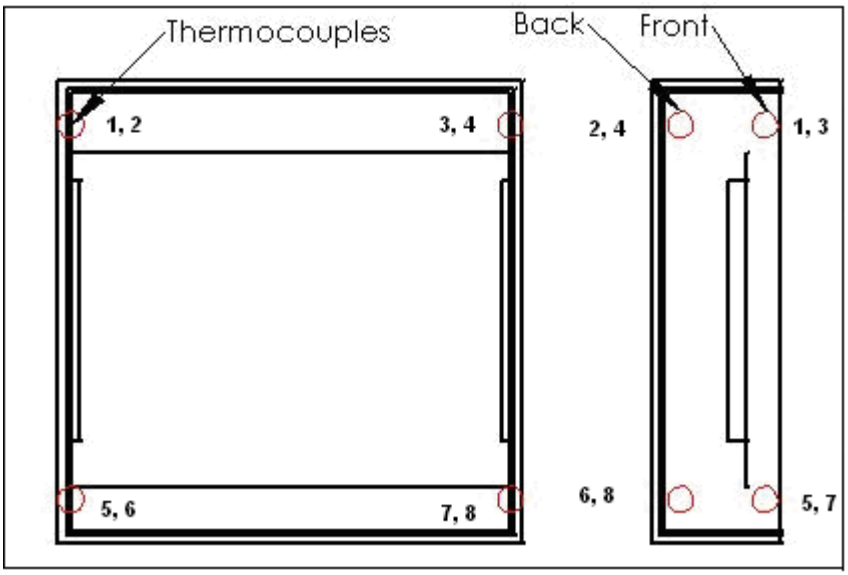

Figure 5.2: Thermocouple Placement in Metering Box for Preliminary Tests

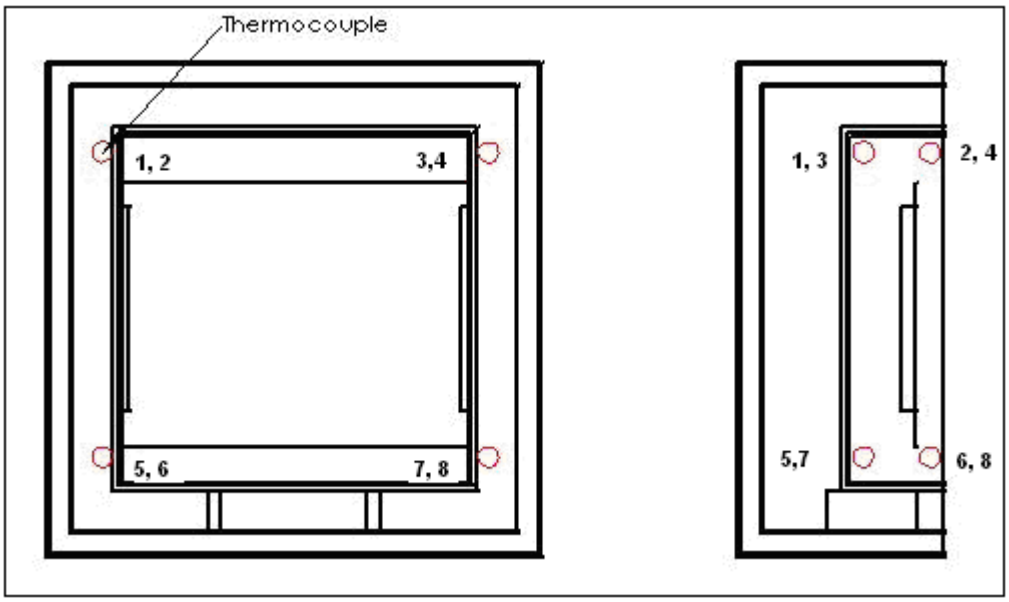

Figure 5.3: Thermocouple Placement in Guard Box for Preliminary Tests

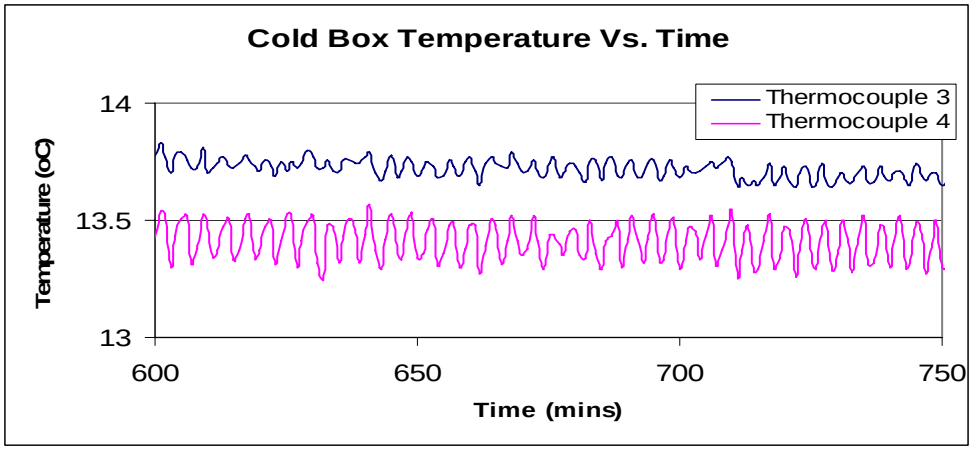

Figure 5.4 T: Air Temperature Distribution in the Cold Box (T600-T750)

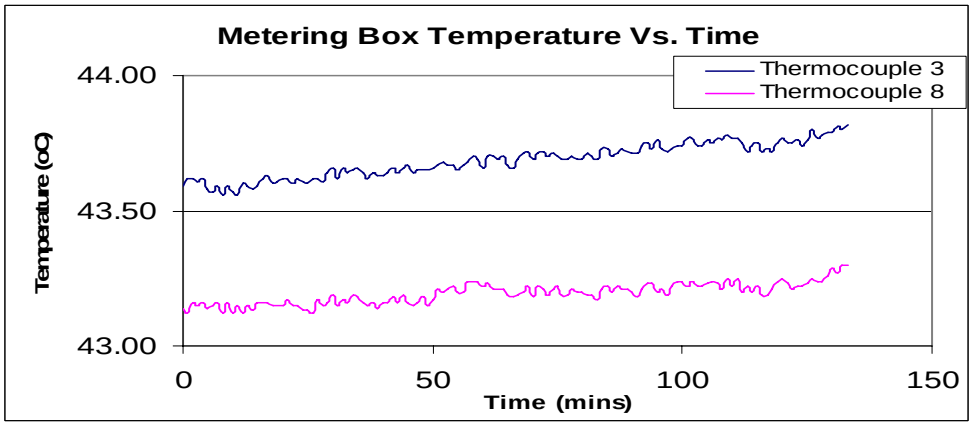

Figure 5.5: Air Temperature Distribution in the Metering Box (T0-T133)

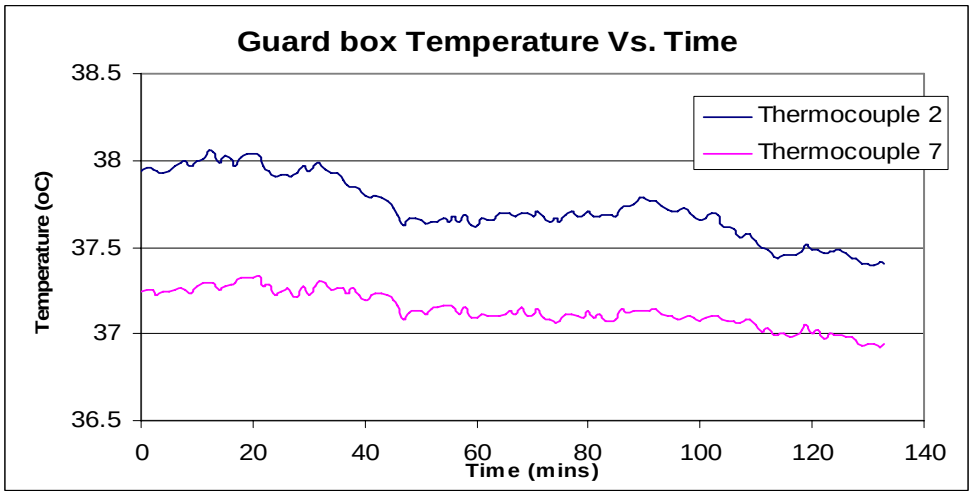

Figure 5.6: Air Temperature Distribution in the Guard Box (T0-T133)

5.2.2 PID Temperature Controller Test

The PID controller was chosen to control the temperature in the guard box. A PID controller would not fluctuate as much as an On – Off controller around the set temperature and therefore was deemed the most suitable type of controller to use. Due to the lack of ports available in the data logger, it was decided to monitor the temperatures in the metering box and the cold box before, during and after tests and assume that the outer wall metering box temperature remained constant in between data collection periods. To ensure this assumption was valid, a preliminary test was carried out to show that the controller kept the temperature of the outer walls of the metering box constant over a period of time. Figure 5.7 shows the results from this test. The power to the metering box was constant. A detailed description of the data collection procedure is described in Section 5.4.1.

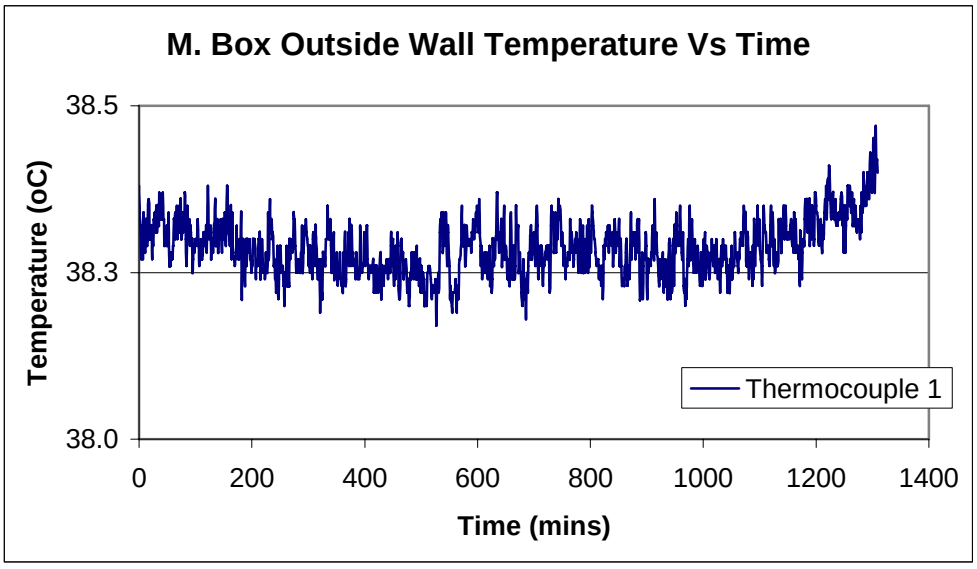

Figure 5.7: Metering Box wall Temperature Vs. Time (T0-T1300)

The conditions in the metering box and the cold box were recorded throughout the testing. The temperature difference across the metering box walls was an important

part of the tests and it was essential that the guard box temperature remained constant throughout the test. The maximum fluctuation in temperature during the 24 hour test period was 0.3 ^{o}C. The location of the thermocouple used for this test is shown in Figure 5.8.

5.3 Thermocouple Placement for Guarded Hot Box Tests

The results from the air distribution tests showed that the temperature variation in the GHB was small and the calibration for the GHB could take place. A decision on the thermocouple placement for these tests was made and implemented. 35 thermocouples were used for the tests. A breakdown of the thermocouple placement was as follows and is shown in Figures 5.8, 5.9:

5 Thermocouples on the outside surface of metering box walls.

5 Thermocouples on the inside surface of metering box walls.

2 Thermocouples on the metering box baffle.

2 Thermocouples for metering box air temperature.

4 Thermocouples on the hot side surface of the surround panel.

4 Thermocouples on the cold side surface of the surround panel.

5 Thermocouples on the hot side surface of the test specimen.

5 Thermocouples on the cold side surface of the test specimen.

2 Thermocouples on the cold side baffle.

1 Thermocouple for the cold box air temperature.

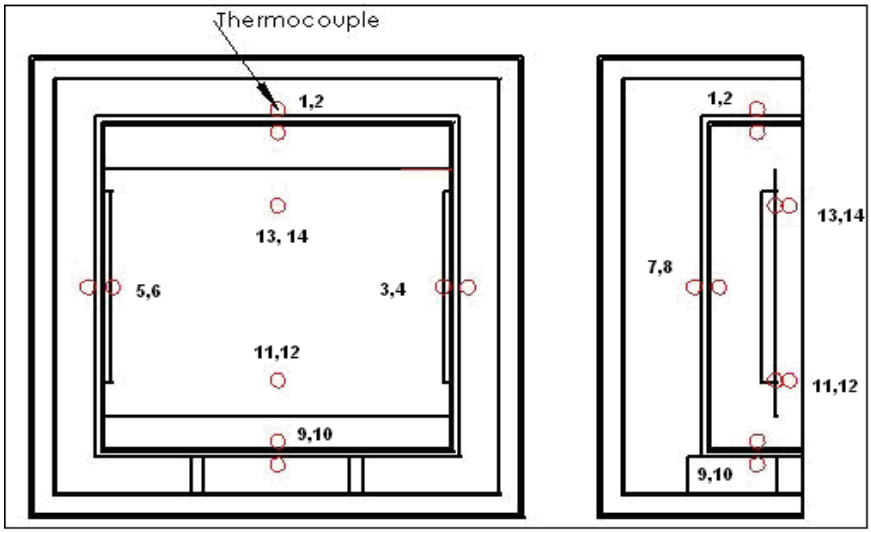

Figure 5.8: Thermocouple Placement in Hot Side

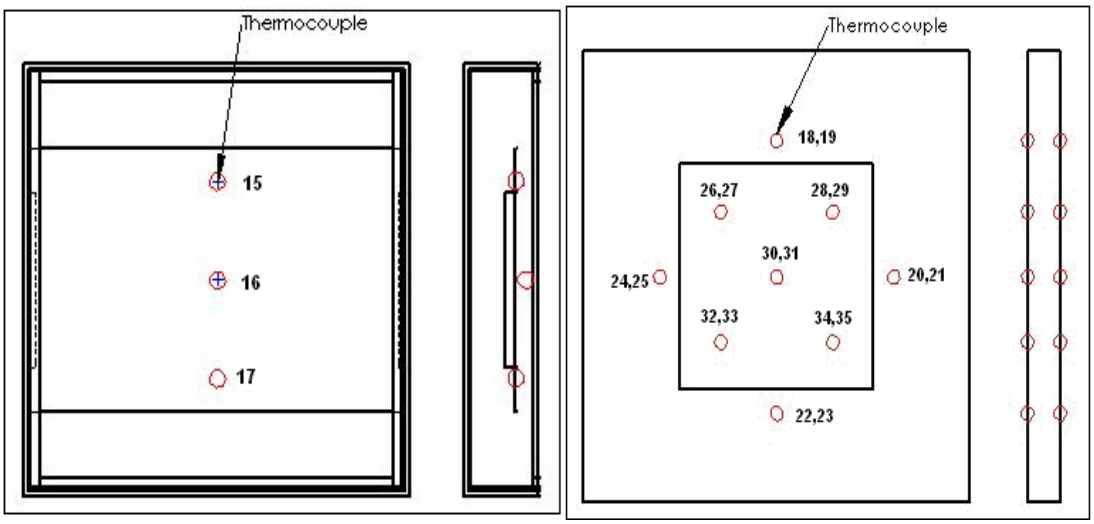

Figure 5.9: Cold Box and Surround Panel/Test Specimen Thermocouple Placement

5.4 Data Acquisition Method

The data logger available for this testing had 8 ports available at any one time to record the temperatures which meant that all 35 temperature readings could not be read at the same time. To overcome this problem a specific procedure was employed.

Temperatures in the metering box and cold box were observed for approximately 16 hours before each test. This was done to ensure that steady state conditions

existed. Following this, readings from all the other thermocouples were recorded three times in one day: morning, afternoon and evening. During and after the readings, the air and baffle temperatures in the metering box and the cold box were recorded to ensure that the temperatures in both chambers did not fluctuate to a large degree.

5.4.1 Data Collection Procedure

Once steady state conditions were reached, the testing period lasted approximately ten hours. This comprised of approximately one hour of collecting data in all thermocouples, on two occasions, in the morning. These temperatures were recorded once every minute for five minutes in two consecutive cycles. This started by recording the surround panel temperatures on the hot and cold sides. Then the test specimen temperatures were recorded, followed by the inside and outside walls of the metering box and then the air and baffle temperatures in the hot and cold chambers. The process was immediately repeated for the second cycle. This resulted in the data from each thermocouple being recorded for ten minutes in the morning, afternoon and evening. Temperatures in the metering box and cold box were recorded in between these data collection procedures to ensure that the temperatures did not change during a test. The thermocouples were physically labelled and the time interval of each thermocouple reading was known. The readings from the data logger could be opened in Microsoft Excel where all the necessary calculations were conducted.

Figure 5.10 shows readings from the data logger that was opened in an Excel spreadsheet. In column A, it can be seen that the time of each reading is given. Temperatures recorded from channels 1 to 8 are in columns B-I, and the cold junction

temperature is given in column J. For each time interval (e.g. 0 – 7 in the example in Figure 5.10), the identity of the thermocouple was known. Following the procedure that was outlined above, the first set of temperatures recorded were the surround panel temperatures on the hot and cold side (from channel 1 – 8). The data logger could then be paused and eight more thermocouples inserted into the data logger, and then the next 8 channels recorded were the test specimen readings (time reading 11 – 17). The procedure was exactly the same for every test that was completed.

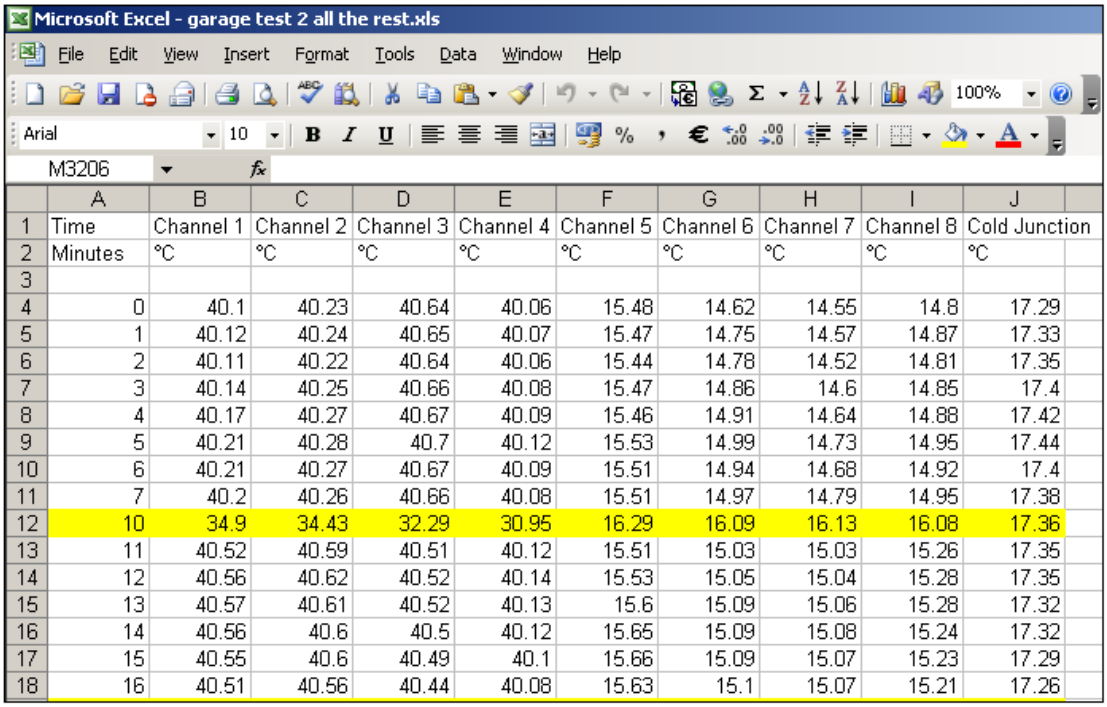

	A	B	C	D	E	F	G	H	I	J
1	Time	Channel 1	Channel 2	Channel 3	Channel 4	Channel 5	Channel 6	Channel 7	Channel 8	Cold Junction
2	Minutes	°C	°C	°C	°C	°C	°C	°C	°C	°C
3										
4	0	40.1	40.23	40.64	40.06	15.48	14.62	14.55	14.8	17.29
5	1	40.12	40.24	40.65	40.07	15.47	14.75	14.57	14.87	17.33
6	2	40.11	40.22	40.64	40.06	15.44	14.78	14.52	14.81	17.35
7	3	40.14	40.25	40.66	40.08	15.47	14.86	14.6	14.85	17.4
8	4	40.17	40.27	40.67	40.09	15.46	14.91	14.64	14.88	17.42
9	5	40.21	40.28	40.7	40.12	15.53	14.99	14.73	14.95	17.44
10	6	40.21	40.27	40.67	40.09	15.51	14.94	14.68	14.92	17.4
11	7	40.2	40.26	40.66	40.08	15.51	14.97	14.79	14.95	17.38
12	10	34.9	34.43	32.29	30.95	16.29	16.09	16.13	16.08	17.36
13	11	40.52	40.59	40.51	40.12	15.51	15.03	15.03	15.26	17.35
14	12	40.56	40.62	40.52	40.14	15.53	15.05	15.04	15.28	17.35
15	13	40.57	40.61	40.52	40.13	15.6	15.09	15.06	15.28	17.32
16	14	40.56	40.6	40.5	40.12	15.65	15.09	15.08	15.24	17.32
17	15	40.55	40.6	40.49	40.1	15.66	15.09	15.07	15.23	17.29
18	16	40.51	40.56	40.44	40.08	15.63	15.1	15.07	15.21	17.26

Figure 5.10: Example of Data Logger Readout

5.5 Test Development

The test development began by examining the GHB test procedure in case studies and standards discussed in the Chapter 3. By applying knowledge gained in this analysis, the most suitable testing procedure for the designed GHB was determined.

5.5.1 Heat Balances in the Guarded Hot Box

When steady state conditions have been reached in a GHB, all the losses must be known to find the specimen's thermal characteristics. Evaluating these losses involved measuring the heat input into the metering box and then subtracting all the losses through the metering box walls, surround panel etc. Figure 5.11 shows a section view through the GHB with the heat balance shown in Equation 5.1.

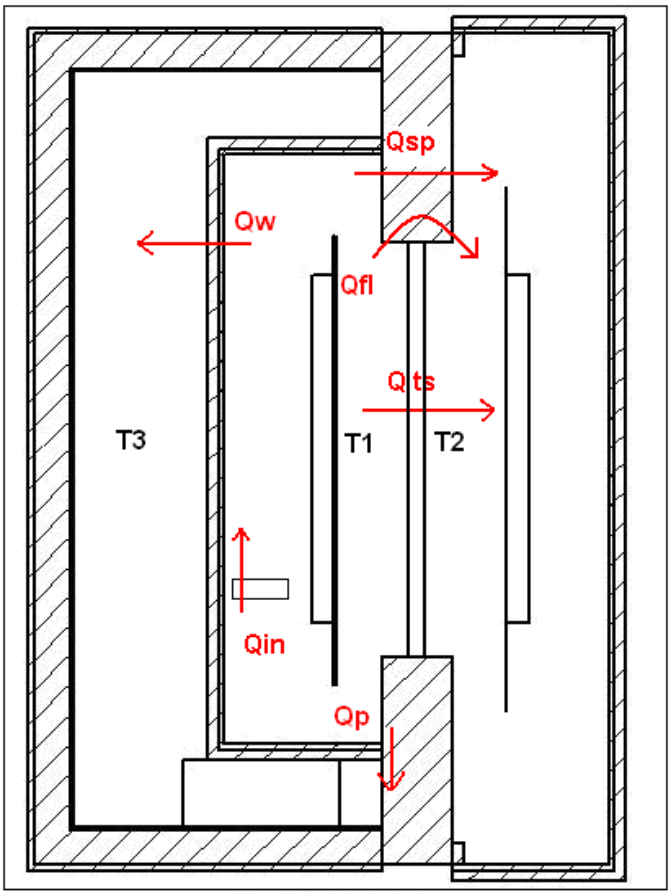

Figure 5.11: Heat Balance of GHB with Flanking Loss

The temperature in the metering box, *T1*, was designed to be higher than the temperature in the Guard box, *T3*. This ensured that no heat flow into the metering box from the guard box would occur. Equation 5.1 shows the heat balance.

$$Q_{ts} = Q_{in} - Q_{sp} - Q_{fl} - Q_w - Q_p \quad \textbf{5.1}$$

The heat input into the metering box, Q_{in}, was the only known parameter as it could be determined from the power supply. All the other parameters could be found from carrying out calibration tests. Some of the heat is lost through the surround panel, Q_{sp}. It can be seen in Figure 5.11 that the test specimen is not as wide as the surround panel. This is when flanking losses, Q_{fl}, have an effect on the heat balance in Equation 5.1. As discussed in Section 3.7, flanking losses are mainly a function of temperature difference across the test specimen and specimen thickness. This loss could be reduced almost to zero by using calibration panels the same thickness as the surround panel and by keeping the temperature difference across the specimen the same. This made it possible to find the other unknown parameters without having to consider the flanking losses.

As the metering box temperature was designed to be greater than the guard box temperature, losses through the metering box walls, Q_w, and parallel loss through the surround panel, Q_p, would exist. These losses were combined and termed Q_l and this is shown in Equation 5.2. A testing procedure was developed to evaluate this loss.

$$Q_l = Q_w + Q_p \quad \textbf{5.2}$$

Where;

Q_l = Combined loss heat transfer (W)

5.5.2 Guarded Hot Box Testing Procedure

A comparative test method was employed in the GHB to be used to calibrate the Hot Box and to test specimens with unknown thermal properties. The basis of this method

was to use the calibration tests to evaluate the losses in the GHB, while keeping the conditions in all compartments as similar as possible for all tests. A heat transfer coefficient for the combined losses was found and used to calculate the thermal properties of an unknown test specimen.

5.5.2.1 Calibration Procedure

Figure 5.12 is a sectional view of the GHB and shows that the test specimen is the same thickness as the surround panel. The thickness of the surround panel was kept the same for all tests conducted in order for flanking losses to be neglected. Heat balance for the GHB is shown in Equation 5.3.

$$Q_l = Q_{in} - Q_{ts} - Q_{sp} \qquad \textbf{5.3}$$

The surround panel was designed to be made with insulation with known thermal properties. The calibration test specimen also had known thermal properties. The surface temperatures on both sides of the surround panel and test specimen were recorded. From these readings, Q_{sp} and Q_{ts} could be calculated using Equation 5.4 to calculate the heat transfer coefficients for the surround panel and test specimen, and then substituting those values into Newton's Law of Cooling shown in its general form in Equation 5.5 **[88]**.

$$U_{ts} = U_{sp} = \frac{k}{L} \qquad \textbf{5.4}$$

Where;

U_{sp} = Heat transfer coefficient of surround panel (W/m^2 ^{o}C)

U_{ts} = Heat transfer coefficient of test specimen (W/m^2 ^{o}C)

k = Thermal conductivity (W/m ^{o}C)

L = Thickness (m)

$$Q = UA\Delta T \qquad \textbf{5.5}$$

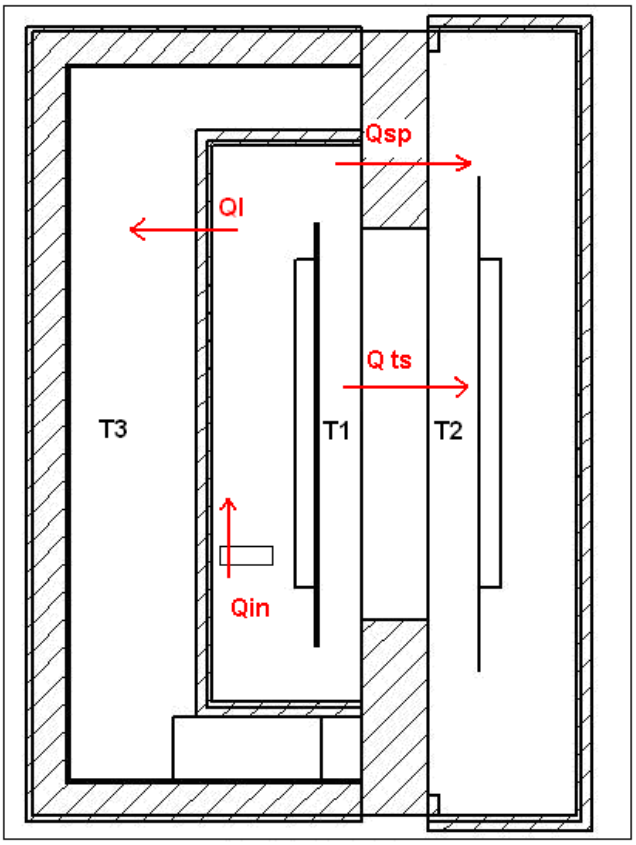

Figure 5.12: Heat Balance without Flanking Loss

The combined loss heat transfer, Q_l, was found by solving Equation 5.3 and from that, a heat transfer coefficient for this combined loss, C_l, was found from Equation 5.6. This coefficient was presented as a function of the metering box wall area and the temperature difference across the walls.

$$C_l = \frac{Q_l}{A_w \Delta T_w} \qquad \textbf{5.6}$$

5.5.2.2 Unknown Test Specimen

Once the combined loss heat transfer coefficient was found, a specimen with unknown

thermal properties could be tested. When testing a specimen with unknown properties, the combined loss heat transfer, Q_l ,was found by solving Equation 5.6. Substituting this value into Equation 5.3, the heat transfer through the test specimen was found. Using the temperature difference across the test specimen from the test data, and the known area, the heat transfer coefficient for the unknown specimen was found by using Equation 5.7.

$$U_{ts} = \frac{Q_{ts}}{A_{ts} \Delta T_{ts}} \qquad \textbf{5.7}$$

5.6 Calibration Tests

The calibration tests were designed to obtain the combined loss coefficient for the metering box walls. In order to get the best possible results, the temperatures in all the chambers were kept as similar as possible for all the tests. Five tests were carried out to calibrate the GHB. This was done to ensure the results from the GHB were repeatable. By keeping as many parameters as possible constant between tests, a direct comparison could be made between test specimens with unknown thermal properties and the calibration test specimen. For example, varying the temperature difference between the metering chamber and the guard chamber would change the temperature difference of the surround panel from the metering chamber to the guard chamber. This would, in turn, affect the combined loss heat transfer.

5.6.1 Description of Calibration Specimens

The calibration specimen was made from the same material (polyiso) and was the same thickness as the surround panel. The panels were cut to the size of the surround

panel aperture, which was 950 mm x 950 mm. The specimen was then inserted into the surround panel and was sealed with duct tape to seal the hot side from the cold side to ensure air tightness. A picture of the surround panel with the calibration panel in place is shown in Figure 5.13. The thermal conductivity of the surround panel and the calibration specimen were known from hot plate tests carried out by the manufacturer of the insulation.

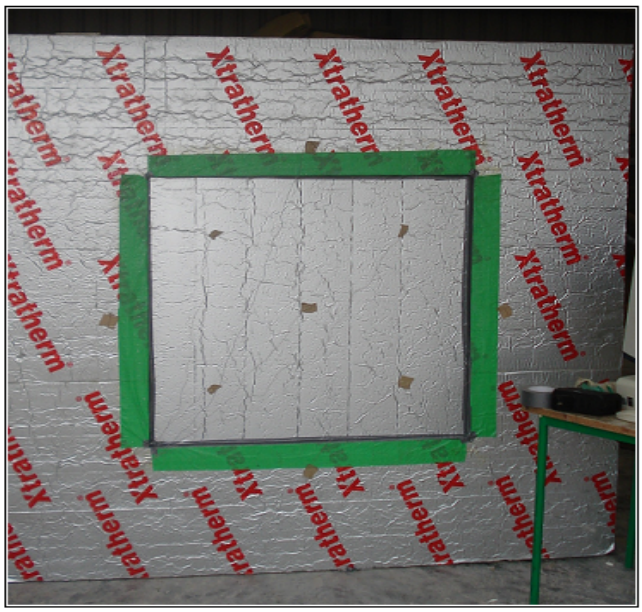

Figure 5.13: Surround Panel with Calibration Test Specimen in place

5.6.2 Calibration Results

Figure 5.14 is a graph of the air temperature in the metering box of calibration Test 2 in Table 5.1 over the testing period. The three gaps in the graph are the periods where the other data was collected from the other thermocouples i.e. the morning, afternoon and the evening. The readings were taken over a 36 hour period. Over that time the temperature fluctuation in the metering chamber was approximately 0.2 ^{o}C. Figure 5.15 is a graph from the same calibration test over the same period of time from the cold box. The cold box temperature was more difficult to control due to the room

temperature changing. The temperature fluctuation in the cold side was approximately 0.7 ^{o}C over the 36 hour period. The thermocouple placements locations for Figures 5.14 and 5.15 are illustrated in Figures 5.8 and 5.9.

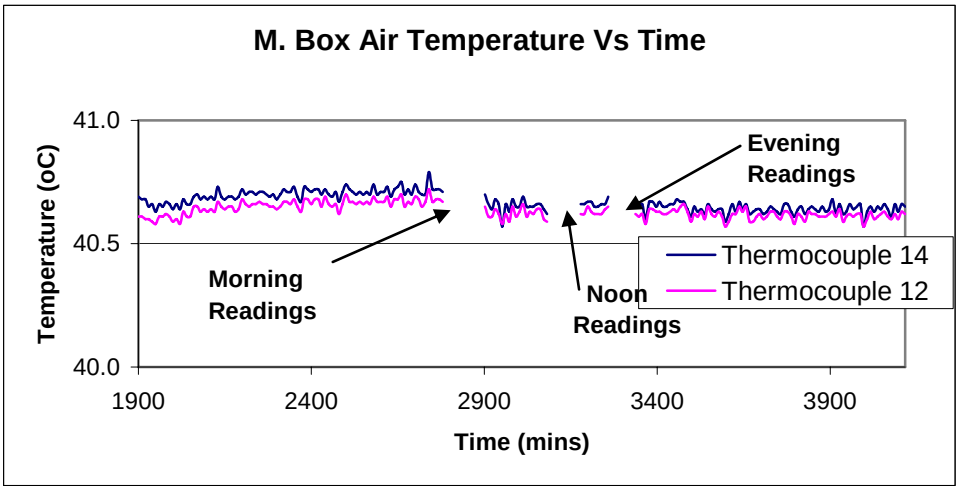

Figure 5.14: Metering Box Air Temperature during Testing (T1900-T4117)

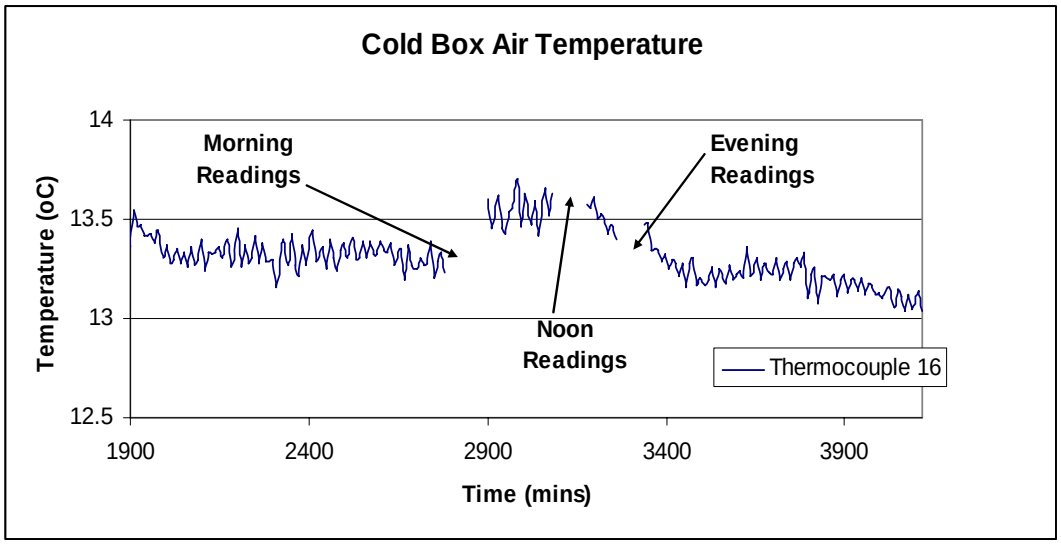

Figure 5.15: Cold Box Air Temperature during Testing (T1900-T4117)

Table 5.1 is a summary of the results of the five calibration tests that were conducted. The combined loss heat transfer coefficient was calculated from the data for each test and is highlighted in yellow in Table 5.1. The values ranged from 1.19 W/m^2 ^{o}C to 1.20

$W/m^2\,^oC$. The results of the tests showed that the GHB was capable of giving repeatable results.

Parameter	Test 1	Test 2	Test 3	Test 4	Test 5
Q_{in} (W)	16.24	16.30	16.34	16.23	16.2
ΔT_{sp} (^oC)	25.9	26.5	26.1	26.1	26.2
ΔT_{ts} (^oC)	25.8	26.2	25.9	25.7	25.9
ΔT_w (^oC)	2.2	2.2	2.2	2.2	2.18
K_{SP} ($W/m\,^oC$)	0.021	0.021	0.021	0.021	0.021
K_{ts} ($W/m\,^oC$)	0.021	0.021	0.021	0.021	0.021
$L_{sp,\,ts}$ (m)	0.16	0.16	0.16	0.16	0.16
U_{sp} ($W/m^2\,^oC$)	0.13	0.13	0.13	0.13	0.13
U_{ts} ($W/m^2\,^oC$)	0.13	0.13	0.13	0.13	0.13
A_w (m^2)	3.82	3.82	3.82	3.82	3.82
A_{ts} (m^2)	0.90	0.90	0.90	0.90	0.90
A_{sp} (m^2)	0.92	0.92	0.92	0.92	0.92
Q_{sp} (W)	3.12	3.20	3.15	3.15	3.17
Q_{ts} (W)	3.05	3.10	3.07	3.04	3.07
Q_l (W)	10.06	10.01	10.11	10.05	10.00
C_l ($W/m^2\,^oC$)	**1.20**	**1.19**	**1.20**	**1.19**	**1.19**

Table 5.1: Calibration Tests Results

5.6.3 Sample Calculations

Using the theory in Section 5.5 and the test results for Test 1 in Table 5.1, the combined loss heat transfer coefficient was calculated as follows:

$K_{sp}, K_{ts}, L_{sp/ts}, U_{sp}, U_{ts}, A_w, A_{ts}$ and A_{sp} were all known before testing took place. The data gathered from carrying out the tests was Q_{in}, ΔT_{sp}, ΔT_{ts} and ΔT_w. The remaining terms were calculated. The heat transfer coefficient for the surround panel and the calibration test specimen was calculated using Equation 5.4.

$$U_{sp} = U_{ts} = \frac{0.021(W/m^oC)}{0.16(m)} \; W/m^2\,^oC$$

$$U_{sp} = U_{ts} = 0.13 \; W/m^2\,^oC$$

Heat transfer through surround panel was calculated using Equation 5.5.

$$Q_{sp} = (0.131)(0.92)(25.9) \; W$$

$$Q_{sp} = 3.12 \; W$$

Heat transfer through calibration test specimen was calculated using Equation 5.5.

$$Q_{ts} = (0.131)(0.90)(25.8) \; W$$

$$Q_{ts} = 3.05 \; W$$

The combined loss heat transfer was calculated using Equation 5.3.

$Q_{in} = 16.24 \; W$

$$Q_l = 16.24 - 3.12 - 3.05 \; W$$

$$Q_l = 10.06 \; W$$

Finally, the combined loss heat transfer coefficient was calculated using Equation 5.6.

$$C_l = \frac{10.06}{(3.82)(2.22)} \; W/m^2\,^oC$$

$$C_l = 1.19 \; W/m^2\,^oC$$

The GHB was now calibrated and the tests were found to be successful. The combined

loss heat transfer coefficient deviated very little over the five tests. Figures 5.15 and 5.16 shows that the GHB had the ability to keep the temperatures and power supply constant over a long period of time to give repeatable results.

5.6.4 Discussion of Calibration Results

The data collection for each test occurred three times a day: in the morning, afternoon and evening. As these tests were comparative, the conditions for all tests had to be kept similar to achieve the best possible results. Table 5.2 is a breakdown of the calibration results that were recorded over the testing period for Test 2 in Table 5.1.

It can be seen from Table 5.2 that the average hot and cold temperatures remained consistent over the testing period. The biggest variation in temperature was in the surround panel cold temperature ($T_{cold\ sp}$) where the temperature varied by approximately 0.5 ^{o}C. The power input (Q_{in}) varied by 0.09 W over the testing period. Test data for the calibration tests are shown in Appendix B. Errors in testing are discussed in Section 5.8.

Parameter	Morning	Afternoon	Evening	Average ΔT
$T_{hot\ SP}$ (^oC)	40.0	40.1	40.1	
$T_{cold\ SP}$ (^oC)	13.7	13.8	13.3	
ΔT_{SP} (^oC)	26.3	26.3	26.8	**26.5**
$T_{inside\ walls}$ (^oC)	40.7	40.7	40.7	
$T_{outside\ walls}$ (^oC)	38.6	38.5	38.6	
ΔT_w (^oC)	2.2	2.2	2.2	**2.2**
$T_{hot\ ts}$ (^oC)	40.3	40.3	40.3	
$T_{cold\ ts}$ (^oC)	14.1	14.3	14.1	
ΔT_{ts} (^oC)	26.2	26.0	26.2	**26.2**
$T_{hot\ air}$ (^oC)	40.9	40.8	40.8	
$T_{cold\ air}$ (^oC)	13.5	13.6	13.6	
ΔT_{air} (^oC)	27.4	27.5	27.3	
Q_{in}	16.25	16.34	16.33	16.30

Table 5.2: Calibration Test Data

5.7 Multi-foil Testing

The temperatures for the Eco-quilt tests were kept as similar as possible to the calibration tests in order to make a direct comparison between the multi-foil and the calibration panel. The heat transfer coefficient for the metering box walls was used in these tests to calculate the heat transfer through the test specimen. The multi-foil

insulation was tested in two different ways. One test was carried out with the recommended unventilated air gap on either side of the multi-foil. The other test was conducted with only one air gap. This was done to replicate a situation where one side of the multi-foil insulation would be in contact with a ventilated cavity in a building. In all these tests, the multi-foil was tested in conjunction with 40 mm polyiso. Polyiso was included in these tests because it was clear from other tests described in Section 4.2 that a layer of multi-foil alone would not meet the building regulations. The results for these tests are shown in Appendix A. By using the polyiso sheet with known thermal properties along with the multi-foil, the results would show if the multi-foil insulation could be used along with another insulation to meet the 0.16 $W/m^2\ ^oC$ required for the roofs of new buildings **[3]**.

5.7.1 Specimen Preparation and Description

Figures 5.16 a and b show how the Eco-quilt specimen was prepared. A wooden frame was constructed from 50 mm x 25 mm battens. The height and width of the frame was 940 mm wide x 940 mm high. This left the dimensions 10 mm short of the height and width of the surround panel aperture. The Eco-quilt was then wrapped around the perimeter of the frame and stapled to it. This allowed the specimen to be tightly installed into the surround panel.

(a)

(b)

Figure 5.16: Eco-quilt Test Specimen a) Front view b) Rear view

5.7.2 Eco-quilt Testing with Two Cavities

Figure 5.17 shows a sectional view schematic of the surround panel with the test specimen in place. The test specimen consisted of three elements, the 40 mm sheet of polyiso, the sheet of multi-foil and a sheet of foiled back plasterboard. The polyiso was on the hot side of the surround panel. The multi-foil was in the middle of the aperture with an air gap on either side. In order to create an unventilated air gap on the cold side, foiled back plasterboard was mounted on the cold side of the surround panel. An air gap of 50 mm existed between the plasterboard and the Eco-quilt, and an air gap of approximately 32 mm existed between the polyiso and the Eco-quilt.

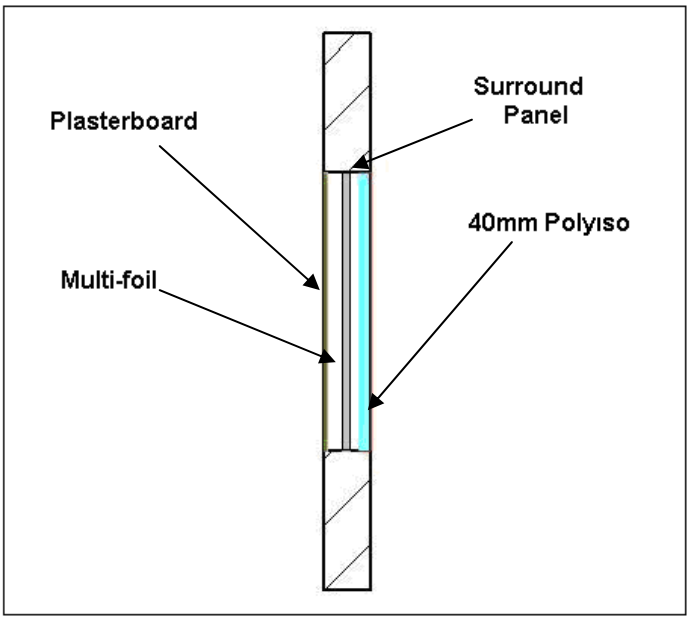

Figure 5.17: Eco-quilt with Two Air Gaps Configuration

5.7.2.1 Test Results

There were four tests carried out on the Eco-quilt with the air gaps on either side. The average combined loss heat transfer coefficient, C_l, calculated from the calibration tests, was used in these tests to calculate the combined loss heat transfer, Q_l. Table 5.3 shows the results for the four tests that were conducted. The heat transfer coefficient for the test specimen, U_{ts}, is highlighted in yellow.

The heat transfer coefficient for the polyiso/Eco-quilt configuration varied from 0.27 W/m^2 ^{o}C to 0.30 W/m^2 ^{o}C. The thermal resistance of Eco-quilt, $R_{Eco-quilt}$, was calculated by subtracting the known thermal resistance of the polyiso from the thermal resistance of the test specimen, R_{ts}. This calculated thermal resistance ($R_{Eco-quilt}$) was for the Eco-quilt with an unventilated air gap on either side plus the sheet of plasterboard. As the thermal resistance of the plasterboard was not known, it could not be subtracted from the test specimen thermal resistance (R_{ts}). The data for these tests can be found in

Appendix B.

Parameter	Test 1	Test 2	Test 3	Test 4
Q_{in} (W)	18.76	18.76	18.73	19.64
ΔT_{sp} (^oC)	25.6	25.6	25.8	25.8
ΔT_{ts} (^oC)	24.7	24.5	24.9	24.8
ΔT_w (^oC)	2.1	2.0	2.0	2.3
C_l ($W/m^2\,^oC$)	**1.19**	**1.19**	**1.19**	**1.19**
A_w (m^2)	3.82	3.82	3.82	3.82
A_{ts} (m^2)	0.90	0.90	0.90	0.90
A_{sp} (m^2)	0.92	0.92	0.92	0.92
U_{sp} ($W/m^2\,^oC$)	0.13	0.13	0.13	0.13
Q_{sp} (W)	3.09	3.09	3.11	3.11
Q_l (W)	9.55	9.09	9.09	10.46
Q_{ts} (W)	6.12	6.58	6.53	6.08
$K_{polyiso}$ (W/m^oC)	0.021	0.021	0.021	0.021
$L_{polyiso}$ (m)	0.040	0.040	0.040	0.040
U_{ts} ($W/m^2\,^oC$)	**0.27**	**0.30**	**0.29**	**0.27**
R_{ts} ($m^2\,^oC/W$)	3.70	3.33	3.45	3.70
$R_{polyiso}$ ($m^2\,^oC/W$)	1.86	1.86	1.86	1.86
$R_{Eco\text{-}quilt}$ ($m^2\,^oC/W$)	1.84	1.47	1.59	1.84

Table 5.3: Results for Eco-quilt with Air Gap on either side

5.7.2.2 Sample Calculation

Using the testing procedure in Section 5.5 and the test results for Test 1 in Table 5.3, the

heat transfer coefficient for the metering box walls was calculated. The constants known before the tests were K_{sp}, $K_{polyiso}$, $L_{sp/ts}$, $L_{polyiso}$, U_{sp}, C_l, A_w, A_{ts} and A_{sp}. The data gathered from carrying out the tests were Q_{in}, ΔT_{sp}, ΔT_{ts} and ΔT_w. The remaining terms were calculated. Using Equation 5.5 the heat transfer through the surround panel was calculated.

$$Q_{sp}=(0.131)(0.92)(25.6)\ W$$

$$Q_{sp}=3.09\ \ W$$

The combined loss heat transfer was calculated using Equation 5.5.

$$Q_l=(1.19)(3.82)(2.1)\ \ W$$

$$Q_l=9.55\ \ \ W$$

Then using Equation 5.3 the heat transfer through the test specimen was found.

$$Q_{ts}=18.76-9.55-3.09\ W$$

$$Q_{ts}=6.12\ \ W$$

The heat transfer coefficient for the test specimen was found using Equation 5.7.

$$U_{ts}=\frac{6.12}{(0.90)(24.7)}\ W/m^2\,^oC$$

$$U_{ts}=0.27\ \ \ W/m^2\,^oC$$

$$R_{ts}=\frac{1}{0.27}\ m^2\,^oC/W$$

$$R_{ts}=3.70\ \ \ m^2\,^oC/W$$

The thermal conductivity and the thickness of the sheet of polyiso were known. This meant that the thermal resistance could be calculated by using Equation 5.8:

$$R_{polyiso} = \frac{L_{polyiso}}{K_{polyiso}} \qquad \textbf{5.8}$$

$$R_{polyiso} = \frac{0.04}{0.0215}\ m^2\ ^oC/W$$

$$R_{polyiso} = 1.86\ m^2\ ^oC/W$$

Using Equation 5.8, the thermal resistance of the Eco-quilt with an air gap on either side was calculated:

$$R_{Eco\text{-}quilt} = R_{ts} - R_{polyiso}$$

$$R_{Eco\text{-}quilt} = 3.70 - 1.86\ \ m^2\ ^oC/W$$

$$R_{Eco\text{-}quilt} = 1.84\ \ m^2\ ^oC/W$$

5.7.3 Testing of Multi-Foil with One Cavity

Figure 5.18 shows a schematic of the surround panel with the test specimen in place. The test specimen consisted of the 40 mm sheet of polyiso, and a sheet of multi-foil. The polyiso was on the hot side of the surround panel. The multi-foil was situated on the cold side of the surround panel. There was an air gap of 95 mm between the polyiso and the multi-foil. Two different multi-foils were tested: one was Eco-quilt, and the other was a prototype multi-foil developed by SmartRinsulations. The aim of these tests was to observe the effect of having the multi-foil with only one unventilated air gap and to compare Eco-Quilt with an alternative multi-foil configuration.

The SmartRinsulation multi-foil consisted of the following:

- 2 outer layers of tear-resistant reinforced reflective films.
- 4 layers of bubble wrap with a reflective film on one side.

- 1 internal reflective film.
- 2 layers of closed cell foam.

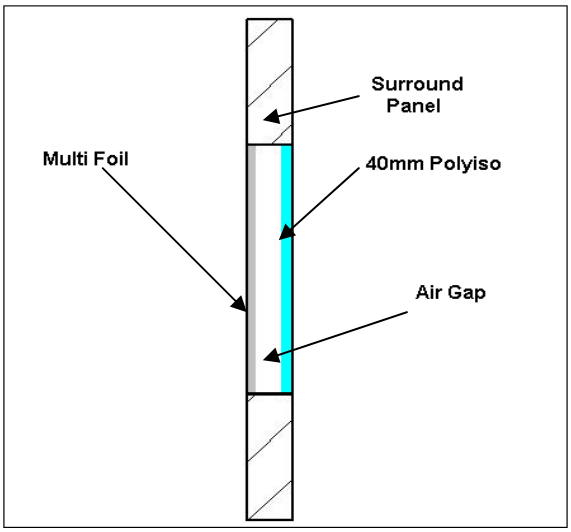

Figure 5.18: Eco-quilt with One Air Gap Configuration

5.7.3.1 Test Results

Table 5.4 shows the results from the two tests that were conducted. The heat transfer coefficient for the test specimens is highlighted in yellow. The results show that when the Eco-quilt was tested with one cavity, the heat transfer coefficient of the test specimen was found to be 0.35 W/m^2 ^{o}C. This equates to a thermal resistance of 2.86 m^2 ^{o}C/W. The average thermal resistance of the Eco-quilt with two air gaps was 3.54 m^2 ^{o}C/W. This showed that the thermal resistance was reduced with one air gap and that multi-foil insulation performs best when it is in between two unventilated air gaps. The heat transfer coefficient for the variation of multi-foil was found to be 0.39 W/m^2 ^{o}C. This equates to a thermal resistance of 2.56 m^2 ^{o}C/W, which is slightly less than the Eco-quilt. The thermal resistance of Eco-quilt ($R_{Eco-quilt}$) and the alternative multi-foil ($R_{multi-foil}$) was calculated by subtracting the known thermal resistance of the polyiso

from the thermal resistance of the test specimen, R_{ts} .The calculation procedure for these tests was the same as the procedure described in Section 5.7.3.2. The data for these tests can be found in Appendix B.

Parameter	**Eco-Quilt**	**Multi-foil**
Q_{in} (W)	21.37	20.96
ΔT_{sp} (^oC)	26.7	27.1
ΔT_{ts} (^oC)	25.5	25.9
ΔT_w (^oC)	2.2	1.9
C_l ($W/m^2\,^oC$)	**1.19**	**1.19**
A_w (m^2)	3.82	3.82
A_{ts} (m^2)	0.90	0.90
A_{sp} (m^2)	0.92	0.92
U_{sp} ($W/m^2\,^oC$)	0.13	0.13
Q_{sp} (W)	3.22	3.27
Q_l (W)	10.00	8.64
Q_{ts} (W)	8.15	9.06
$K_{polyiso}$ (W/m^oC)	0.0215	0.0215
$L_{polyiso}$ (m)	0.040	0.040
U_{TS} ($W/m^2\,^oC$)	0.35	0.39
R_{ts} ($m^2\,^oC/W$)	2.86	2.56
$R_{polyiso}$ ($m^2\,^oC/W$)	1.86	1.86
$R_{Eco\text{-}quilt,\ multi\text{-}foil}$ ($m^2\,^oC/W$)	1.00	0.70

Table 5.4: Results for Multi-foil with one Air gap

5.7.3.2 Sample Calculation

Using the testing procedure in Section 5.5 and the test results for the Eco-quilt test in Table 5.4, the heat transfer coefficient for the metering box walls was calculated. The constants known before the tests were K_{sp}, $K_{polyiso}$, $L_{sp/ts}$, $L_{polyiso}$, U_{sp}, C_l, A_w, A_{ts} and A_{sp}. The data gathered from carrying out the tests were Q_{in}, ΔT_{sp}, ΔT_{ts} and ΔT_w. The remaining terms were calculated. Using Equation 5.5 the heat transfer through the surround panel was calculated.

$$Q_{sp}=(0.131)(0.92)(26.7)\ W$$

$$Q_{sp}= 3.22\ W$$

The combined loss heat transfer was calculated using Equation 5.5.

$$Q_l= (1.19)(3.82)(2.2)\ W$$

$$Q_l=10.00\ W$$

Then using Equation 5.3 the heat transfer through the test specimen was found.

$$Q_{ts} = 21.37 - 10.00 - 3.22\ W$$

$$Q_{ts} = 8.15\ W$$

The heat transfer coefficient for the test specimen was found using Equation 5.7.

$$U_{ts} = \frac{8.15}{(0.90)(25.5)}\ W/m^2\,^oC$$

$$U_{ts}= 0.35\quad W/m^2\,^oC$$

$$R_{ts} = \frac{1}{0.35}\ m^2\,^oC/W$$

$$R_{ts} =2.86\quad m^2\,^oC/W$$

The thermal conductivity and the thickness of the sheet of polyiso were known. This meant that the thermal resistance could be calculated by using Equation 5.8:

$$R_{polyiso} = \frac{L_{polyiso}}{K_{polyiso}} \qquad \textbf{5.8}$$

$$R_{polyiso} = \frac{0.04}{0.0215}\ m^2\ ^oC/W$$

$$R_{polyiso} = 1.86\ m^2\ ^oC/W$$

Using Equation 5.8, the thermal resistance of the Eco-quilt with an air gap on either side was calculated:

$$R_{Eco\text{-}quilt} = R_{ts} - R_{polyiso}$$

$$R_{Eco\text{-}quilt} = 2.86 - 1.86\ \ m^2\ ^oC/W$$

$$R_{Eco\text{-}quilt} = 1.00\ m^2\ ^oC/W$$

This calculated thermal resistance ($R_{Eco\text{-}quilt}$) was for the Eco-quilt and 1 unventilated air gap.

5.7.4 Discussion of Multi-foil Testing Results

Even though the Eco-quilt was tested with 40 mm polyiso, the heat transfer coefficient was not found to be near the 0.16 W/m^2 ^{o}C required for the roofs of new buildings **[3]**. The heat transfer coefficient of the sheet of polyiso was known to be 0.54 W/m^2 ^{o}C before the tests took place. Using that heat transfer coefficient, the average thermal resistance of the Eco-quilt with an air gap on either side of the insulation plus the sheet of plasterboard was found to be 1.68 m^2 ^{o}C/W. This value would be equivalent to using

67 mm of fibre glass, with a conductivity of 0.04 W/m^{o}C, or 36 mm of polyiso insulation.

A sample calculation was performed to estimate the thermal resistance of the Eco-quilt insulation with no air gaps on either side. This was done by estimating the thermal resistances of each unventilated air gap and the sheet of plasterboard and subtracting this resistance from 1.68 m^{2} ^{o}C/W. BS EN ISO 6946 outlines the following procedure to estimate the thermal resistance of unventilated air gaps **[93]**. The resistance of each air gap *($R_{airgaps}$)* was estimated using Equation 5.9.

$$R_{airgaps} = \frac{1}{h_a + h_r} \qquad \textbf{5.9}$$

Where;

h_a =The conduction/convection coefficient (W/m^{2} ^{o}C)

h_r =The radiative coefficient (W/m^{2} ^{o}C)

For horizontal heat flow, h_a is the larger of 1.25 W/m^{2} ^{o}C and 0.025/d (W/m^{2} ^{0}C) **[93]**.

Where ;

d = The thickness of the airspace (m)

h_r is given by Equation 5.10

$$h_r = Eh_{ro} \qquad \textbf{5.10}$$

Where;

E = The intersurface emittance

h_{ro} =The radiative coefficient for a black body surface (W/m^{2} ^{o}C)

h_{ro} was chosen to be 5.1 W/m^{2} ^{o}C from a table A1 in this standard **[93].** The intersurface emittance was calculated using Equation 5.11

$$E = \frac{1}{\frac{1}{\varepsilon_1} + \frac{1}{\varepsilon_2} - 1} \qquad \textbf{5.11}$$

Where;

$\varepsilon_1, \varepsilon_2$ = Emissivities of the surfaces bounding the air space

By assuming ε_1 and ε_2 for both air gaps were 0.08, the intersurface emmitance was found to be 0.041 from Equation 5.11.Using this value and h_{ro} = 5.1 W/m^2 ^{o}C, the radiative coefficient was calculated to be 0.212 W/m^2 ^{o}C using equation 5.10. Using h_a = 1.25 W/m^2 ^{o}C , the thermal resistance of each air gap was estimated to be 0.68 m^2 ^{o}C/W. The thermal conductivity of the 12.5mm thick plasterboard was assumed to be 0.25 W/m ^{o}C **[51],** giving it a calculated thermal resistance of 0.05 m^2 ^{o}C/W.

The total thermal resistance of the two air layers plus the sheet of plasterboard amounted to 1.41 m^2 ^{o}C/W. Although this was only an estimation, it suggests that the thermal resistance of Eco-quilt with no air gaps on either side is quite small (estimated to be 0.27m^2 ^{o}C/W) and that the thermal performance of multi-foil is highly dependant on having an air gap on either side of the insulation.

Figure 5.19 compares some of the test results described in the literature survey with the average result for Eco-quilt with two air gaps. Both tests conducted by Sheffield Hallam University (see Section 2.4.1) quoted a thermal resistance of 6.1 m^2 ^{o}C/W and at least 5 m^2 ^{o}C/W respectively. The second of those tests was conducted under steady state laboratory conditions. The TRADA (see Section 2.4.2) tests found the thermal resistance of TRI-ISO Super 10 to be 5.25 m^2 ^{o}C/W. These test results were not in good agreement with this research. Tests conducted by the NPL and the BRE found the thermal resistance of the multi-foils to be 1.71 m^2 ^{o}C/W and 1.72 m^2 ^{o}C/W respectively.

These results were in excellent agreement with this research. The main difference between these tests and this research was that a different type of multi-foil insulation was examined and that most of the test specimens were tested at an inclination that replicated a pitched roof. This research tested the multi-foils with horizontal heat flow (instead of an inclined angle), which would have affected the thermal resistances of the air gaps when comparing the results. The extra thermal resistance of the plasterboard is also incorporated into the 1.68 m^2 $^oC/W$ that was found in this research. The conditions for each of the tests also varied. It is still quite clear, however, that this research is in good agreement with the tests carried out by the NPL and the BRE, even though the testing conditions may not have been exactly the same.

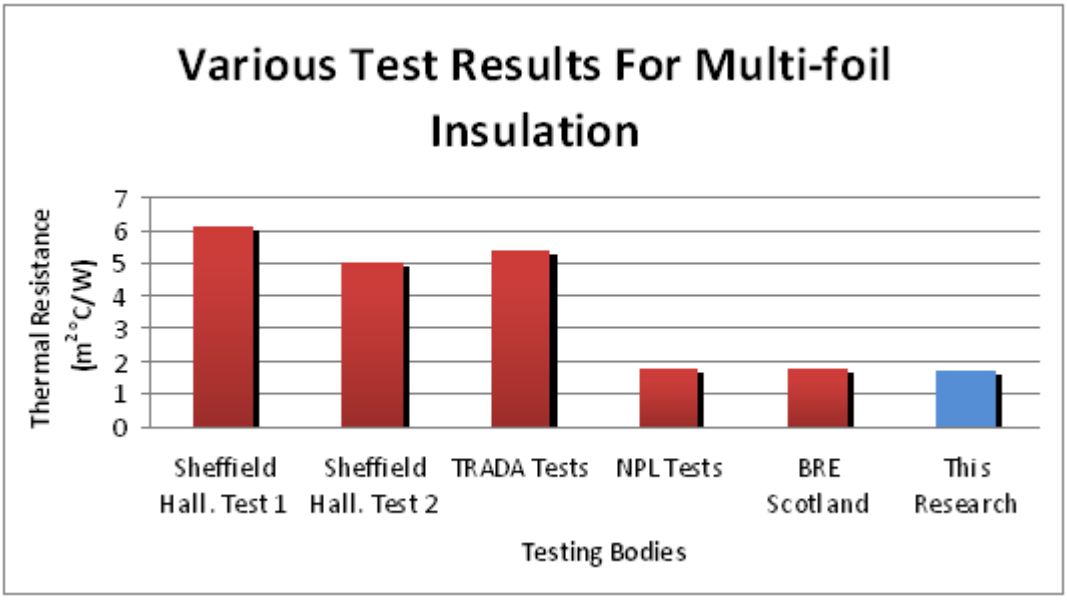

Figure 5.19: Comparison of Multi-foil Test Results with Two Air Gaps

Where multi-foil was tested with only one air gap, results showed that its thermal performance is reduced. After subtracting the thermal resistance for the known sheet of polyiso, $R_{polyiso,}$ from the test specimen, R_{ts}, Eco-quilt had a thermal resistance of 1.00 m^2 $^oC/W$ with the other multi-foil being 0.76 m^2 $^oC/W$. For the Eco-quilt, this

would be equivalent to using 40 mm of fibre glass, with a conductivity of 0.04 W/m ^{o}C or 22 mm of polyiso insulation.

5.8 Error Sources

The heat transfer coefficient for the test specimen ranged from 0.27 W/m^2 ^{o}C to 0.30 W/m^2 ^{o}C, where Eco-quilt was tested with two air gaps. This amounted to a 10 % difference over the four tests. The difference in these values can be attributed to the conditions not being exactly the same for all of the tests. Every effort was made (see Section 5.9) to keep the testing conditions the same but due to the room conditions not being the same for each test, other values such as cold box temperature, and the temperatures in the guard box changing affected the results. It can be seen in the calibration results (see Section 5.6.2) that the average temperature difference across the metering box wall was constant at 2.2 ^{o}C but in the Eco-quilt tests with two air gaps, the temperature difference varied from 2.0 ^{o}C to 2.3 ^{o}C. The maximum fluctuation in the input power for any one test fluctuated by 0.2 W and can be seen in Appendix B. In most tests conducted, the input power fluctuation was less than 0.1 W. Temperatures and input power for calculation purposes were collected three times a day for each test. This could have caused an error as minor fluctuations in between the data collection periods could have occurred.

5.9 Problems Encountered in Early Stages of Testing

One of the main problems encountered was controlling the cold box temperature over a long period of time. The GHB was located in a room in which the temperature changed regularly due to the weather varying from day to day. This affected the refrigeration unit

because the room temperature was sometimes colder than the set temperature on the unit and this in turn affected the air temperature travelling into the cold box.

Figure 5.20 is a graph that shows a graph of the cold side of the surround panel temperature over a period of approximately eight hours. Four thermocouples were monitoring the temperature on the cold side of the surround panel. The thermocouple that is shown on Figure 5.20 was located on the Left side of the surround panel. The other three temperature readings are not included in the graph for clarity of viewing. It can be seen that the temperature varies significantly over this time.

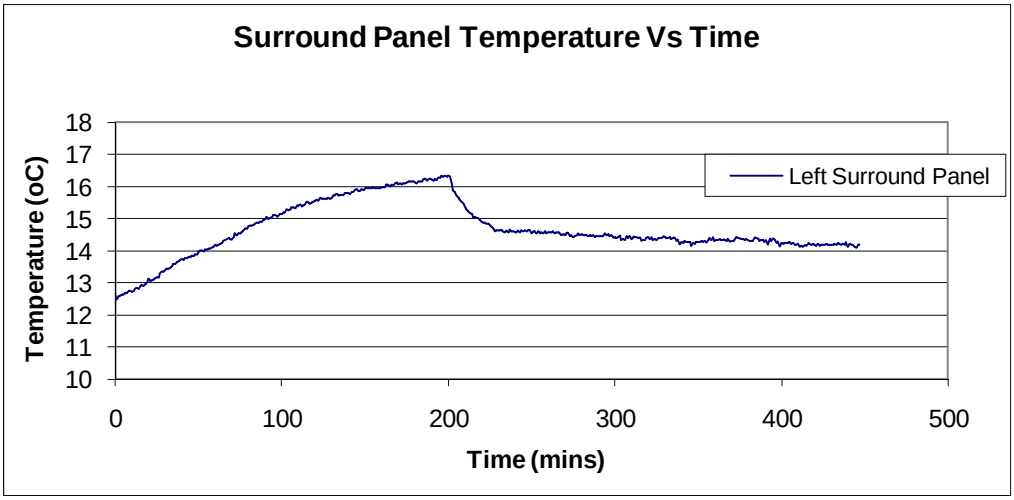

Figure 5.20: Cold Side Temperature Variation

Another problematic aspect of this testing was that the test data (e.g. readings of all thermocouples for calculation procedures) was collected once a day over a period of two hours. This also may not have been representative of the conditions due to the weather conditions.

The room temperature had to be raised above the set temperature in the cold box to solve this problem. The location of the testing facility was changed from an industrial

unit to a much smaller room and is shown in Figure 5.22. A 1 kW heater wired up to a thermostat was used to heat the room. A fan was used to circulate the air around the room. A picture of the fan and heater is shown in Figure 5.21. This resulted in a more uniform temperature in the cold box over a period of time. The result of changing the test location can be seen in Figure 5.15. It is clear that the cold box air temperature was more uniform and more reliable than the previous method. A test could now be completed without having to rely on weather conditions.

Figure 5.21: Fan and Heater in Place

Figure 5.22: New Testing Location

The data collection procedure was also changed. Test results were taken three times a day as opposed to once during initial testing. These measures were taken to ensure the temperatures in the GHB did not fluctuate during tests and was found to be a more accountable method of testing that produced repeatable results. This procedure is explained in Section 5.4.1. The observation period of temperatures before tests was also increased.

5.10 Testing Conclusions

The testing began by examining the air temperature distribution in the guard box, the

metering box and the cold box. These tests showed that the equipment was functioning the way it was designed to by achieving relatively uniform air temperature in each enclosure. A comparative test method was developed by analysing the losses in the GHB and combining the metering box wall losses with the parallel losses in the surround panel to calibrate the GHB and then test a specimen with unknown thermal properties.

The calibration tests evaluated this combined loss, and by repeating the tests, it was shown that the GHB was capable of giving meaningful and repeatable results. Four tests were conducted testing Eco-quilt insulation with an air gap on either side with 40 mm of polyiso insulation. The tests conditions were kept as similar as possible to the calibration tests and the results showed that Eco-quilt was closer to the thermal resistance of 1.71 m^2 $^oC/W$ than the thermal resistance of 5 m^2 $^oC/W$ quoted in the literature survey. Tests conducted on multi-foils with only one air gap showed that the thermal resistance of Eco-quilt and the other multi-foil insulation is reduced.

Possible errors in the GHB were discussed by examining the test results. This chapter also highlighted the problems that occurred in the early stages of testing. By changing the testing location and taking measures to control the surrounding room temperature these problems were overcome. The test procedure was also changed as a result of these problems.

CHAPTER 6 – CONCLUSIONS AND RECOMMENDATIONS

6.1 Conclusions

The main aim of this research was to test and examine the thermal properties of Eco-quilt multi-foil insulation. In order to achieve this, a list of project objectives are set out in Section 1.5.

The properties and characteristics of multi-foil insulation were researched and it was found that there was differing opinions on its thermal resistance. The difference in opinions is generally based on the test method that is used to evaluate multi-foils. All the tests that were conducted in real weather conditions found that multi-foils performed better than 200 mm of glass wool and, from that, it was claimed that the multi-foils had a thermal resistance of approximately 5 $m^2\,^oC/W$. Only one steady state test conducted agreed with these results. Other steady state tests found the thermal resistance was approximately 1.7 $m^2\,^oC/W$.

Eco-quilt was tested with two separate test rigs. The first test rig was constructed prior to this research and tests conducted using this rig offered a general idea of how multi-foils would perform. The results for these tests were in agreement that the thermal resistance of multi-foils was closer to 1.7 $m^2\,^oC/W$. These results indicated that Eco-quilt would have to be used with an additional insulation in order to meet the current building regulations.

There were some limitations with the preliminary test rig and, accordingly, a new

improved testing facility was successfully designed and manufactured to ensure the reliability and accountability of these results. Three different types of Hot Box were studied and a decision to base the design on a GHB was made. Key parameters such as the GHB dimensions, heaters and fans sizing and selection, and temperature and power measurements were all taken into account in the design. Evaluating the disadvantages of the preliminary test rig also helped in the design of the GHB.

A comparative test method was used to calibrate the GHB. This was done by using a test specimen with known thermal properties to evaluate the losses in the GHB. The same test was conducted on five different occasions and the combined loss heat transfer coefficient ranged from 1.19 $W/m^2\ ^oC$ to 1.20 $W/m^2\ ^oC$. The results showed that the GHB produced repeatable results.

The results for the Eco-quilt with an air gap on both sides and 40 mm polyiso ranged from 0.27 $W/m^2\ ^oC$ to 0.30 $W/m^2\ ^oC$. These results further showed that the GHB was successful due to the consistency of the results. The average thermal resistance of the Eco-quilt with two air gaps was found to be 1.68 $m^2\ ^oC/W$. This result was in good agreement with the tests that were conducted on other multi-foils using EN ISO test methods. These tests were conducted on ACTIS TRI-ISO Super 9 insulation, which consists of the same amount of layers and has the same thickness as Eco-quilt.

When Eco-quilt was tested with one air gap and with the sheet of polyiso, the results showed that its thermal performance is reduced. Another type of multi-foil was also tested in this configuration to compare it to Eco-quilt. The Eco-quilt performed better, with a heat transfer coefficient of 0.35 $W/m^2\ ^oC$ as opposed to 0.39 $W/m^2\ ^oC$ for the other multi-foil.

The test results show that the GHB used in this research can offer a good estimation of the thermal properties of different materials. This could be of benefit to companies developing new forms of insulation or looking to improve an already existing product.

Tests could also be conducted to test different methods of installing insulation and its effect on the thermal performance. For example, the tests conducted on multi-foil with only one air gap showed that its thermal resistance was reduced.

6.2 Recommendations

1 The tests that were conducted took place in a small, poorly-insulated room in an out-building. Over all the calibration and multi-foil tests, the room temperature varied by approximately 9 ^{o}C. By having a well insulated room for this testing where the temperature variation could be reduced, the repeatability of the GHB could be improved. Adding more layers of insulation around the guard area would also improve the repeatability.

2 By using a data logger with many more ports available, all the different temperatures could be measured at the same time during the testing period. Also, increasing the number of thermocouples would give a better and more accurate temperature profile for the different enclosures.

3 Inclusion of a method for continuously measuring the power input to the metering box could improve the average input power measurements for calculations.

4 The temperature difference across the metering box walls is currently controlled by setting the temperature on the PID controller in the guard box and adjusting

the power input into the metering box to achieve a temperature difference of approximately 2 ^{o}C. Designing a PID controller whose set point is controlled to keep the temperature difference across the metering box walls constant would also improve the repeatability of the GHB tests.

REFERENCES

All websites were accessed on the date 01/03/08

1. (2006) "Green Paper - Towards a sustainable energy future for Ireland" *Department of Communications, Marine and Natural resources pp. 8*
2. O'Leary F., Howley M., Ó Gallachóir B. (2007) "Energy Statistics 1990-2006*"*
3. Part L, Irish Building regulations "Conservation of Fuel and Energy" Section 0.3, pp. 9-10
4. (2002) "Directive 2002/91/EC of the European Parliament and of the Council of 16 December 2002 on the energy performance of buildings" *Official Journal of the European Communities L1/65.*
5. (Building Energy Rating) information leaflet. Website: www.sei.ie
6. BS EN ISO 8990 (1996): " Thermal Insulation – Determination of steady state thermal transmission properties- Calibrated and Guarded hot box"
7. Bolaturk A. (2006) "Determination of Optimum insulation thickness for building walls with respect to various fuels and climate zones in Turkey" *Applied thermal engineering 26 pp. 1301- 1309*
8. Guger E. C., Brownwell D. L. (1999) "Handbook of Applied Thermal Design" *Part 3, Chapter 1 pp.3-2. Published by Taylor & Francis, 1999.*
9. Polystyrene image. Website: http://www.atlasroofing.com/gallery/commercial/polystyrene.asp#
10. Fibre glass image. Website: www.timberframe.ie/index.php?page=build_sections
11. Vercumilite image. Website : www.pinchin.com/.../vermiculite16.htm

12. Multi-foil image, and installation Information http://www.insulation-actis.com/home.php?p=3&l=3

13. Dr. Mohammad S. Al-Homoud (2005) "Performance characteristics and practical application of common building thermal insulation materials" *Building and Environment 40 (2005) pp 353-366.*

14. Insulation Fact sheet – Department of Energy USA. Website: http://www.ornl.gov/sci/roofs+walls/insulation/ins_02.html

15. Mechanical insulation design guide – materials and systems- National institute of building science. Website: http://www.wbdg.org/design/midg_materials.php

16. Bardy E.R., Mollendorf J.C., Pendergast D. "Thermal Conductivity and Compressive Strain of Aerogel Insulation Blankets Under Applied Hydrostatic Pressure"

17. Ackerman W.C., Vlachos M., Rouanet S., Fruendt J. (2001) "Use of surface treated aerogerls derived from various silica precursers in translucent insulation panels". *Journal of Non-Crystalline Solids 285 pp. 264-271*

18. Brunner S , Simmler H. (2007)"In-situ Performance Assessment of Vacuum insulated panels in a flat roof construction". *Vacuum (2008) Vol. 82, issue 7, pp. 700-707*

19. Frike J., Heinemann U., Erbert H.P. (2007) "Vacuum Insulation Panels- From Research to market". *Vacuum 82 (2008) 680-690*

20. Alawadhi E.M. (2007) "Thermal analysis of a building brick containing phase changing material". *Energy and Buildings 40 (2008) pp.351-357*

21. Medina M. A., King J.B., Zhang M. "On the heat transfer rate reduction of structural insulated panels (SIPs) outfitted with phase change materials (PCMs)"

Energy 33(2008) pp.667-678

22. Kosny J., Miller W., Mohiuddin Syed A.(2007)"Field Testing of Second-Generation Residential Attic Using Inorganic PCM Thermal Storage" *Oak ridge national laboratory (ORNL)*

23. Reflective Insulation Manufacturers Association (RIMA) 2002; Understanding and Using Reflective Insulation, Radiant Barriers and Radiation control Coatings"

24. Bynum Jr, R.T., Rubino D. L. (2000) "Insulation Handbook" *Chapter 12 pp 250. Published by Mc Graw 2000*

25. Radiant Barrier image. Website: www.neo.ne.gov/.../aug2007/aug2007.loan.htm

26. Justice B. "Insulation Comparison Demonstration" Louisiana Department of Natural Resources. Department of Energy USA

27. Miranville F., Boyer H., Lauret P., Lucas F. (2007) " A Combined approach for determining the thermal performance of radiant barriers under field conditions" *Solar Energy 82 (2008) 339-410*

28. Shabica C.W. (1984) "Effects of Reflective Radiant Barrier on Heat Loss in Attic Floors and Metal Building Installations" *Reflective Insulation Manufacturers Association (RIMA)*

29. Michels C., Lamberts R., Guths S. (2007) "Theoretical/experimental comparison of heat flux reduction in roofs achieved with the use of reflective thermal insulators" *Energy & buildings 40 (2008), pp. 438-444*

30. Medina M.A. (2000) "On the performance of radiant barriers in combination with different attic insulation levels" *Energy and Buildings 33 (2000) pp. 31-40*

31. Medina M.A., Young B. (2005) "A perspective on the effect of climate and local

environmental variables on the performance of attic radiant barriers in the United states" *Building and Environment 41 (2006) pp. 1767-1778*

32. Information on TRI-ISO Super 9. Website: www.tri-isosuper9.co.uk

33. Thinsulex installation Website: www.thinsulex.co.uk

34. YBS installation manual. Website: www.ybsinsulation.com

35. ACTIS TRI ISO Super 10 information leaflet. Website: www.roof-solutions.co.uk/ourshop_158894_33485.html

36. Description of Sheffield Hallam University. Website: http://www.shu.ac.uk/research/cim/index.html

37. O'Flaherty F. (2005) "Evaluation of SuperQuilt multi-layer insulation Blankets in Roofs" Report No. CIM 122/r3. *Centre for Infrastructure Management, Sheffield Hallam University City campus Howard St. S1 1WB UK*

38. O'Flaherty F (2005) "Assesment of Alumaflex Thermo-reflective Insulation in Roofs" Report No. CIM 126/21. *Centre for Infrastructure Management, Sheffield Hallam University City campus Howard St. S1 1WB UK*

39. Description of BM TRADA. Website: www.bmtrada.com/index.php

40. Kearly V. (2006) "Multifoil Testing at TRADA" power point presentation

41. Description of Fraunhofer institute for Building Physics description. Website: http://www.ibp.fraunhofer.de

42. König N. (2007) "Thermal insulation with IR-reflective multifoil products" *NORMAPME Conference Stuttgart: PowerPoint Presentation.*

43. SFIRMM (Syndicat Français des Isolants Reflecteurs Minces Multicouches) "For the promotion of thin reflective insulation products for the creation of European certificate applied to these products" *Powerpoint presentation*

44. National Physics Laboratory description. Website: www.npl.co.uk

45. Williams R. (2004) "Measurement of the thermal resistance of an air cavity insulated with ACTIS TRI-ISO Super 9" Report reference No. PP31/E04060280

46. Williams R. TMAN meeting (2005)-Thermal Imaging for Building Fabric Insulation Compliance- "Evaluating the thermal performance of reflective insulation systems"

47. Ward T. I. Doran S.M.(2005)-"The thermal performance of multi-foil insulation" BRE, Scottish Enterprise Technology Park, East Kilbride, Glasgow, G75 0RZ.

48. Rooney G. (2006)"Thermal Insulation Performance Appraisal 139b & 141b Victoria Road, Torry, Aberdeen. Report no. 25035" Alba Building Sciences LTD.

49. Alba building Sciences description. Website: www.alba-sciences.co.uk

50. ASA (Advertising Standards Authority) Adjudication on ACTIS TRI ISO SUPER 9 (23rd April 2008) Website: www.asab.org.uk

51. Anderson B.(2006 edition) "Conventions for U-value calculations BR443" BRE Sctotland

52. Royal Court of Justice, London. Case No. CO/9218/2006, Date 2/11/2007. **Claimants:** ACTIS insulation Ltd. **Defendant:** The Secretary of State for Communities and Local Government. Approved Judgement

53. CMM (Confederation of multi-foil manufactures). Website: www.confederationmultifoil.org

54. Thinsulex multi-foil insulation BBA certificate. Website: www.webdynamics.co.uk

55. Curcija D. PHD "Trends and developments in Window Testing Methods" *University of Massachusetts, Centre for Energy Efficiency and Renewable Energy.*

56. Aviram D.P., Fried A.N, Roberts J.J. (2001)"Thermal properties of a variable cavity wall" *Building and Environment 36 (2001) 1057-1072*

57. Ghazi Wakili K., Tanner Ch. "U-value of a dried wall made of perforated porous clay bricks. Hot box measurement versus numerical analysis" *Energy and Buildings 35 (2003) 675-680*

58. Williams R. (2002) "Overview of a project to determine the thermal resistance of masonry walls in dry and moist states and a conversion procedure to determine the appropriate design value" *Session 12: Hygrothermal Properties of Materials*. *Building Physics 2002- 6th Nordic symposium*.

59. Nussbaumer T, Ghazi Wakili K., Tanner C.H "Experimental and numerical investigation of a protected vacuum insulation system applied to a concrete wall" *Applied Energy 83 (2006) 841-855*

60. Adam E. A., Jones P.J. (1995) "Thermophysical Properties of Stabilised Soil Building Blocks" *Building and Environment, Vol. 30, No. 2 pp245-253 (1995)*

61. Nader R. Elhajj (2003) – American Iron and Steel Institute Technology Roadmap Program Office, Pittsburgh, PA 15220. "Development of Cost Effective, Energy-Efficient Steel Framing"

62. Amunddarain A., Tero J.L., Usamani A., Al-Remal A.M. "Light Steel Framing : Improving the Integral design" *University of Edinburgh*

63. Nieminen J, Salonvaara M. (2000) "Hygrothermal Performance of Light Steel-Framed Walls" *VTT Technical Research Centre Finland*.

64. Yuan S. (2001) "Experimental and Analytical Heat Transfer analysis For a calibrated Hot Box and Fenestration System" *University of Massachusetts Amherst. UMI No.3027279*

65. Shah B., Curcjia D (2000): "A pilot Project to establish the technical Basis and Institutional Framework for assuring the Energy Efficiency of fenestration Building Products in Certain Transitional Economy Countries". *University of Massachusetts Amherst*

66. Simko, T.M.; Elmahdy, A.H.; Collins, R.E. (1999) "Determination of the overall heat transmission coefficient (U-value) of vacuum Glazing" *ASHRAE Transactions, v. 105, pt. 2, 1999, pp. 1-9.*

67. Burch D.M., Zarr R.R., Fanney A.H (1995) "Experimental verification of a moisture and heat transfer model in the hygroscopic regime" *Thermal performance of exterior envelopes of Building VI, Cleawater Beach FL. pp273-282*

68. Rose J, Svendsen S. (2004) "Validating Numerical Calculations against Guarded hot box Measurements" *Nordic Journal of Building Physics Vol.4, 2004;*

69. Zarr,R.R (2001) "A History of Testing Heat Insulators at the National Instituteof Standards and Technology" *ASHRAE Transactions 2001, V. 107, Pt.2., June 2001*

70. Burch, D.M., Zarr, R. R.,and Lacitra B.A. " A Dynamic Test method for determining Transfer function Coefficients for a wall Specimen using a Calibrated Hot Box" *Insulating Materials, testing and applications, Astm Stp 1030, D.L. Mcelroy and J.F. Kimlen, Eds., American society for testing*

Materials, Philadelphia, 1990 pp. 3454-361

71. Mumaw, J.R. 1974 "Thermal Research Facility- A large calibrated Hot box For horizontal Building Elements". *Thermal Insulation Performance, ASTM STP 718, D.l. McElroy and R.T. Tyre, Eds. American society for testing and materials, 1980 pp. 195-207*

72. Gao Y., Roux J.J., Teodosiu C., Zhao L.H. (2004) "Reduced linear steady state model of hollow block walls validation using hot box measurements". *Energy and Buildings 36 (2004) pp. 1107-1115*

73. Goss W.P. and Oplank, Ahmet "Design and Calibration of a Rotatable Thermal Test Facility" *Thermal Insulation, Materials, and Systems for Energy Conservation in the 80's, ASTM STP 789, F.A.Govan, D.M. Greason, and J.D. Mc Allister Eds., American Society for testing Materials, 1983, pp. 215-233*

74. Guarded Hot Box Image. Website: www.zebayern.comga

75. Desjarlais A.O., Tye R. P. (1989) "The Thermal Performance of Reflective Insulation Materials and Systems with Vertical Heat Flow: a Parametric study". *Thermal conductivity 21: The 21st International Thermal Conductivity Conference, October 15 – 18 1989, Lexinton Kentucky, pp. 291 -309.*

76. Velersluis R. MSC. Oversloot F.P. (2005) "Calibration of the TNO Guarded hotbox as specified by BS ISO 12567-1: 2000" *Netherlands Organisation for Applied Scientific Research.*

77. Kosney J, Dejarlais A. and Christian J. (1999) "Whole rating /Label for Structural Insulated Panels : Steady State Thermal Analysis" *Oak Ridge National Laboratory Building Technology Centre*

78. Nussbaumer T., Bundi R., Tanner, Ch, Muehlebach H. "Thermal Analysis of a

Wooden Door System with Integrated Vacuum Insulated Panels" *Energy and Buildings 37 (2005) 1107-1113*

79. Elmahdy, A.H.; Haddad, K. "Experimental procedure and uncertainty analysis of a guarded hotbox method to determine the thermal transmission coefficient of skylights and sloped glazing" *ASHRAE Transactions, v. 106, pt. 2, 2000, pp. 601-613*

80. Fang Y " An experimental and theoretical investigation into the design, development and performance of evacuated glazing*". PhD thesis, the University of Ulster, Northern Ireland, UK, 2002*

81. Fang Y., Eames P.C., Hyde T.J., Norton B. (2005)"Complex multimaterial insulating frames for windows with evacuated glazing" *Solar Energy 79 (2005) pp. 245-261*

82. Fang Y., Eames P.C., Hyde T.J., Norton B. (2006) "Experimental validation of a numerical model for heat transfer in vacuum glazing" *Solar Energy 80 (2006) pp.564-577*

83. Gatland S.D., Goss W.P., Baumgardener R. , Williams R., Millar R.G. "A wall and edge guarded Hot Box for Fenestration Testing" *Insulation Materials: Testing and Applications: Third Volume, ASTM STP 1320, R.S.Graves and R.R. Zarr, Eds., American Society for Testing and Materials, 1997.*

84. Williams R., Ballard G. (2003)"Validation of the NPL (National Physics Laboratory) rotatable Wall guarded hot box with horizontal heat flow Project PT0142 Milestone 4.2.a.02 June 2003" *NPL Report No. CBTLM25*

85. EN 1946-4 (2000) "Thermal performance of building products and components – Specific criteria for the assessment of laboratories measuring heat transfer

properties – part 4: Measurements by hot box methods".

86. BS EN ISO 12567-1 (2000) "Thermal performance of windows and doors – Determination of thermal transmittance by hot box method".

87. Lavine A.G., Rucker, J.L. and Wilkes, K.E. "Flanking Loss for a Calibrated Hot Box", *Thermal Insulation, Materials, and Systems for Energy Conservation in the 80's, ASTM STP 789, F. A. Govan, D.M.Greason, and J.D.Mc Allister Eds., American Society for testing Materials, 1983 pp. 234-247*

88. Incropera F.P. and DeWitt D.P. "Fundementals of Heat and Mass Transfer" *Fourth edition*

89. Fans, heaters and Fluke 189 multimeter technical specifications. Website: www.radionics.ie

90. DATALOGIC QS/QD specifications.

91. Specifications of Fluke 70 III multimeter

92. Pico Technology (2005): TC08 Thermocouple Data Logger User guide. Website: www.picotech.com

93. EN ISO 6946 (1998) "Building components and building elements – Thermal resistance and thermal transmittance – Calculation method" Table 1- Surface resistances pg. 5

94. Ye Z. (2001) "Development, Calibration and Application of a Guarded Hot Box to Determine the Thermal Resistance of Wool Insulation" *Masters of Science Thesis, University of Otago, Dunedin, Newzealand*

APPENDIX A – PRELIMINARY TEST RESULTS

A-1 Introduction

A series of tests were conducted with a preliminary test rig and the results are detailed in this section. The aim of these tests was to measure the thermal resistance of three types of multilayer reflective insulation in different configurations.

The apparatus used was a simplified Rotatable Calibrated Hot Box developed in the academic year of 05/06. This apparatus and testing theory is discussed in Section 4.2. All the tests were carried out at an angle of approximately 30^{o} to represent a roof structure as seen in Figure A1.

Figure A1: Picture of Test Rig

A-2 Specimen Preparation and Description

The specimen size for all tests was 1130 mm x 1380 mm. The plasterboard and the

polyisocyanurate were cut to size with a hand saw. As multi-foil is quilted, a suitable skeleton frame was built from 50 mm x 22 mm battens to support the material and avoid the sagging of the quilt during testing. The multi-foil was then stapled to the wooden frame using 14 mm staples. This is shown in Figure A2.

Figure A2: Preparation of Multi-foil Specimen

There were three types of multi-foil insulation being tested. One was Eco-quilt, another had a type of foam wadding and the last had no wadding present. All insulations were 25 mm thick. A description of each type of insulation follows:

Eco-quilt:

- 2 tear-resistant reinforced reflective films.
- 2 layers of soft, flexible wadding.
- 6 layers of closed cell foam.
- 4 internal reflective films.

Multi-foil with Wadding (W)*:

- 2 outer layers of tear-resistant reinforced reflective films.
- 4 layers of bubble wrap with a reflective film on one side.
- 1 layer of soft flexible wadding.

Multi-foil with no wadding (NW)**:

- 2 outer layers of tear-resistant reinforced reflective films.
- 4 layers of bubble wrap with a reflective film on one side.
- 1 internal reflective film.
- 2 layers of semi transparent plastic foam.

* = **With wadding**
** = **No Wadding**

A-3 Test Methodology

All tests were carried out as follows:

1. All test specimens were placed in the surround panel and duct tape was used around the perimeter of the test specimen to ensure no mass transfer (air leakage) occurred.
2. The surround panel was then clamped to the Hot Box using ratchets and straps.
3. The heaters were switched on and left for approximately 20 hours for steady state conditions to exist.
4. Power meters and the data logger were then used to collect the relevant data.

The inside temperature of the hot box was controlled by a thermostat and kept at approximately 39 ^{o}C.

A-4 Results

A-4-1 Calibration Test

The first test that was carried out was a calibration test. 12.5 mm plasterboard and 80 mm of polyiso insulation were tested together. The thermal properties of both were known. Table A1 gives all the parameters required to calculate the heat transfer coefficient (highlighted in yellow) in W/^{o}C for the box walls and surround panel. All thermocouples recorded air temperatures, and no surface temperature measurements were taken.

Conductivity $_{polyiso}$ (W/m ^{o}C)	0.0215
L (m)	0.08
R_{s1} (m^2 ^{o}C/W)	0.13
R_{s2} (m^2 ^{o}C/W)	0.04
R_{PB} (m^2 ^{o}C/W	0.038
Q_{in} (W)	53
ΔT_a(^{o}C)	28.9
A_{ts} (m^2)	1.56
R_{TT} (m^2 ^{o}C/W)	3.93
Q_{ts} (W)	11.49
UA_w (W/ ^{o}C)	1.45
U_{TT} (W/ m^2 ^{o}C)	0.25

Table A1: Calibration Results

The sample calculations use the testing theory discussed in Section 4.2.2. The thermal transmittance was known before testing. The two surface resistances were chosen from EN ISO 6946 and substituted into equation 4.2 **[93].**

$$U_{TT} = \frac{1}{R_{s1} + R_{ts} + R_{pb} + R_{s2}}$$

$$U_{TT} = \frac{1}{0.13 + 3.72 + 0.038 + 0.04}$$

$$U_{TT} = 0.25\ W/m^{2\,o}C$$

Using Equation 4.4 the heat transfer coefficient for the metering box walls was:

$$(UA)_w = \frac{(Q_{in} - (U_{TT} A_{ts} \Delta T_a))}{\Delta T_a}$$

$$(UA)_w = \frac{(53.1 - ((0.25)(1.56)(28.9))}{28.9}$$

$$(UA)_w = 1.45\ W/^oC$$

A-4-2 Multi-foil Test results

Ten tests were conducted on the three types of Multi-foil in different configurations. The configuration of the test specimen is given with the thermal resistance for each test highlighted in yellow in the following tables. The theory described in section 4.2.2 was used to calculate the thermal resistance of each test specimen.

Test 2 - Plasterboard - air gap - sheet of multi-foil (NW)

Q_{in} (W)	84.0
Δ T (^{o}C)	31.5
A_{ts} (m^2)	1.56
Q_w (W)	46.0
Q_{ts} (W)	38.0
U_{TT} ($W/m^2\,^{o}CK$)	0.77
R_{TT} ($m^2\,^{o}C/W$)	1.30

Table A2: Data for Test 2

- Equivalent to 52 mm of fibre glass or 30 mm of polyiso insulation.

Test 3 – Plasterboard - air gap – sheet of multi-foil (NW) - air gap – sheet of multi-foil (NW)

Q_{in} (W)	84.0
Δ T (^{o}C)	37.3
A_{ts} (m^2)	1.56
Q_w (W)	54.0
Q_{ts} (W)	30.0
U_{TT} ($W/m^2\,^{o}CK$)	0.52
R_{TT} ($m^2\,^{o}C/W$)	1.92

Table A3: Data for Test 3

- Equivalent to 76 mm of fibre glass or 41 mm of polyiso insulation

Test 4 -Plasterboard - air gap - sheet of multi-foil (W)

Q_{in} (W)	100
Δ T (^{o}C)	35.8
A_{ts} (m^2)	1.56
Q_w (W)	52
Q_{ts} (W)	48
U_{ts} (W/m^2 ^{o}CK)	0.86
R_{TT} (m2 oC/W)	1.16

Table A4: Data for Test 4

- Equivalent to 46 mm of fibre glass or 25 mm of polyiso insulation

Test 5 - Plasterboard - air gap – sheet of multi-foil (W) - air gap – sheet of multi-foil (W)

Q_{in} (W)	85
Δ T (^{o}C)	34.8
A_{ts} (m^2)	1.56
Q_w (W)	50
Q_{ts} (W)	35
U_{TT} (W/m^2 ^{o}CK)	0.64
R_{TT} (m^{2o}C/ W)	1.56

Table A5: Data for Test 5

- Equivalent to 62 mm of fibre glass or 34 mm of polyiso insulation

Test 6 - Plasterboard – 25 mm polyiso - air gap – sheet of multi-foil (W)

Q_{in} (W)	71
Δ T (^{o}C)	31.6
A_{ts} (m^2)	1.56
Q_w (W)	46
Q_{ts} (W)	25
U_{ts} ($W/m^2\,^{o}C$)	0.51
R_{TT} ($m^{2o}C/W$)	1.96

Table A6: Data for Test 6

- Equivalent to 78 mm of fibre glass or 42 mm of polyiso insulation.

Test 7 - Plasterboard -25 mm polyiso - air gap – sheet of multi-foil (W) - air gap – sheet of multi-foil (W)

Q_{in} (W)	72
Δ T (^{o}C)	32.7
A_{ts} (m^2)	1.56
Q_w (W)	47
Q_{ts} (W)	25
U_{ts} ($W/m^2\,^{o}C$)	0.49
R_{TT} ($m^{2o}C/W$)	2.04

Table A7: Data for Test 7

- Equivalent to 82 mm of fibre glass or 44 mm of polyiso insulation

Test 8 - Plasterboard – 25 mm polyiso - air gap – sheet of multi-foil (NW)

Q_{in} (W)	79
Δ T (^{o}C)	36.6
A_{ts} (m^2)	1.56
Q_w (W)	53
Q_{ts} (W)	26
U_{ts} ($W/m^2\,^{o}CK$)	0.46
R_{TT} ($m^{2o}C/W$)	2.17

Table A8: Data for Test 8

- Equivalent to 87 mm of fibre glass or 47 mm of polyiso insulation.

Test 9 - Plasterboard -25 mm polyiso - air gap – sheet of multi-foil (NW) - air gap – sheet of multi-foil (NW)

Q_{in} (W)	77
Δ T (^{o}C)	37.2
A_{ts} (m^2)	1.56
Q_w (W)	54
Q_{ts} (W)	24
U_{ts} (W/m2 oCK)	0.40
R_{TT} ($m^{2o}C/W$)	2.50

Table A9: Data for Test 9

- Equivalent to 100 mm of fibre glass or 53 mm of polyiso insulation

Test 10 - Plasterboard - air gap – Eco-quilt - air gap – Plasterboard

Q_{in} (W)	59
Δ T (^{o}C)	25.4
A_{ts} (m^2)	1.56
Q_w (W)	37
Q_{ts} (W)	22
U_{TT} (W/m2 oCK)	0.56
R_{TT} (m^{2o}C/ W)	1.79

Table A10: Data for Test 10

- Equivalent to 72 mm of fibre glass or 38 mm of polyiso insulation

Test 11 - Plasterboard - air gap – Eco-quilt

Q_{in} (W)	77
Δ T (^{o}C)	27.2
A_{ts} (m^2)	1.56
Q_w (W)	39
Q_{ts} (W)	38
U_{ts} (W/m2 oCK)	0.90
R_{TT} (m^{2o}C/ W)	1.11

Table A11: Data for Test 11

- Equivalent to 44 mm of fibre glass or 24 mm of polyiso insulation

This sample calculation is for the results shown in Table A2 for Test 2. For test specimens with unknown thermal properties, Equation 4.5 is used to calculate the heat transfer through the test specimen.

$$Q_{ts} = Q_{in} - Q_w$$

$$Q_{ts} = 84 - ((1.45)(31.5))$$

$$Q_{ts} = 38\ \text{W}$$

Finally Equation 4.6 was used to calculate the thermal transmittance for the unknown test specimen.

$$U_{TT} = \frac{(Q_{in} - (UA)_w \Delta T_a))}{\Delta T_a A_{ts}} = \frac{(Q_{ts})}{\Delta T_a A_{ts}}$$

$$U_{TT} = 0.77\ \text{W/m}^2\,^{\text{o}}\text{C}$$

$$\text{R}_{\text{TT}} = 1.30\ \text{m}^2\,^{\text{o}}\text{C/W}$$

APPENDIX B – GUARDED HOT BOX TEST DATA RESULTS

B-1 Introduction

The following tables correspond to the raw data for the calibration and multi-foil tests discussed in Chapter 5. The methodology applied in collecting the data is outlined in section 5.6.4.

B-2 Calibration Tests

Tables B1 – B4 display data collected from the calibration tests. Note that the data for calibration test 2 is shown in table 5.2.

	Morning	Afternoon	Evening	Average ΔT
$T_{hot\ SP}$ (^oC)	40.1	40.1	40.1	
$T_{cold\ SP}$ (^oC)	14.6	14	14	
ΔT_{SP} (^oC)	25.5	26.1	26.1	25.9
$T_{inside\ walls}$ (^oC)	40.7	40.7	40.7	
$T_{outside\ walls}$ (^oC)	38.5	38.5	38.5	
ΔT_{walls} (^oC)	2.2	2.2	2.2	2.2
$T_{hot\ ts}$ (^oC)	40.3	40.2	40.2	
$T_{cold\ ts}$ (^oC)	14.8	14.2	14.2	
ΔT_{ts} (^oC)	25.5	26	26.1	25.8
$T_{hot\ air}$ (^oC)	40.8	40.8	40.8	
$T_{cold\ air}$ (^oC)	13.9	13.5	13.4	
ΔT_{air} (^oC)	26.8	27.3	27.4	27.2
Q_{in}	16.13	16.34	16.25	16.24

Table B1: Calibration Test 1

	Morning	Afternoon	Evening	Average ΔT
$T_{hot\ SP}$ (^oC)	40.1	40.1	39.9	
$T_{cold\ SP}$ (^oC)	14.1	14	13.9	
ΔT_{SP} (^oC)	26	26.1	26.2	26.1
$T_{inside\ walls}$ (^oC)	40.8	40.8	40.7	
$T_{outside\ walls}$ (^oC)	38.6	38.5	38.5	
ΔT_{walls} (^oC)	2.2	2.3	2.2	2.2
$T_{hot\ ts}$ (^oC)	40.4	40.3	40.4	
$T_{cold\ ts}$ (^oC)	14.6	14.4	14.5	
ΔT_{ts} (^oC)	25.8	26	26	25.9
$T_{hot\ air}$ (^oC)	41	40.9	40.9	
$T_{cold\ air}$ (^oC)	13.8	13.6	13.6	
ΔT_{air} (^oC)	27.2	27.3	27.3	27.3
Q_{in}	16.34	16.33	16.33	16.33

Table B2: Calibration Test 3

	Morning	Afternoon	Evening	Average ΔT
$T_{hot\ SP}$ (^oC)	40	39.9	40	
$T_{cold\ SP}$ (^oC)	13.8	14.1	13.8	
ΔT_{SP} (^oC)	26.1	25.8	26.3	26.1
$T_{inside\ walls}$ (^oC)	40.7	40.6	40.6	
$T_{outside\ walls}$ (^oC)	38.4	38.4	38.4	
ΔT_{walls} (^oC)	2.3	2.2	2.2	2.2
$T_{hot\ ts}$ (^oC)	40.2	40.2	40.2	
$T_{cold\ ts}$ (^oC)	14.5	14.7	14.4	
ΔT_{ts} (^oC)	25.7	25.5	25.8	25.7
$T_{hot\ air}$ (^oC)	40.8	40.8	40.8	
$T_{cold\ air}$ (^oC)	13.7	13.8	13.5	
ΔT_{air} (^oC)	27.1	27	27.2	27.1
Q_{in}	16.21	16.25	16.23	16.23

Table B3: Calibration Test 4

	Morning	Afternoon	Evening	Average ΔT
$T_{hot\ SP}$ (^oC)	40	40	40.1	
$T_{cold\ SP}$ (^oC)	13.7	13.9	13.7	
ΔT_{SP} (^oC)	26.3	26.1	26.3	26.2
$T_{inside\ walls}$ (^oC)	40.7	40.7	40.7	
$T_{outside\ walls}$ (^oC)	38.5	38.4	38.6	
ΔT_{walls} (^oC)	2.2	2.3	2.1	2.2
$T_{hot\ ts}$ (^oC)	40.3	40.3	40.3	
$T_{cold\ ts}$ (^oC)	14.4	14.4	14.4	
ΔT_{ts} (^oC)	25.9	25.9	26	25.9
$T_{hot\ air}$ (^oC)	41	40.9	40.9	
$T_{cold\ air}$ (^oC)	13.8	13.5	13.5	
ΔT_{air} (^oC)	27.2	27.4	27.4	27.3
Q_{in}	16.22	16.24	16.25	16.24

Table B4: Calibration Test 5

B-3 Eco-quilt with Two Air Gaps

Tables B5 – B8 display data collected from the Eco-quilt tests with two air gaps.

	Morning	Afternoon	Evening	Average ΔT
$T_{hot\ SP}$ (^oC)	40.2	40.1	40.2	
$T_{cold\ SP}$ (^oC)	14.4	14.6	14.7	
ΔT_{SP} (^oC)	25.8	25.5	25.5	25.6
$T_{inside\ walls}$ (^oC)	40.6	40.6	40.6	
$T_{outside\ walls}$ (^oC)	38.6	38.5	38.5	
ΔT_{walls} (^oC)	2	2.1	2.1	2.1
$T_{hot\ ts}$ (^oC)	39.8	39.7	39.8	
$T_{cold\ ts}$ (^oC)	14.9	15	15.2	
ΔT_{ts} (^oC)	24.9	24.8	24.6	24.7
$T_{hot\ air}$ (^oC)	40.8	40.8	40.8	
$T_{cold\ air}$ (^oC)	13.6	13.6	13.7	
ΔT_{air} (^oC)	27.3	27.2	27.1	27.2
Q_{in}	18.76	18.77	18.74	18.76

Table B5: Eco-quilt Test 1

	Morning	Afternoon	Evening	Average ΔT
$T_{hot\ SP}$ (^oC)	40.3	40.1	4.03	
$T_{cold\ SP}$ (^oC)	14.6	14.8	14.6	
ΔT_{SP} (^oC)	25.7	25.3	25.7	25.6
$T_{inside\ walls}$ (^oC)	40.5	40.5	40.5	
$T_{outside\ walls}$ (^oC)	38.5	38.5	38.6	
ΔT_{walls} (^oC)	2	2.1	2	2
$T_{hot\ ts}$ (^oC)	39.8	39.7	39.8	
$T_{cold\ ts}$ (^oC)	15.2	15.3	15.2	
ΔT_{ts} (^oC)	24.5	24.5	24.6	24.5
$T_{hot\ air}$ (^oC)	40.8	40.7	40.8	
$T_{cold\ air}$ (^oC)	13.7	13.9	13.7	
ΔT_{air} (^oC)	27.1	26.8	27.1	27
Q_{in}	18.77	18.74	18.76	18.76

Table B6: Eco-quilt Test 2

	Morning	Afternoon	Evening	Average ΔT
$T_{hot\ SP}$ (^oC)	40.3	40.2	40.3	
$T_{cold\ SP}$ (^oC)	14.4	14.7	14.3	
ΔT_{SP} (^oC)	25.9	25.5	26	25.8
$T_{inside\ walls}$ (^oC)	40.7	40.4	40.6	
$T_{outside\ walls}$ (^oC)	38.7	38.5	38.8	
ΔT_{walls} (^oC)	2	1.9	2.1	2
$T_{hot\ ts}$ (^oC)	39.8	39.8	39.8	
$T_{cold\ ts}$ (^oC)	14.8	15.1	14.8	
ΔT_{ts} (^oC)	25	24.7	25	24.9
$T_{hot\ air}$ (^oC)	40.8	40.8	40.9	
$T_{cold\ air}$ (^oC)	13.4	13.5	13.4	
ΔT_{air} (^oC)	27.4	27.3	27.5	27.4
Q_{in}	18.78	18.66	18.74	18.73

Table B7: Eco-quilt Test 3

	Morning	Afternoon	Evening	Average ΔT
$T_{hot\ SP}$ (^oC)	40.5	40.5	40.5	
$T_{cold\ SP}$ (^oC)	14.7	14.7	14.7	
ΔT_{SP} (^oC)	25.8	25.8	25.8	25.8
$T_{inside\ walls}$ (^oC)	40.8	40.8	40.8	
$T_{outside\ walls}$ (^oC)	38.6	38.5	35.5	
ΔT_{walls} (^oC)	2.2	2.3	2.3	2.3
$T_{hot\ ts}$ (^oC)	40.2	40	40.1	
$T_{cold\ ts}$ (^oC)	15.1	15.4	15.2	
ΔT_{ts} (^oC)	25.1	24.6	24.8	24.8
$T_{hot\ air}$ (^oC)	41	41	41.1	
$T_{cold\ air}$ (^oC)	13.7	13.7	13.6	
ΔT_{air} (^oC)	27.4	27.3	27.4	27.3
Q_{in}	19.65	19.63	19.63	19.64

Table B8: Eco-quilt Test 4

B-4 Multi-foil Testing- with One Air Gap

Table B9 displays data collected from the Eco-quilt tested with one air gap and table B10 displays data collected from a multi-foil variant test also with one air cavity.

	Morning	Afternoon	Evening	Average ΔT
$T_{hot\ SP}$ (^oC)	40.5	40.6	40.6	
$T_{cold\ SP}$ (^oC)	13.9	13.9	13.8	
ΔT_{SP} (^oC)	26.7	26.6	26.8	26.7
$T_{inside\ walls}$ (^oC)	41	41	41	
$T_{outside\ walls}$ (^oC)	38.8	38.8	38.8	
ΔT_{walls} (^oC)	2.2	2.2	2.2	2.2
$T_{hot\ ts}$ (^oC)	40.1	40.1	40	
$T_{cold\ ts}$ (^oC)	14.6	14.7	14.5	
ΔT_{ts} (^oC)	25.5	25.4	25.5	25.5
$T_{hot\ air}$ (^oC)	41.2	41.2	41.2	
$T_{cold\ air}$ (^oC)	13.4	13.6	13.4	
ΔT_{air} (^oC)	27.8	27.6	27.8	27.7
Q_{in}	21.33	21.37	21.4	21.37

Table B9: Eco-quilt Test with One Air Gap

	Morning	Afternoon	Evening	Average ΔT
$T_{hot\ SP}$ (^oC)	40.3	40.4	40.4	
$T_{cold\ SP}$ (^oC)	13.1	13.3	13.3	
ΔT_{SP} (^oC)	27.2	27.1	27.1	27.1
$T_{inside\ walls}$ (^oC)	41	41	41	
$T_{outside\ walls}$ (^oC)	39.1	39.1	39.1	
ΔT_{walls} (^oC)	1.9	1.9	1.9	1.9
$T_{hot\ ts}$ (^oC)	40.1	40.1	40.1	
$T_{cold\ ts}$ (^oC)	14.1	14.3	14.2	
ΔT_{ts} (^oC)	26	25.8	25.9	25.9
$T_{hot\ air}$ (^oC)	41.1	41.2	41.2	
$T_{cold\ air}$ (^oC)	12.5	12.6	12.6	
ΔT_{air} (^oC)	28.6	28.6	28.6	28.6
Q_{in}	20.9	20.89	21.08	20.96

Table B10: Multi-foil Variant Test with One Air Gap

APPENDIX C – THERMOCOUPLE CALIBRATION

C1- Introduction

Type T thermocouples were used for temperature measurement in this research. The thermocouples were connected up to a PICO TCO8 data logger for the testing of the GHB. This data logger contains software that was compatible with Type T thermocouples and a temperature resolution of 0.1^{o}C could be achieved. To check this, the readings from the data logger were compared with an ISOTECH Venus Calibrator.

C2- Procedure

The ISOTECH Venus Calibrator has a liquid bath and the set-point temperature of the liquid can be adjusted. A digital readout displays the temperature of the bath. Three temperatures were chosen (20^{o}C, 25^{o}C and 40^{o}C) to compare the thermocouple readings with the readings of the ISOTECH calibrator. These temperatures were chosen because it was similar to the intended testing temperatures that were used in the GHB tests. Ten thermocouples were chosen from different parts of the GHB and were placed in the bath. The temperature readings from the digital readout on the calibrator and the data logger were compared and observed. This procedure was repeated before and after each testing period.

C3- Results

The readings from the ISOTECH Venus Calibrator always agreed with the readings from the data logger to the nearest 0.1 ^{o}C.